Photon statistics and power-law blinking of single semiconductor nanocrystals

Verberk, R.

Photon statistics and power-law blinking of single semiconductor nanocrystals

PROEFSCHRIFT

ter verkrijging van
de graad van Doctor aan de Universiteit Leiden,
op gezag van de Rector Magnificus Dr. D.D. Breimer,
hoogleraar in de faculteit der Wiskunde en
Natuurwetenschappen en die der Geneeskunde,
volgens besluit van het College voor Promoties
te verdedigen op woensdag 6 april 2005
klokke 15:15 uur

door

Rogier Verberk
geboren te Papendrecht
in 1976

Promotiecommissie:

Promotoren:	Prof. Dr. M. A. G. J. Orrit
	Prof. Dr. J. Schmidt
Referent:	Dr. M. Dahan
Overige Leden:	Prof. Dr. P. H. Kes
	Prof. Dr. A. Meijerink
	Prof. Dr. Th. Schmidt

The present work is part of the research program of the Stichting voor Fundamenteel Onderzoek der Materie (FOM), which is financially supported by the Nederlandse Organisatie voor Wetenschappelijk Onderzoek (NWO).

Contents

1 Introduction

Semiconductor nanocrystals, sometimes called nanocrystallites or quantum dots, are very small spheres of semiconductor material, with a diameter of 2–20 nm. They possess unique (optical) properties and many interesting applications of semiconductor nanocrystals have already been demonstrated. The most striking property of semiconductor nanocrystals is their blinking behavior. The luminescence of nanocrystals under continuous excitation is interrupted at random times and for random durations, see Figure 1.1. The reason for this is still not fully understood. Next to an interesting scientific question it is also important for all applications to understand the processes behind it. A single photon source would for example be more reliable if the nanocrystal would not blink. This intriguing phenomenon is also the limiting factor for the brightness of nanocrystals and therefore for their use as biological labels. The research described in this thesis is intended to get a better understanding of the blinking behavior of semiconductor nanocrystals. A new model is proposed to describe the physical processes that cause blinking. Model predictions and their agreement with experimental results are illustrated by numerical simulations. Also described here are several experiments on nanocrystals in different environments, that were performed to investigate the influence of the surrounding matrix on the blinking behavior. The statistics that governs the rhythm of blinking is different from the statistics of everyday life and complicates the interpretation of experimental data. It is discussed here within a general description of photon statistics in the fluorescence of single molecules and nanocrystals.

The nanocrystals (NC's) discussed in this thesis are all colloidal II–VI semiconductor nanocrystals. Self-assembled quantum dots or quantum wells, i.e., semiconductor nanocrystals embedded in another semiconductor, are not considered here. Those are often built from III–V semiconductors and are part of the bigger class of semiconductor heterostructures. Yet another type of quantum dots are silicon NC's [1, 2]. Although details are different, developments in the knowledge of silicon NC's follow those in the field of II–VI semiconductor NC's. First, it was discovered that the II–VI semiconductor nanocrystals require a protecting shell for efficient emission. Shortly after that, blinking was observed. The statistics to describe the blinking turned out to be based

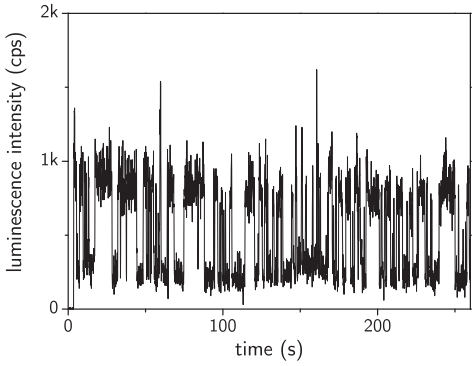

Figure 1.1: The intensity of the luminescence of a single (capped) nanocrystal under continuous illumination is not constant in time. It switches between two levels, high and low, like a telegraph switching on and off when receiving a Morse code.

on power laws, and statistical aging was demonstrated. Physical models to explain the processes that cause blinking require charge traps, tunneling, and the surrounding matrix for charge trapping. The two topics meet again in the debate about the physical nature and location of the traps [3].

The characteristics of semiconductor nanocrystals depend on their size. This size dependence is unique for this type of crystalline material. In this introduction we first discuss the major effects that cause this size dependence and other intriguing properties. After that, some of the many applications of NC's are discussed. This demonstrates the relevant properties and versatility of these little particles. At the end of this introduction, a more detailed overview is given of the research described in the rest of this thesis.

1.1 Semiconductor nanocrystals

The most important properties of bulk crystalline materials are fairly well understood from solid state physics. Below a certain size, however, the properties start to deviate significantly from bulk properties and become dependent on size. In case of semiconductors, these so called quantum size effects manifest themselves already in relatively large particles [4]. Quantum size effects in these semiconductor nanocrystals, which are still large enough to have a core resembling, to some extent, bulk material, are a unique opportunity to study the transition between atomic and solid state physics. The difference between semiconductors and, for example, metals can be understood by considering

the density of states. For increasing size of a crystalline solid, starting from a single atom to bulk material, the atomic energy levels broaden gradually to bands of allowed energy levels (band structure), see Figure 1.2. The energy level scheme of a single atom shows discrete levels (S, P, ...) for the energy of the electrons. In a small cluster of e.g. Si–atoms the connections between the atoms are hybridized sp^3-bonds. There are both bonding and antibonding molecular orbitals and a discrete energy spectrum. For bigger clusters or small crystals the orbital sets develop into conduction and valence bands. The highest occupied molecular orbital (HOMO) becomes the top of the valence band and the lowest unoccupied molecular orbital (LUMO) becomes the bottom of the conduction band [4, 5].

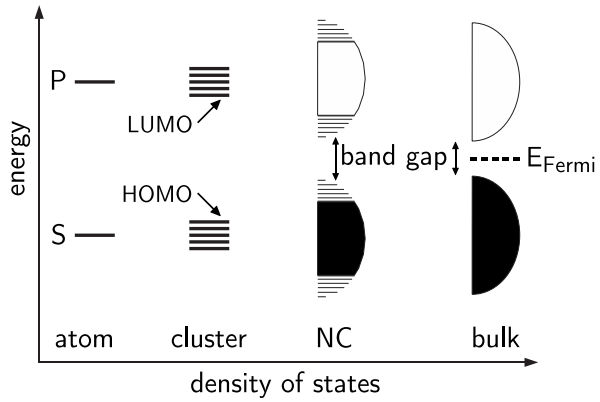

Figure 1.2: The density of states (DOS) in a semiconductor depends on the size of the crystal. A single atom is described by atomic energy levels (atom). A small cluster is governed by molecular orbitals (cluster). For nanocrystals and bulk material the DOS is condensed in continuous bands. For a nanocrystal (NC), the edges of the band structure are not completely developed, and show discrete levels. Because the Fermi level lies somewhere in the band gap, the optical properties of a NC are determined by these discrete levels.

For semiconductors (Figure 1.2), the Fermi level lies between two bands and the optical and electronic properties are dominated by the structure of the edges of the conduction and valence bands. For NC's, the center of a band has already developed into a continuum, but the edges consist of discrete energy levels. The combination of material and size causes the mixed continuous/discrete spectrum of semiconductor nanocrystals. Metals, on the other hand, have a Fermi level close to the center of a band, and already for very small particles the relevant energy levels are very closely spaced. For temperatures above a few Kelvin the spectrum resembles a continuum.

The energy spectrum of NC's is roughly as described above, but the optical properties depend critically on size. For CdS, the most studied NC material, the band gap can be tuned between 2.5 and 4 eV, or 500 and 300 nm, by changing the size of the particles. Smaller NC's are "blue shifted" with respect to bigger ones. The band gap in NC's is always bigger than in bulk semiconductor (see Figure 1.2). But not only the energy of the first transition changes, also the spacing between the consecutive transitions depends on size, like for a particle in a box. Also the radiative rate varies from several nanoseconds to tens of picoseconds, depending on the size of the NC [6]. This makes NC's very well suited for optical investigations of confinement effects.

Another consequence of the size of NC's is that adding a charge to it does not always cost the same energy, like in large crystals. Owing to the screening of charges, which can be significant in the case of semiconductors with large values of the relative dielectric constants, the additional charges can move independently through the bulk crystal. In NC's, however, the wavefunctions of the charges, which are confined in the small volume of the NC, overlap significantly. Screening cannot prevent interaction between the charges and the presence of a single charge makes adding another (similar) charge very expensive (in energy). This "Coulomb blockade" is the reason that current–voltage curves of single NC's resemble a staircase [7]. This effect is clearly very interesting for electronic applications, but it will also be discussed in relation to optical excitation in Chapter 4.

The surface–to–volume ratio of a sphere increases with decreasing size. This means that NC's have a relatively large surface area. Not surprisingly, surface effects are important when up to 40% of the atoms are at the surface. At the surface of a pure semiconductor, reconstructions occur in the atomic positions [8]. As a consequence, numerous surface energy levels lie in the band gap of the bulk crystal, acting as traps for electrons or holes. To prevent degradation of the optical properties, the surface has to be "passivated". For colloidal NC's this can be done either by organic or inorganic compounds. In the former case, large ligands like TOPO (trioctylphosphine oxide) are used, which attaches to the Cd-atoms via its oxygen. TOPO also takes care of the solubility of the NC and prevents aggregation [4]. Unfortunately, many questions about this coating are still not answered. The size of the ligand compared to the size of the NC makes it unlikely that all Cd-positions are passivated [8]. A few traps will remain. Molecular dynamics simulations indicate that the coverage varies with the size of the NC and is different for different surface types (sides) [9]. On the other hand, the ligands may still form a closed sphere around the NC, making it impossible for other molecules to react with its surface [10].

The second type of passivation is by capping with a thin layer of semiconductor with higher band gap, e.g., ZnS around a core of CdSe. A capping layer of a few monolayers is enough to remove the trap energy levels from the band gap. It has been demonstrated that the quantum yield increases dramatically by adding this capping layer [11]. New surface traps occur at the outer surface of the capping layer, but they are further away from the core. Moreover, a capped NC can be coated again by organic ligands. A thicker capping layer does not improve the passivation, as new defects may appear at the interface between the two semiconductors due to the large lattice mismatch [11]. An old explanation for the working of the capping layer is that the material of higher band gap prevents ionization and neutralization of the NC [12]. A new explanation for the effect of the capping layer is presented in Chapter 4.

1.2 Properties and applications

Owing to their special properties, semiconductor nanocrystals are a popular subject in several fields of physics, chemistry, and biology. For a few of these fields, the most important properties and possible applications of NC's are described hereafter. Again, this list is limited to the optical properties of NC's.

i) Optics

Several applications in quantum optics, like quantum computing or communication, require the controlled generation of individual photons. Not long after the introduction of single-molecule microscopy and spectroscopy, experiments were started with single molecules as single-photon sources. Nice results were obtained, first at low temperature [13] and later at room temperature [14, 15]. The high quantum yield [16] and photostability of nanocrystals recently attracted the attention of this community [17]. The main problem of NC's in this application is their fluorescence intermittency or blinking (vide infra).

For the same reasons NC's are now also used as light sources in photonic crystals [18]. Another interesting property of NC's is their circular emission dipole (2-D degenerate) [19, 20]. Finally, NC's may even be used to build color-selective lasers [21–23].

ii) Solid state physics

From the point of view of solid state physics, one of the most interesting aspects of NC's is the crossover from bulk material to the regime of strong quantization. Relaxation of the exciton energy in bulk II-VI semiconductors is dominated by Fröhlich interaction with phonons [24]. For nanocrystals, how-

ever, the generation of phonons is restricted by conservation rules of energy and momentum, due to their small size. This limitation called the "phonon bottleneck" is expected to slow down the relaxation process. Its existence and the relevance of Auger-like processes are studied in NC's [25]. Multi-particle Auger recombination can take place between two or three charges. The difference can be studied in NC's in relation to the confinement regime of differently shaped NC's [26]. Also the relevance of other, competing, decay channels like radiative electron–hole recombination and carrier trapping at defects or surface states are investigated in NC's [27].

iii) Nano-electronics
New ideas about the role of NC's in small electronic devices are proposed regularly. LED's and photovoltaic cells [28] could be based on NC's. What has been shown already includes photo-refractive polymer composites sensitized by NC's [29], 3-dimensional data storage [30], and electrical pumping necessary for many applications in electronics [31]. In combination with their photostability, the temperature dependence of the luminescence intensity and emission spectrum make NC's even suited for temperature probing [32].

iv) Biology
Biologists are mainly interested in the applications of semiconductor nanocrystals as fluorescent labels. For example, NC's have been used to track glycine receptors in the neuronal membrane of living cells [33]. The use of NC's as fluorescent labels in biological systems is reviewed in Refs. [34, 35].

Nanocrystals have many advantages compared to conventional fluorescent labels (dyes, e.g. Cy5, rhodamine 6G, or GFP). The emission wavelength can be tuned by changing the size of the NC's. On the other hand, they can be excited far over the band gap, exciting the electron to the continuous part of the conduction band, where the exact wavelength is not important. This means that NC's of different sizes can be used in a single experiment. All NC's are excited with the same blue laser, but the emission is different for NC's of different sizes. Due to the narrow emission peak (only 20–30 nm full width at half maximum), the emission of NC's of different sizes can be separated (multiplexing) [36, 37]. Another advantage of nanocrystals is their large absorption cross section ($\sim 10^{-14}$ cm^2 for NC's [36, 38] compared to e.g. $3 \cdot 10^{-16}$ cm^2 for rhodamine 6G in PVA [39]). Even three-photon excitation has been demonstrated [40]. The fluorescence intensity may be as high as that of 20 rhodamine 6G molecules [41]. Moreover, they are far more stable against photo degradation than the conventional dyes [36]. (Nearly 100

times more stable than rhodamine 6G [41].) Finally, the most recent progress in the synthesis of NC's makes it possible to make them suitable for use in numerous environments, including those relevant for biology [42]. Although their size may still be a problem for some applications, nanocrystals are a good compromise between small fluorophores and large beads for single-molecule experiments in living cells [33].

Several techniques that are used for investigating the structure of biological macromolecules or the folding and unfolding of proteins are based on fluorescence resonant energy transfer (FRET) [43]. This type of energy transfer has already been demonstrated for nanocrystals in 1996 [44] and many improvements have been proposed since then.

v) Photophysics
Finally, NC are studied for their intrinsic, interesting physics. In this context the contributions of the groups of Bawendi and Guyot-Sionnest are mentioned. They studied for example the quantum-confined Stark effect [45], intraband relaxation [46], and charge-tunable optical properties [47] in NC's. Interesting theoretical problems remain in the description on the confinement effects. It is not completely determined which interactions have to be taken into account in calculations on the energy levels and optical band gap [48, 49]. Recently, the topic that attracted most attention is the blinking behavior of NC's.

1.3 Outline of the thesis

Experimental setup and basic concepts

Blinking of semiconductor nanocrystals could only be observed after the introduction of single-molecule spectroscopy. This young field of research has shown many interesting results already. The development of the field is described in Chapter 2, together with the experimental requirements, up to the level required for experiments on single NC's. This is continued by a short description of our initial experiments on NC's, based on continuous-wave two-photon excitation. During these experiments we observed blinking. The difference between blinking and bleaching is explained. This is followed by an introduction to Lévy statistics, which describes the rhythm at which photons are emitted by single nanocrystals under continuous illumination. It appears in several other fields, too, but deviates profoundly from usual statistics. A good understanding is important to the research discussed in the subsequent chapters. The synthesis of semiconductor nanocrystals is described at the end

of this chapter.

Photon statistics in the fluorescence of single molecules and nanocrystals

The stream of photons emitted by a single molecule or nanocrystal can be explored in several ways. Common methods are based on the investigation of the distributions of delays or the correlation function. The former is used more often in experiments, the latter is easier to relate to models. It is therefore desirable to know the relation between these two methods. This relation is derived analytically in Chapter 3. An important aspect of this derivation is that it applies to any distribution of delays and to random telegraphs. This means that also the non-exponential distributions found in single-NC blinking are included. Topics that are discussed include switching between two states with different distributions (and various statistics of switching), correlations at long times that can only be observed via the second-order correlation function, changes in the detection quantum yield or the presence of background, and power-law distributions of on- and off-times. This last item is important for blinking NC's, as simple treatments dealing with exponential distributions cannot cope with this type of statistics.

Model for nanocrystal blinking

Experiments have been done on two types of nanocrystals; capped and uncapped. They show different kinds of blinking statistics, but no satisfying explanation for this difference has been given, yet. Moreover, the statistics of capped NC's seems to deviate considerably from what could be expected from simple physical arguments. The model presented in Chapter 4 may have the answers to both questions. Bright and dark periods are no longer simply related to neutral and charged states of the NC. Instead, a charged but bright state will be introduced, which is necessary to explain the wide distribution (in duration) of bright periods for capped NC's. The capping layer plays a key role in this model. It makes the introduction of the charged, bright state possible and effects thus the statistics of the bright periods. The model is compared to experimental data and simulations for validation.

Simulations of the blinking behavior of individual nanocrystals

Details of the numerical simulations that are based on the model presented in Chapter 4, which help to get a better understanding of the model, are described

in Chapter 5. The relations between the parameters in the simulations and physical observables in the model are explained. Also the influence of a few individual parameters is investigated explicitly. In the end, simulations based on a single model could reproduce the experimental data for both uncapped and capped nanocrystals. Luminescence time traces, distributions of on- and off-times, and correlations functions are all considered.

Influence of the environment on nanocrystal blinking

The environment has a significant influence on the blinking behavior of NC's. Chapter 6 presents several experiments dealing with this problem. The influence of the atmosphere is discussed first. Then, we show that the blinking statistics also depends on the local environment. NC's situated in different materials or on different substrates behave differently. This important role of the matrix was assumed in the model of Chapter 4. Finally, the blinking statistics is investigated as a function of excitation intensity. In this chapter, special attention is payed to the relation between the blinking statistics of individual NC's and the ensemble-averaged luminescence intensity. This relation is derived analytically and investigated experimentally. Good agreement has been found between theory and experiment, and between blinking statistics of single NC's and the fluorescence decay of ensembles.

2 Experimental setup and basic concepts

2.1 Single-molecule spectroscopy

An important development for nanoscience was the introduction of techniques to investigate materials at the level of single molecules. Individual molecules could now be addressed by optical microscopy and spectroscopy, or by means of scanning probe microscopy if they were located at the surface. With statistical physics the observed properties of bulk materials can be explained as the combined behavior of the molecules building up the material. The molecules building up the ensemble are assumed to behave all in a statistically identical manner. This assumption may not be correct, however. After all, the environment on a microscopic scale is not exactly identical for all molecules. Local disorder, defects and impurities in the material cause stress or small changes in the local potential. Investigation of an individual molecule gives information on the interactions between this molecule and its surrounding. This leads to a better understanding of the local interactions as well as the bulk properties. Instead of measuring ensemble averages, details about the statistical distribution can now be unravelled. An overview of the statistical methods that are often used in single-molecule spectroscopy can be found in Ref. [50]. Note that still many molecules have to be investigated to give a reliable picture of the system under interest. In fact, the sum of responses of many individual molecules should resemble the ensemble response. In the end, it is possible to judge whether the assumption that all molecules behave in a statistically identical manner is true or not. And even if this assumption turns out to be correct, additional information can be obtained. Several properties that were hidden under the ensemble average have been discovered in this way. Examples are luminescence intermittency (blinking) and spectral diffusion.

Scanning probe microscopy (scanning tunneling microscopy [51] and atomic force microscopy [52]) turned out to be a very useful way to investigate surfaces. The advantage of optical microscopy and spectroscopy on transparent materials is that it is not limited to surfaces. Despite several limitations, single-molecule spectroscopy has opened an interesting, new field of research. Although the first single molecules were detected via their absorbtion [53], the most popular method is to look at their fluorescence [54].

Figure 2.1 shows a schematic representation of the physical mechanism leading to fluorescence in case of an aromatic hydrocarbon of the type that is often used for single-molecule studies. The excitation source is tuned in resonance with the electronic transition between the singlet ground state S_0 and the singlet excited state S_1 of the molecule. The excitation wavelength λ_{exc} thus exactly matches the energy difference between these states. After absorption of a photon, the molecule is excited to S_1, where it will stay for typically a few nanoseconds. If the molecule decays to the ground state under emission of a photon with wavelength λ_{exc} (longest gray arrow in Figure 2.1), this fluorescence cannot be separated from the excitation light. This part of the fluorescence is called the zero phonon line. Slightly higher in energy than the pure electronic states are the associated vibronic levels (dashed lines in the figure, distances not to scale). A significant fraction of times, the molecule decays under emission of a photon with longer wavelength than λ_{exc} (shorter three gray arrows) to one of the vibronic levels of the ground state. This fluorescence is labeled as the phonon side bands in an emission spectrum. By use of dielectric filters it can easily be separated from the excitation light. By analyzing the emission spectrum carefully, information is obtained on the energy differences between the vibronic levels of the ground state (fluorescence–emission spectroscopy). Relaxation from the vibronic levels to the electronic states is very fast compared to the lifetime of the excited state and is accompanied by the creation of a phonon. For investigation of the emission spectrum, the molecule could also be excited to one of the vibronic levels of the excited state. This increases the spectral difference between the excitation light and the fluorescence. By accurately scanning the excitation wavelength through the vibronic levels of the excited state, information is obtained on their mutual distances (fluorescence–excitation spectroscopy).

The fluorescence signal can be hundreds to hundreds of thousands of photons per second, depending on the system under investigation. Under the right experimental conditions this signal can easily be detected. More important than the count rate of the signal is the intensity of the background signal. We distinguish four contributions to the total background signal. The first contribution consists of dark counts of the detector, fluorescence or scattered light from optical elements (lenses, filters), etc. By use of modern equipment this instrumental contribution to the total background is limited to tens of counts per second. The second contribution to the background consists of fluorescence of molecules that are situated in the sample, but outside the detection volume. One has to ensure that the excitation volume and the detection volume overlap well and that the microscope has a sufficiently high resolution in

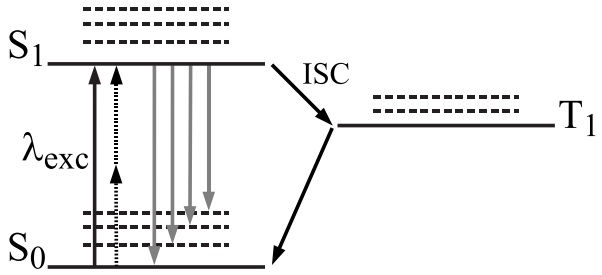

Figure 2.1: Jablonski diagram of an aromatic hydrocarbon. The molecule is excited from the singlet ground state S_0 to the first singlet excited state S_1 by absorption of a photon with wavelength λ_{exc} or shorter. The wavelength of the fluorescence is either λ_{exc} (zero phonon line, longest gray arrow) or a longer, i.e., it is red shifted (shorter three gray arrows). This shift is big enough to make spectral separation between excitation and fluorescence possible. Decay from a vibronic level (dashed lines, distances not to scale) to the lowest vibration level, i.e., the pure electronic state, is fast compared to the lifetime of the excited state. The long-lived triplet state T_1 is accessible via intersystem crossing (ISC) from the first excited state. The dashed black arrows represent two-photon excitation. The difference in wavelength between excitation and emission is then about a factor of two, which makes separation by filtering easier.

the lateral as well as the axial dimensions to minimize this contribution. The axial resolution is improved by using a pinhole in the detection path, as will be explained in the next section. More than one molecule in the detection volume and in resonance with the excitation source leads to a third contribution to the background. This can be molecules of the type under investigation or impurities. Obviously, the sample has to be prepared with great care to minimize the number of impurity molecules in the detection volume. Also the concentration of the molecules of interest has to be sufficiently low. The next section describes how a combination of microscopy and spectral selection reduces this contribution. Finally, laser light that is reflected (or scattered) by the sample leads to a higher background signal. This contribution can be filtered out because fluorescence and excitation light have different wavelengths.

Since the first experiments on aromatic hydrocarbons at low temperature the field of single-molecule spectroscopy has greatly expanded. Not only are the same systems now studied at room temperature, also new systems are addressed. Well known examples are green fluorescent proteins (GFP) [55, 56] and light harvesting (LH) complexes [57]. These experiments demonstrated the relevance of single-molecule spectroscopy to biology and increased the interest in this technique. The field also extended in the directions of polymers

[58] and nanoparticles like nanocrystals [12] and carbon nanotubes [59]. Note that spectroscopy on individual quantum systems does not provide information on the particle or molecule alone, but on the combination of the quantum system plus its local environment. Well investigated particles can thus be used to obtain information about the host material on very small scales. An example of "nanoprobing" is the work on Shpol'skii systems done in our group [60, 61]. An overview of recent developments in single-molecule spectroscopy can be found in [62].

2.2 Experimental setup

The confocal arrangement discussed here and shown in Figure 2.2 is nowadays the standard setup for single-molecule microscopy/spectroscopy and described in more detail elsewhere [63]. It can easily be extended for specialized measurements like, for example, polarization experiments. Light from the excitation source, typically a laser, is directed to the objective via the dichroic mirror, the scan mirror and the telecentric lens system. The objective is required to focus the excitation light tightly onto the sample. A smaller excitation and detection volume causes less background. This volume is typically 1–10 μm^3. It is desirable to scan the focus over the sample to search for molecules. The scan mirror is therefore used to deflect the excitation beam in a controlled way, such that the light enters the objective under different angles. Regarding the dimensions of the objective and the distance between scan mirror and objective, this is not possible without a pair of lenses (mutual distance equals the sum of their focal lengths) between the scan mirror and the objective. This so-called telecentric system "images" the point where the beam hits the scan mirror onto the back focal plane of the objective. In this way the angular displacement caused by the scan mirror is translated to a change in entrance angle in the objective. Ultimately this causes a small displacement of the focus on the sample. Fluorescence is collected by the same objective. Objectives with high numerical aperture (N.A.$= n \sin\alpha$, n is the refractive index of the propagating medium, α is the half-angle of the cone of collection) are preferred for more efficient collection of the fluorescence light. The fluorescence follows the inverse path of the excitation light up to the dichroic mirror. This mirror has a dielectric coating such that it reflects excitation light, but transmits fluorescence light. This is possible because the fluorescence light has a different (longer) wavelength than the excitation light. Residual scattered laser light is suppressed by appropriate filters. The fluorescence is focussed on a detection pinhole and then collected by a detector. The pinhole helps to suppress

the background signal. Both scattered light and fluorescence originating from other positions than the focal plane in the sample is not correctly focussed onto the pinhole and is attenuated accordingly. The most widely used detector is the avalanche photo diode, which is a sensitive single-photon counter with a small sensitive area, having a few tens of background counts per second.

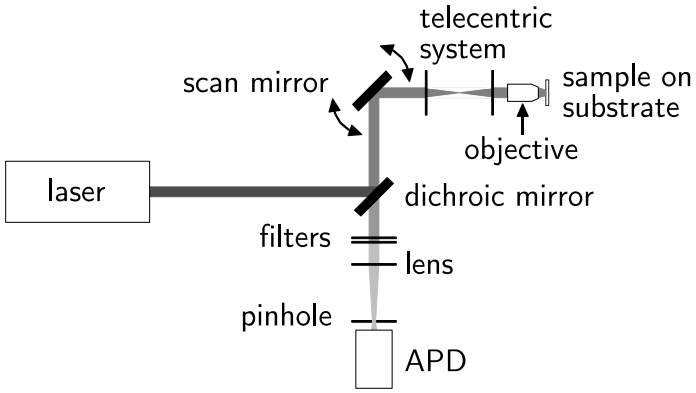

Figure 2.2: Schematic picture of a basic confocal arrangement. The laser light is focused on the sample by the same objective that collects the fluorescence. The dichroic mirror and filters suppress the laser light so that only fluorescence is directed to the detector (APD).

The confocal arrangement reduces the excitation or detection volume to several cubic microns. The sample has to be very dilute, in the order of 10^{-10} molar or lower, to have only one molecule of interest in this volume. This would mean that workable concentrations are limited to a narrow range and that for the investigation of every molecule a new sample position has to be selected. Fortunately, the differences in the behavior between individual molecules in which we are interested, are also very useful. Small local differences in the surrounding of the molecules make every molecule–environment system unique. As a result, the absorption energy is slightly different from one molecule to another at low temperatures. This is why the absorption spectrum of an ensemble is always broader than the absorption spectrum of an individual molecule. This effect is called inhomogeneous broadening. By use of modern lasers with very narrow linewidth, the excitation energy can be scanned through the inhomogeneously broadened absorption spectrum of an ensemble to address individual molecules. This spectral selection makes measurements on samples with much higher concentration possible.

2.3 Two-photon excitation of nanocrystals

An apparent difficulty with microscopy on individual nanocrystals is their very small Stokes shift. Separation between excitation light and fluorescence is very difficult if the spectral difference is (too) small. There are three alternatives to obtain information on the energy levels at the edges of the band gap. The first method is emission spectroscopy by excitation high above the band gap. The emission light can be analyzed with a monochromator. Unfortunately, this technique is limited by the spectral resolution of the monochromator, typically 1 cm^{-1} or 30 GHz. The second method is based on separation of the excitation light and emission in the time domain. Delayed emission can be detected after pulsed excitation due to the finite lifetime of the excited state (gated detection). (This technique is also used, for example, to improve the signal–to–noise ratio for biological imaging with NC's [64].) We have chosen for the third possibility; two-photon excitation spectroscopy. With this technique the NC is excited via absorption of two photons at the same time. Each of the photons provides only half of the required energy, which means that photons with far less energy are used. The wavelength is thus two times bigger than the wavelength of the fluorescence, making spectral filtering possible. (Compare to Figure 2.1: the wavelength of the two dashed arrows is very different from the wavelength of the longest gray arrow.) Because the probability is very low to absorb two photons simultaneously, the intensity of the excitation beam has to be high. Pulsed lasers are often used for this technique to reach sufficiently high excitation intensities, but this limits the spectral resolution. For example picosecond pulses cause a line-broadening of several tens of gigahertz. Better spectral resolution is obtained by using continuous-wave excitation. Single-mode cw lasers can have a spectral linewidth of less than 1 MHz. Owing to the fact that the absorption cross section of NC's is relatively large compared to dye molecules, cw two-photon and even three-photon excitation is possible [30].

We have performed continuous-wave two-photon excitation measurements on individual CdS nanocrystals. The goal was high-resolution fluorescence–excitation spectroscopy on the electronic states near the band edge. Those states are hardly accessible by one-photon spectroscopy due to the small Stokes shift.

Nanocrystals of CdS with a diameter of 5 nm were added to a solution of demineralized water with 0.5 (weight) % poly(vinyl alcohol) (PVA, molecular weight 125000). This solution was spin-cast on a substrate of fused silica to obtain films with an estimated thickness of less than 1 μm. At a concentration of 5×10^{-11} M, individual NC's could be observed. The sample was mounted in a helium bath cryostat and cooled down to 2 K. Fluores-

cence microscopy was performed with a home-built beam-scanning confocal microscope. The 457.9 nm line of an argon-ion laser was used for one-photon excitation and a single-mode continuous-wave titanium:sapphire laser for two-photon excitation. Figure 2.3 shows two images of CdS nanocrystals embedded in a spin-coated PVA film. Figure 2.3(a) is obtained by excitation with light at a wavelength of 810 nm and an intensity of 6 MW/cm^2. Figure 2.3(b) shows the same part of the sample as obtained by excitation at 457.9 nm and 1.2 kW/cm^2. The correspondence between the two pictures demonstrates that continuous-wave two-photon excitation is possible. This was proven by a measurement of the fluorescence intensity as a function of excitation intensity. The experimental data were fitted with a power law with exponent 2.2 ± 0.1. In these experiments the NC's were excited fairly high over the band gap, which is just below 500 nm or 2.5 eV for this type of NC's.

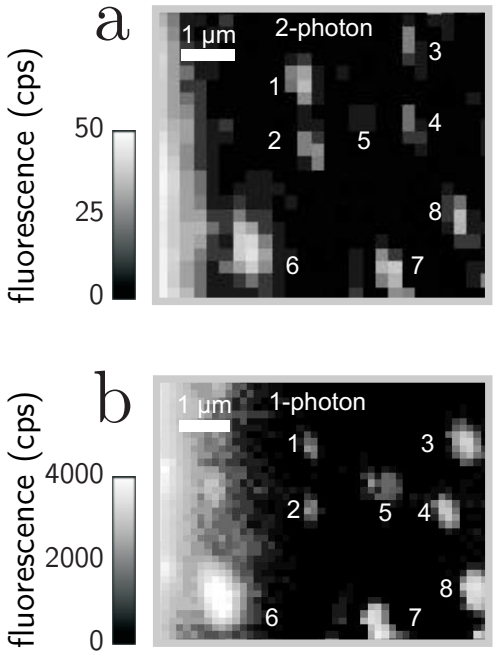

Figure 2.3: Individual CdS nanocrystals in a PVA film. Image (a) is obtained by two-photon excitation at 810 nm and 6 MW/cm^2. Image (b) depicts the same part of the sample, as obtained by one-photon excitation over the band gap at 457.9 nm. The same group of nanocrystals is observed in both cases.

In a second type of experiment we have tried to perform high-resolution fluorescence-excitation spectroscopy to observe the pure exciton transition just below the band gap. Severe experimental problems then appeared. First, it is

difficult to scan the laser over a broad spectral range at the required excitation wavelength. Moreover, the linewidth of the laser and the electronic transition are both relatively narrow and the exact position of the exciton transition is not known because it depends on the size of the individual NC. Spectral diffusion complicates the experiments even further [65, 66]. Another problem in these experiments are the fluctuations of the fluorescence intensity, which reduces the photon yield. Moreover, some transitions are very weak, because they are not allowed by two-photon excitation. A transition based on two-photon absorption is only allowed between two states of equal parity (whereas absorption of a single photon causes a change in parity). Even though some mixing of states is expected (due to symmetry breaking in the unit cell or because the NC is polar), two-photon transitions are probably very weak [67]. All these problems prevented us from observing the pure exciton transition by cw two-photon excitation.

Fluctuations in the luminescence intensity were observed both for one-photon and two-photon excitation. Although this interesting phenomenon called blinking is well known for single molecules, the physical processes causing it in NC's were unknown at the start of this work.

2.4 Blinking and bleaching

Blinking, or luminescence intermittency, is known since the first optical experiments on single molecules. Almost all single-molecule systems studied so far show fluctuations in the emission intensity under continuous-wave (cw) excitation [68]. If the fluctuations are so strong that the luminescence is virtually switched on and off, this effect is called blinking. An example of this is given in Figure 1.1 for a single capped NC under cw excitation. A graph of the intensity of the luminescence as a function of time is called a luminescence time trace. The durations of bright or dark periods range at least from microseconds to hours for NC's. For molecules, typical timescales are microseconds to milliseconds. Blinking could not be observed before the introduction of single-molecule microscopy. In general the molecules of an ensemble are not synchronized, which means that an ensemble shows no blinking. The only effect of blinking on the emission of an ensemble is that the intensity, the sum of the emissions of all single molecules, is lower than it would be without blinking. The discovery of blinking is the most clear and well known example of information that is normally hidden under ensemble averaging but is accessible by means of single-molecule microscopy.

There are several possible reasons for a molecule to blink. Investigation

of blinking behavior led to new insight into the photophysical properties of numerous systems. The best known process to cause blinking is an excursion to the triplet state, see Figure 2.1. Aromatic hydrocarbons have singlet ground- and excited states between which a fast cycle of excitation and emission (fluorescence) is possible under cw excitation. The lifetime of the excited state is typically in the order of nanoseconds. With finite probability a triplet state is accessed from the excited state via intersystem crossing. Due to the much longer lifetime of the triplet state, the fluorescence is interrupted for the lifetime of the triplet state [69]. Other processes causing blinking are intramolecular (charge transfer [70], photochemical changes [71]) or intermolecular (two-level tunneling systems [72], environmental fluctuations [73], enzymatic dynamics [74] or energy transfer to an acceptor or donor [43]).

In all these cases, the luminescence is interrupted for a short time and resumed again. This means that the processes that cause the interruptions are reversible, like an excursion to a triplet state. This is different for the phenomenon called bleaching. In case of bleaching the luminescence is terminated by an irreversible process and the luminescence will not be resumed. A photo-induced chemical reaction is the most likely explanation. Although bleaching often takes place at longer timescales than blinking, the only correct way to distinguish the two is to check whether the luminescence is resumed or not. The luminescence of an ensemble of single-quantum systems may decrease in time due to blinking, bleaching or a combination of blinking and bleaching [39]. In the next section we explain how blinking (in the absence of bleaching) can cause a decay of ensemble luminescence.

2.5 An introduction to Lévy statistics

The blinking of semiconductor nanocrystals leads to bright and dark periods. The following chapters exploit the statistical information on these on- and off-times to learn about the physical processes that take place in a NC. One could try to obtain the required information simply from the average duration, variance, maximum duration, etc. of the on- and off-times. However, the on- and off-times of blinking NC's are governed by a particular type of statistics, called Lévy statistics, which is different from the statistics that is commonly used in everyday life. One of the particularities is, for example, that average values cannot be calculated. This leads to complications, but also to very interesting properties. Here, we give a short introduction to Lévy statistics.

Characteristic for Lévy statistics is its scale invariance. The same mathematical relations describe the physical properties on different scales. This

property is generic for fractals. If one zooms in on a small part of a fractal and blows up the image to the original size, the result is statistically identical to the original image. Although not so common in everyday life, Lévy statistics and the corresponding power-law distributions (vide infra) are far from unique for blinking nanocrystals. For example, the size distribution of fragments from an exploded object follows a power law [75]. Another example is the study of complex, scale-free networks, a popular application of graph theory [76]. The distribution of edges (links), also called degree distribution, follows a power law. This is relevant for, e.g., a network like the internet or modeling disease outbreaks in social networks [77]. Other examples of Lévy statistics can be found in biology or economic studies (extinction of species or companies [78] and response of stock exchange [79]). Here, the properties of Lévy statistics are explained in relation to blinking NC's.

As an example of "ordinary" statistics, we consider the light from an attenuated (continuous wave) laser, that is detected by a sensitive camera. This is an example of a Poisson process. The average number of detected photons during a fixed period of time is independent of time. In other words, the probability to detect a certain number of photons in the first two minutes of the experiment is equal to the probability to detect the same number of photons in the last two minutes of the experiment. (We assume no overlap of time intervals.) This probability is determined by the well known Poisson distribution:

$$P(n) = \frac{\alpha^n}{n!} e^{-\alpha} ,$$

with n the number of detected photons and α the average number of photons detected during a chosen interval. The time between two successively detected photons is the delay time. If the first photon is detected at $t = 0$, the possibility to detect the next photon is a random event. This means that it may be detected at any time, a time that cannot be predicted. The distribution of delay times follows an exponential distribution:

$$C(t) = \alpha e^{-\alpha t} . \tag{2.1}$$

The constant α is the probability per unit time that a photon is emitted. In other words, the probability that a photon has been emitted during an interval of duration $1/\alpha$ equals 1. Short delay times occur often, and the possibility that no photon was emitted for a long time is much lower. The average delay time of this exponential function can be calculated to be $1/\alpha$.

Imagine that the delay times are now distributed according to

$$C(t) = ct^{-\beta} . \tag{2.2}$$

This function is called a power law, β its exponent, and c is a proportionality constant. This function decays much slower than an exponential distribution. This means that very long delay times, which happen less often than short times, are not as rare as in the case of an exponential distribution. They have a significant contribution to the "average" value. But for $\beta < 2$ the average value of a power-law distribution is not even defined.

It has been shown that the on- and off-time distributions of blinking NC's are often governed by power laws. The distribution of off-times is similar to the distribution of delay times mentioned above. A series of photons emitted shortly after each other without interruption by an off-time is regarded an on-time. The on-times are supposed to follow a power-law distribution as well.

For exponential distributions, every on- or off-time will be of the same order of magnitude as the average value of on- or off-times. For Lévy statistics, however, the next period can be much longer. This can be illustrated by calculating the total time that the NC has spent in the off-state so far. This value is the sum of all off-times that were recorded up to present time. It is dominated by only a few long events of the same order of magnitude as the total value. There is even a finite probability that the next off-time lasts infinitely long. As long as the experiment continues, the probability to record such long off-times increases. As a consequence of this, the probability that the NC switches from off to on decreases in time. The same is true for switching-off events. The fact that this probability depends on time means that the system ages. The physical processes related to luminescence are independent of time, however. The aging, or observables being non-stationary, is purely due to statistics.

An important property in single-molecule microscopy is ergodicity. A system is ergodic if the time average of an observable is equal to the ensemble average. The average luminescence intensity of a single molecule can for example be calculated by measuring the intensity over a long time and dividing the total number of photons by the duration of the experiment. Another way is to measure the intensity of an ensemble of molecules and divide by the number of molecules in this ensemble. Generally, these two averages are equal and the system is ergodic. We have seen in the former paragraph, however, that for example the average off-time cannot be calculated for blinking NC's. There is no timescale over which physical observables can be averaged. This is also characteristic for Lévy statistics. The ergodicity is clearly broken for the on- and off-time distributions of blinking NC's.

Although the time- and ensemble averages of on- and off-times are not equal

(or not defined), there is still an interesting relation between the blinking behavior of single NC's and the fluorescence intensity of NC ensembles. The exponent of the on-time distribution is often somewhat bigger than that of the off-times, which means that long on-times are relatively more rare than long off-times. For an ensemble of NC's this means that the off-times dominate over the on-times at long times. In other words, after a long time, the fraction of NC's in the off-state is larger than the fraction in the on-state. The ensemble luminescence decreases therefore slowly in time. This time dependence is again completely due to statistics and called statistical aging. To prove that bleaching does not play a role here, one could simply interrupt the experiment. After a long time without excitation light, all NC's are in their state of lowest energy. Resuming the experiment will show a luminescence level similar to the level at the beginning of the experiment, which is higher than the level just before the break. The processes that caused the decrease of the ensemble luminescence are thus reversible. The rate at which the ensemble luminescence level decreases in time is related to the difference between the exponents of the on- and off-time distributions. In Chapter 6 this relation is worked out, and the information obtained from single-NC blinking is related to that obtained from ensemble measurements.

2.6 Synthesis of semiconductor nanocrystals

Since the first experiments on single semiconductor nanocrystals, the control over the process of synthesis has improved significantly [80]. As a consequence of this, the size distributions are much narrower and the crystal quality is better. Besides this, the variety of nanocrystals has increased dramatically. NC's are now available in many different shapes and sizes, suitable for several different environments (due to new capping and coating materials), and with many types of chemical groups at the surface for biological labeling. Here, the important steps in the production of CdSe NC's are described briefly as an example. The exact conditions like temperature, atmosphere, and Cd:Se molar ratio are critical to obtain NC's with high quantum yield [81].

To synthesize CdSe nanocrystals, a mixture of hexadecylamine (HDA) and trioctylphosphine oxide [TOPO, $(CH_3(CH_2)_7)_3PO$] is slowly heated in a flask to 330° C, under argon atmosphere. The exact composition of this solvent is important to achieve slow growth of the NC's later on in this fabrication process. TOPO slows down the growth process by binding to cadmium sites on the seeds through its oxygen. This improves the final crystal quality. The flask is then allowed to cool down. At 300° C a solution of trioctylphosphine [TOP,

$(CH_3(CH_2)_7)_3P$]/selenium/dimethyl cadmium [$Cd(CH_3)_2$] is quickly injected into the mixture using a syringe. Organometallic precursors (like dimethyl cadmium in this case) decompose at these high temperatures and small seeds of CdSe are formed. High concentrations of species containing Cd or Se in the solution are important to limit the time during which nucleation takes place. A shorter period of nucleation helps to create monodisperse particles. The temperature is now allowed to drop to 150° C, which is below the temperature of growth. Next, the temperature is stabilized at the desired growth temperature (170–280° C). Once the NC's have the desired size, after minutes to hours, the temperature is quickly lowered below the minimum temperature at which growth can take place. Other tricks like controlling the concentration of residual moisture present in the solvents are known to the experts [81].

3 Photon statistics in the fluorescence of single molecules and nanocrystals

abstract – The stream of photons emitted by a single quantum system such as a molecule or a nanocrystal is often statistically characterized by the distribution of delays between consecutive photons, or by the autocorrelation function of the intensity, or by the distributions of on- and off-times. In this chapter the general relations between the Laplace transforms of these distributions and correlation function are derived and discussed, addressing the influence of detection yield and background. Our analytical treatment applies to any distribution of delays and to random telegraph signals, including non-exponential distributions. We examine the special case of systems switching between two states characterized by different distributions of delays, where the switching can obey various statistics. We show that the second-order autocorrelation function keeps track of long-time fluctuations which are obviously lost in averaging the distributions of delays. We apply our formalism to random telegraphs, in particular to those with power-law distributions of on- and/or of off-times, which are encountered in the blinking of single semiconductor nanocrystals.

3.1 Introduction

All current optical studies of single nano-objects [82] (molecules, nanocrystals, quantum dots, etc.) are based on counting single photo-electrons. The photo-electrons arise from fluorescence (or luminescence) photons emitted under continuous wave (cw) or pulsed laser excitation. Fluctuations or variations of the emission rate can be related to various processes, intramolecular (triplet [69], charge transfer [70], photochemical changes [71]) or intermolecular (two-level tunneling systems [72], environmental fluctuations [73], enzymatic dynamics [83], energy transfer to an acceptor or from a donor [43], etc.). These strong emission fluctuations, which have been conspicuous from the very first optical experiments on single molecules, are now considered as deeply characteristic for single object luminescence [68]. Although they were largely ignored in conventional experiments on ensembles because their synchronization is in general impossible, they turn out to be very powerful means to investigate basic processes at nanometer scales. The present work aims at giving a general description of the statistics of the photons emitted by single objects, gathering various experimental results, procedures, and ways of exploiting the data, within a single frame. Some systems display Poisson statistics, single- or bi-exponential distributions [84], whereas more complicated non-Markov or non-exponential distributions are found in enzymatic dynamics [74, 74], or in nanocrystal blinking [85, 86]. Our treatment therefore has to go beyond earlier work dealing with exponential statistics [87, 88]. The formalism has to encompass various experimental methods, including start-stop measurements, correlation functions, and the distributions of on- and off-times. All these methods are based on coincidence measurements, i.e. on the detection of photon pairs. We will not enter the field of higher-order correlation functions involving coincidences of more than two photons, whose general theoretical treatment was introduced recently by Barsegov and Mukamel [89, 90].

The case of power-law distributions is of special interest for nanocrystal research. We will demonstrate that the correlation functions corresponding to power-law distributions, which have been observed in the blinking of individual nanocrystals, have simple expressions which can be related to published experiment data.

In the present work, our "signal" will be the series of photo-electrons (which we call "photons" in the following for the sake of brevity) detected from a single emitting nano-object under continuous or quasi-continuous illumination. To establish relations between absorbed laser photons and detected photo-electrons, random processes with specific yields will have to be introduced for emission and detection. Here, we assume we have continuous excitation

and a single detection channel, i.e. we do not consider cross-correlations, nor the time-resolved response to pulsed excitations [91, 92]. A basic hypothesis will be that the detection of each photon resets the system to zero for a given set of quantities (Markov variables), whereas other quantities can keep memories of the past history of the system (non-Markov variables). The most basic quantity we start from will be the waiting time distribution, or *delay distribution* between *consecutive* photons. After each photon detection event, the probability density to observe the next photon is given by a distribution function $C(\tau)$ of the delay τ between the photons. This distribution of waiting times can itself vary on longer timescales according to dynamics of a higher order. We will suppose that such changes in the delay distribution will be sudden and triggered by the absorption or emission of a photon.

A second important assumption in the present work is that measurements are stationary, i.e., the averaging time for the measured quantities is long enough for all states to be sampled with their steady-state probability. Only then can averages for a distribution of consecutive pairs (which would be measured in a start-stop experiment), for a correlation function (distribution function for all pairs), or for a distribution of on- and off-times be defined in a unique way. In order to define on-times and off-times, we have to arbitrarily set at least one threshold for the signal, and decide that the system will be "on" if the signal is higher than this threshold, "off" if it is lower. Besides the arbitrary choice of the threshold value, it is difficult to describe on- and off-times in general mathematical terms because they depend on several other parameters (background, quantum yield, time-resolution). In the present work, the on- and off-times will be one of the three following cases:

i) the off-times are delays between photons. No on-times are defined, only point-like photons separate two off-times;

ii) alternation of bright and dark periods due to sudden changes, for example in emission or detection quantum yields (Sections 3.3, 3.4); in that case, we shall suppose that these periods are known exactly. Real measurements are obviously distorted by background and noise;

iii) the on- and off-times are defined by the values of a random telegraph suddenly jumping between the values 0 and 1 (Section 3.5); these time distributions are again supposed to be known, or experimentally accessible without too much distortion.

Section 3.2 starts with the simple case of a single delay distribution, and its relation to the correlation function. We examine the influence of a non-unity quantum yield and of background. In Section 3.3, we consider random jumps between two waiting-time distributions. The probabilities of the jumps

obey a simple kinetic system. Along with the general solution, we discuss a few important special cases. Then, in Section 3.4, we consider the case of quantum yield fluctuations, which might be caused by motion of a quencher, conformational changes, etc. If the quantum yield is much smaller in one of the two states, the system behaves like a random telegraph, with on- and off-times, and a constant intensity during the on-times. The classical random telegraph will be treated in Section 3.5, and we shall derive relations between the on- and off-time distributions and the correlation function. We shall then focus on the case of power-law distributions in the context of semiconductor nanocrystals.

3.2 Single distribution of delays

We define a delay distribution $C(\tau)$ as the probability *density* that, after any photon, the next one is detected a duration τ later. $C(\tau)d\tau$ is the probability that the *next* photon is observed between τ and $\tau + d\tau$, and therefore $\int_0^\infty C(\tau)d\tau = 1$. Note that the duration of the next delay is randomly drawn from this distribution, and that there cannot be any memory effect in this model. We wish to relate $C(\tau)$ to the *conditional probability density* $G(t+\tau \mid t)$ to find *any* other photon at time $t+\tau$ if one was observed at time t. This conditional probability will be noted $G(\tau)$ for short in the rest of this paper. $G(\tau)$ is related to the familiar second-order correlation function of the intensity $I(t)$ by

$$g^{(2)}(\tau) = \frac{G(\tau)}{\langle I(t)\rangle} .$$

For a classical light source, the probability to observe a photon can be considered as a classical function of time. The correlation function can therefore be rewritten in the usual form [93]:

$$g^{(2)}(\tau) = \frac{\langle I(t)I(t+\tau)\rangle}{\langle I(t)\rangle^2} .$$

In quantum mechanics, however, the "instantaneous intensity" is an operator, whose expectation value depends on former measurements, and is therefore not a classical function of time. In the rest of this paper, in order to avoid speaking of a time-dependent intensity, we shall work mainly with the general conditional probability density $G(\tau)$, which does not refer to the classical or

quantum character of the emission. We will also call $G(\tau)$ the non-normalized correlation function.

In order to obtain this function $G(\tau)$, we note that the probability to observe any other photon at a later time writes as a sum of probabilities for this photon to be the first, the second, etc., which is easily expressed using convolution products of the probability density $C(\tau)$:

$$G(\tau) = C(\tau) + \int_0^\tau C(\tau - \alpha)C(\alpha)d\alpha + \dots \ .$$

Introducing lower-case symbols for the Laplace transforms $c(s)$ of $C(\tau)$, and $g(s)$ of $G(\tau)$, convolutions are replaced by simple products. Summing the geometrical series, we obtain a well-know relation [94], already derived by Reynaud [95]:

$$g(s) = \frac{c(s)}{1 - c(s)} \ . \tag{3.1}$$

Figure 3.1 compares the shapes of the delay distribution and of the correlation function for two simple cases. In the first case (dashed lines), photons are emitted at random, as is the case for a Poisson light source e.g. a well-stabilized cw laser. The distribution of waiting times is a single exponential, $C(\tau) = ae^{-a\tau}$, with $c(s) = a/(s + a)$. We therefore conclude that $g(s) = a/s$, which corresponds to a flat correlation function, $G(\tau) = a$. In that case, the detection of a photon does not tell us anything about the probability of detection of any other one at a later time. In the second example (solid lines), we consider a stream of "anti-bunched" photons such as could be emitted by a single molecule at room temperature [14, 96] or by a capped semiconductor nanocrystal [97–99]. Anti-bunching means that the detection of one photon projects the system (molecule or nanocrystal) into the ground state, and that a new emission will require a certain time, typically the fluorescence lifetime at low power. Therefore, photons tend to arrive separately, they are anti-bunched. Figure 3.1 shows that the delay distribution coincides with the correlation function at short times, but decreases exponentially at longer times, because it is very unlikely to observe two consecutive photons separated by a long waiting time.

Alternatively, photon statistics can be characterized by the time-dependent Mandel parameter $Q(T)$ [100], defined as

$$Q(T) = \frac{\langle n^2 \rangle_T - \langle n \rangle_T^2}{\langle n \rangle_T} - 1 \ ,$$

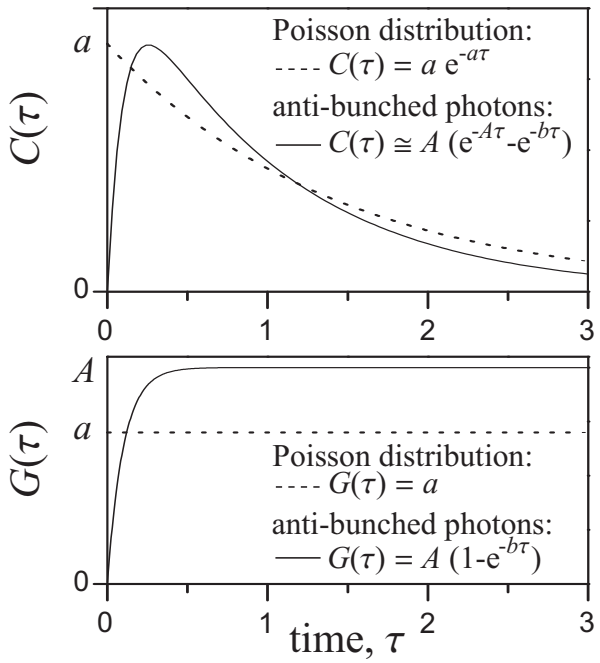

Figure 3.1: Comparison of delay distributions (top) and correlation functions (bottom) in two simple cases: independent random distribution of photons -i.e. Poisson distribution- (dashed lines), and "anti-bunched" photons, where two photons cannot be emitted at the same time (solid lines).

where $\langle \ldots \rangle_T$ means average over an interval T. It is a measure for the deviation from Poisson statistics, for which $Q(T) = 0$. A negative Q indicates anti-bunching (sub-Poisson statistics), a positive Q indicates bunching (super-Poisson). $Q(T)$ is related to the normalized correlation function $g^{(2)}(\tau)$ by [100]

$$Q(T) = \frac{2\langle I(t)\rangle}{T} \int_0^T d\tau \int_0^\tau d\tau' (g^{(2)}(\tau') - 1) \, .$$

In the rest of this paper we consider only the correlation function, from which the Mandel parameter can be immediately obtained.

We will now apply relation 3.1 to a few important cases.

Random additional waiting time before each emission

A random delay may exist before each emission process, e.g. because absorption involves a long waiting time. This is particulary true at low laser power. Assuming there is no correlation between the waiting times of the absorption and of the emission, the two random processes are independent. If $D(\tau)$ is the distribution of these additional absorption delays, and $d(s)$ its Laplace tranform, we can express the new delay distribution between consecutive photons as a convolution product of $C(\tau)$ and $D(\tau)$, from which we get, replacing the Laplace transform of the delay distribution by the product cd:

$$g = \frac{cd}{1 - cd} \,. \tag{3.2}$$

Non-unity detection yield

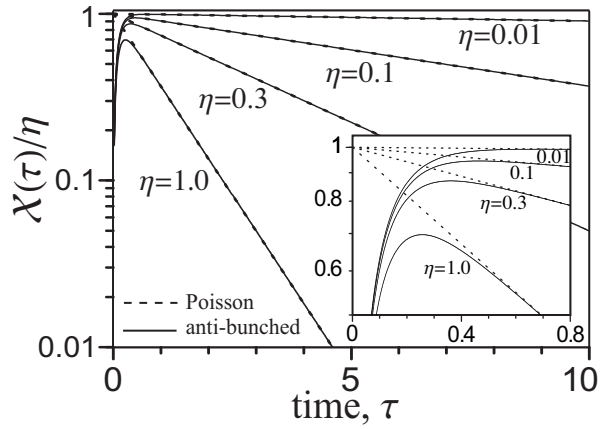

Figure 3.2: Influence of the detection quantum yield on the delay distribution of consecutive photo-electrons in the anti-bunched case (solid line) and in the Poisson case (dashed lines, single exponentials). For vanishing yield, the delay distribution resembles more and more the correlation function.

Let us call η the overall detection yield, i.e. the probability that an absorbed photon gives rise to a detected photo-electron. The distribution of delays between consecutive detected photons can be written as a sum of probabilities of detecting two photons while missing 0, 1, 2,... in between. Because the probability of not detecting a photon is $1-\eta$, we find for the Laplace transform $\chi(s)$ of the delay distribution of consecutive photo-electrons $X(\tau)$:

$$\chi(s) = \frac{\eta c}{1 - (1 - \eta)c} \,, \tag{3.3}$$

which, applying equation 3.1, gives the Laplace transform $\gamma(s)$ of the non-normalized correlation function for photo-electrons $\Gamma(\tau)$:

$$\gamma = \frac{\chi(s)}{1-\chi(s)} = \frac{\eta c}{1-c} = \eta g \,.$$

Therefore, a non-unity detection quantum yield does not change the shape of the correlation function (and leaves the normalized correlation function $g^{(2)}(\tau)$ invariant). Note also that, if the detection yield is much smaller than unity, the distribution of consecutive photo-electrons is nearly proportional to the correlation function [94, 98].

Figure 3.2 presents the influence of the quantum yield on the delay distribution of consecutive photon-electrons in the case of a Poisson distribution and in the anti-bunched case of Figure 3.1. When the yield decreases, the exponential decay becomes slower and slower, and the delay distribution resembles more and more the correlation function, $\chi \approx \eta g$.

Table 3.1 summarizes the analytical forms of the various functions plotted in Figures 3.1 and 3.2.

Poisson distribution

Consecutive emitted photons	$C(\tau)$	$=$	$ae^{-a\tau}$
Consecutive detected photo-electrons	$X(\tau)$	$=$	$\eta a e^{-\eta a\tau}$
Non-normalized correlation function	$G(\tau)$	$=$	a
Correlation function of detected photons	$\Gamma(\tau)$	$=$	ηa

"Anti-bunched" photons

Consecutive emitted photons	$C(\tau)$	$\cong$	$A(e^{-A\tau} - e^{-b\tau})$
Consecutive detected photo-electrons	$X(\tau)$	$\cong$	$\eta A(e^{-\eta A\tau} - e^{-b\tau})$
Non-normalized correlation function	$G(\tau)$	$=$	$A(1 - e^{-b\tau})$
Correlation function of detected photons	$\Gamma(\tau)$	$=$	$\eta A(1 - e^{-b\tau})$

Table 3.1: Analytical forms of the delay distributions of emitted photons and detected photo-electrons, and the corresponding correlation functions in two simple cases: Poisson distribution and "anti-bunched" photons.

Influence of a Poisson background

A constant Poisson background B added to the signal with average intensity $\langle I \rangle$ only changes the contrast of the normalized correlation function $g^{(2)}(\tau)$.

The new correlation function with background added to the signal, $g_B^{(2)}(\tau)$, becomes

$$g_B^{(2)}(\tau) = 1 + \frac{1}{\left(1 + \frac{B}{\langle I \rangle}\right)^2}(g^{(2)}(\tau) - 1)\,. \tag{3.4}$$

In order to show how the background changes the form of the distribution of delays, we derive the consecutive-pair distribution function of the total stream of photons (i.e. signal plus background), corresponding to this new correlation function. To discuss this in the time domain, we introduce two auxiliary probabilities, derived from the distribution of delays $C(\tau)$ of the initial signal.

i) Probability $C_I(\tau)$ that no photon is emitted between 0 and τ, knowing that one photon was emitted at $t = 0$:

$$C_I(\tau) = \int_\tau^\infty C(\alpha)d\alpha\,.$$

Note that $\int_0^\infty C_I(\alpha)d\alpha = \int_0^\infty \alpha C(\alpha)d\alpha = \langle I \rangle^{-1} = T_0$ is the average delay between consecutive photons.

ii) Probability $C_{II}(\tau)$ that no photon is emitted between 0 and τ, without any further knowledge. This is an integral of the probability density that one photon has been emitted at a time α earlier than 0, and that no photon is observed until τ. It can thus be written:

$$C_{II}(\tau) = \int_0^\infty \langle I \rangle C_I(\alpha + \tau)d\alpha = \langle I \rangle \int_\tau^\infty C_I(\alpha)d\alpha\,.$$

For a Poisson background, $C^{'}(\tau) = Be^{-B\tau}$, these probabilities are simply $C_I^{'} = C_{II}^{'} = e^{-B\tau}$. We now look for the probability density of observing a photon at τ, having observed one at $t = 0$, and none in between. We must consider four cases:

i) The first and second photons are signal ones; the product of the probabilities that the first photon is signal, that the next one is too, and that no background photon has come in between is

$$(1 + BT_0)^{-1} \times C(\tau) \times C_{II}^{'}(\tau)\,.$$

ii) The first photon is signal, the second is background:

$$(1 + BT_0)^{-1} \times C^{'}(\tau) \times C_I(\tau)\,.$$

iii) The first photon is background, the second is signal:

$$BT_0(1+BT_0)^{-1} \times C_I(\tau)T_0^{-1} \times C_I'(\tau)\,.$$

iv) The first and second photons are background:

$$BT_0(1+BT_0)^{-1} \times BC_I'(\tau) \times C_{II}(\tau)\,.$$

Therefore, the expression for the distribution of delays $C_B(\tau)$ between consecutive photons in the presence of background writes:

$$C_B(\tau) = (1+BT_0)^{-1}e^{-B\tau}[C(\tau) + 2BC_I(\tau) + B^2T_0C_{II}(\tau)]\,.$$

This form is not related in a simple way to that of $C(\tau)$. Although the background does not change the form of the correlation function, it does change that of the distribution of delays in a complicated way. Therefore, a distribution of "off-times" as measured by the waiting times between consecutive photons will depend not only on detection quantum yield, but also on background. Provided a straightforward correction of the contrast is made according to Equation 3.4, the correlation function is insensitive to background, and is therefore easier to compare to models.

Case of Rabi oscillations (optical nutation)

The distribution function of delays is often much more complex than single-exponential. A simple example is the emission probability of a two-level system resonantly driven by a laser field. The associated phenomenon, called optical nutation, is well-known in time-resolved ensemble measurements [101], where all two-level systems are synchronized by the sudden application of a Stark shift or of the laser wave. The normalized correlation function goes from zero at $t = 0$ to 1 at long times, with Rabi oscillations for a large enough Rabi frequency. The delay distribution therefore also presents several exponential and/or oscillating components [94]. Figure 3.3 shows delay distributions with different quantum yields, for a two-level system with Rabi oscillations. Note that, for unity detection yield, the delay distribution falls to zero after each Rabi period. This is because we have assumed zero dephasing, i.e. that relaxation is caused by emission only. Therefore, having observed no intermediate photon between the two detection events in the pair means that no relaxation occurred. The two-level system is thus exactly in the ground state again after each Rabi period.

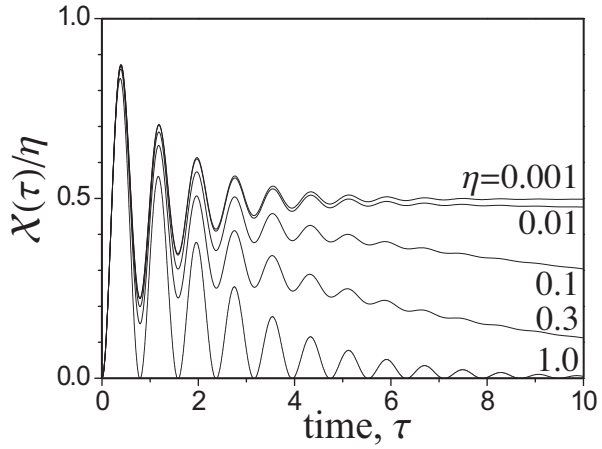

Figure 3.3: Delay distributions of consecutive detected photons emitted by a two-level system under intense illumination [94]. We have assumed a long coherence lifetime, which allows damped Rabi oscillations to appear. The curves are plotted for various values of the detection quantum yield.

3.3 Two distributions of delays

We now consider a two-state system, where the delays between consecutive photons can be drawn from two different distributions $C_1(\tau)$ and $C_2(\tau)$, corresponding to two states of the emitter. Switching between these two states is a random process, which we assume to coincide with excitation or emission, with a given probability. Although not essential for slow changes, this assumption considerably simplifies the subsequent reasoning. Even if they are difficult to access experimentally, the distributions $C_1(\tau)$ and $C_2(\tau)$ can be considered as on- and off-times distributions, because they will in general be associated to states of the emitter of different brightness. Let us call ϵ_1 the probability to change from state 1 to 2 after each absorption/emission, and ϵ_2 that to change from 2 to 1.

In order to treat the general case, we need some auxiliary quantities. The probability to have n (and only n) 1-type intervals in a row is $(1-\epsilon_1)^{n-1}\epsilon_1$, i.e. the probability to have $n-1$ 1-intervals following a first one. From the average number $\langle n-1\rangle = (1-\epsilon_1)/\epsilon_1$, the average number of 1-intervals in a row follows $\langle n\rangle = \epsilon_1^{-1}$, and the probability that any photon starts a 1-type interval is

$$w_1 = \frac{\epsilon_2}{\epsilon_1+\epsilon_2}\,.$$

The occupation probability of state 1, p_1, involves the average delay time

between consecutive photons $\tau_1 = \int_0^\infty \tau C_1(\tau) d\tau$:

$$p_1 = \frac{w_1 \tau_1}{w_1 \tau_1 + w_2 \tau_2} ,$$

with similar definitions for state 2. In the rest of this Section, we assume the quantum yield to be independent on the emitter's state.

Distribution of consecutive pairs

The overall delay distribution of the photon stream is given by adding the delay distributions in each state with the proper weights, i.e. $C = w_1 C_1 + w_2 C_2$, which is just the average distribution of delays, and is therefore insensitive to long-term correlation of many periods of one type.

Correlation function

We again sum the probabilities of all possible sequences between two photons, making use of auxiliary functions corresponding to sequences of 1-times or 2-times only, expressed with the Laplace transform $c_1(s)$ of $C_1(\tau)$:

$$g_1 = \frac{c_1}{1 - (1 - \epsilon_1) c_1} , \tag{3.5}$$

and a similar relation for state 2. Note that these functions are identical to Equation 3.1 except for the factor $1 - \epsilon$, which represents the probability to stay in the same state. The final expression of the Laplace transform $g(s)$ of the G function of the photon stream is a sum over all possible sequences of alternating state-1 and state-2 sequences, starting (with the correct weighting factors) in either one of these states:

$$\begin{aligned} g &= w_1 \left[\frac{g_1 + \epsilon_1 g_1 g_2}{1 - \epsilon_1 \epsilon_2 g_1 g_2} \right] + w_2 \left[\frac{g_2 + \epsilon_2 g_1 g_2}{1 - \epsilon_1 \epsilon_2 g_1 g_2} \right] \\ &= \frac{w_1 c_1 + w_2 c_2 + (\epsilon_1 + \epsilon_2 - 1) c_1 c_2}{1 - (1 - \epsilon_1) c_1 - (1 - \epsilon_2) c_2 + c_1 c_2 (1 - \epsilon_1 - \epsilon_2)} . \end{aligned} \tag{3.6}$$

If the two distributions are identical, $c_1 = c_2$, we retrieve equation 3.1, independently of the switching probabilities.

From this general formula, we can derive a few interesting cases in the two-dimensional space of parameters (see Figure 3.4):

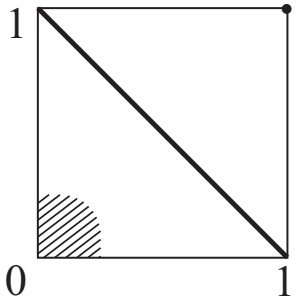

Figure 3.4: Two-dimensional space of parameters ϵ_1, ϵ_2 describing the statistical correlation between states 1 and 2 of an emitter. The hatched region around (0,0) corresponds to series of many 1-times or 2-times, i.e. to long dwell times in either state. The point (1,1) represents a deterministic alternation of states 1 and 2. On the inverse diagonal (solid line between (1,0) and (0,1)) random jumps take place between states 1 and 2, with occupation probabilities determined by the point on the line.

i) $\epsilon_1 = \epsilon_2 = 1$: we have a deterministic alternation of delays, 1-times and 2-times, drawn from the two distributions in turn. We obtain

$$g = \frac{1}{2}\frac{c_1 + c_2 + 2c_1c_2}{1 - c_1c_2} ,$$

which, of course, is different from $c_1c_2/(1 - c_1c_2)$ (see equation 3.2) because a photon is now emitted after each 1- or 2-interval.

ii) $\epsilon_1 + \epsilon_2 = 1$: we have random (Markovian) jumps between the two states, since the end-state after each jump does not depend on the state before. The occupation probabilities of the two states depend on the ratio of ϵ_1 and ϵ_2. We get

$$g = \frac{w_1c_1 + w_2c_2}{1 - w_1c_1 - w_2c_2} ,$$

which could have been obtained directly from Equation 3.1 and from the average delay distribution of section 3.3. Note therefore that the correlation function (Equation 3.6) always contains more information than the average delay distribution, except in the present case of random transitions, where the two quantities are directly related. In the average delay distribution, information about possible correlations or anti-correlations between 1- and 2-times is obviously lost.

iii) $\epsilon_1, \epsilon_2 \ll 1$: in this limit of a slow modulation, we have long periods in states 1 and 2. At the lowest order, we can neglect all products of ϵ's, to obtain

$$g \approx w_1g_1 + w_2g_2 ,$$

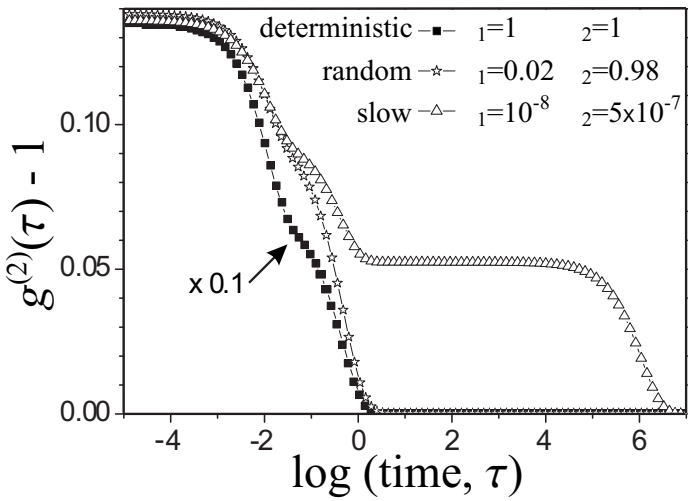

Figure 3.5: Example of correlation functions for an emitter switching in a deterministic way (squares, multiplied by a factor 0.1), randomly (stars) or with long correlation times (triangles) between two states with different emission statistics and brightnesses. Note the long exponential tail of the correlation function in the latter case, due to slow intensity fluctuations which are absent in the other cases.

which is simply, as could be expected, the average of the correlation functions in each state. However, this solution is valid for short times only. At longer times, $G(\tau)$, the intensity correlation function, gives us information about the slow transitions between states 1 and 2. For example, for single-exponential delay distributions with emission rates a_1 and a_2, Equation 3.6 writes as a rational function of s:

$$g = \frac{1}{s}\frac{(w_1 a_1 + w_2 a_2)s + a_1 a_2(\epsilon_1 + \epsilon_2)}{s + a_1\epsilon_1 + a_2\epsilon_2} ,$$

whose inverse Laplace transform will display an additional exponential decay component at the sum of the transition rates $a_1\epsilon_1$ from state 1 to 2, and $a_2\epsilon_2$ from 2 to 1, as expected from a two-state model [72]. Figure 3.5 shows examples of correlation functions calculated for an emitter switching between different brightness in these three cases. For the slow modulation case, in addition to the features of each distribution (taken as bunching at short times in the present example), we find strong intensity fluctuations at long times, which appear clearly in the correlation function. We should stress again that this information cannot be obtained from the average delay distribution, which is insensitive to the correlations between 1-type and 2-type intervals.

3.4 Variations of the detection quantum yield

We now assume that the detection yields η_1, η_2 are different for photons emitted in 1- and 2-states, and differ from unity. This may result from a variation in emission yield, spectrum, polarization, etc.

Distribution of consecutive pairs

We have to consider the probabilities of all different ways of detecting the next photon at time τ once one has been detected at $t = 0$. If only 1-type intervals occur in this interval, the Laplace transform of the delay distribution is

$$\chi_1 = \frac{c_1}{1 - (1 - \epsilon_1)(1 - \eta_1)c_1} \, .$$

Note the resemblance with Equation 3.3 (Single distribution of delays and non-unity detection yield: factor $1 - \eta$.) and Equation 3.5 (Two distributions of delays and unity detection yield: factor $1 - \epsilon$.). Taking all the combinations of 1- and 2-times between 0 and τ, we obtain the total delay distribution[1]:

$$\chi = \frac{w_1(\chi_1\eta_1 + \chi_1(1 - \eta_1)\epsilon_1\chi_2\eta_2) + w_2(\chi_2\eta_2 + \chi_2(1 - \eta_2)\epsilon_2\chi_1\eta_1)}{1 - \epsilon_1\epsilon_2(1 - \eta_1)(1 - \eta_2)\chi_1\chi_2} \, ,$$

where the weighting factors are now corrected for the detection yields:

$$w_1 = \frac{\eta_1\epsilon_2}{\eta_1\epsilon_2 + \eta_2\epsilon_1} \, .$$

Correlation function

The calculation proceeds the same way as for the consecutive pairs, only now we don't know whether the intermediate photons have been detected or not. Therefore, all factors $(1 - \eta)$ in the χ's are replaced by 1. Introducing again the Laplace tranforms of correlation functions:

$$\gamma_1 = \frac{c_1}{1 - (1 - \epsilon_1)c_1} \, ,$$

we obtain for the total correlation function

$$\gamma = \frac{w_1(\eta_1 g_1 + g_1\epsilon_1 g_2\eta_2) + w_2(\eta_2 g_2 + g_2\epsilon_2 g_1\eta_1)}{1 - \epsilon_1\epsilon_2 g_1 g_2} \, .$$

[1] This result was published as equation (8) in Reference [102]. The factors $(1 - \eta_1)$ and $(1 - \eta_2)$ were then omitted by mistake.

In the special case where $\eta_1 = \eta_2 = \eta$, we of course recover the g function of Section 3.3 (Equation 3.6), multiplied by η. We find again that the normalized correlation function is invariable under a global change of detection quantum yield (see Section 3.3).

3.5 Random telegraph

An important special case is that of a signal randomly switching between high and low detection yields, which we will represent as on- and off-times, respectively. We suppose that the detection rate is very high during the on-times, so that the signal has negligible shot noise and is practically constant, and that it is nil during the off-times. We are interested in the long-term correlation function, which may not be single-exponential. We are therefore looking for the correlation function of a random telegraph, with alternating periods of signals 0 and 1 (see Figure 3.6). Note that here, on- and off-times are defined unambiguously, and are independent of experimental quantities such as photon noise, quantum yield, and background.

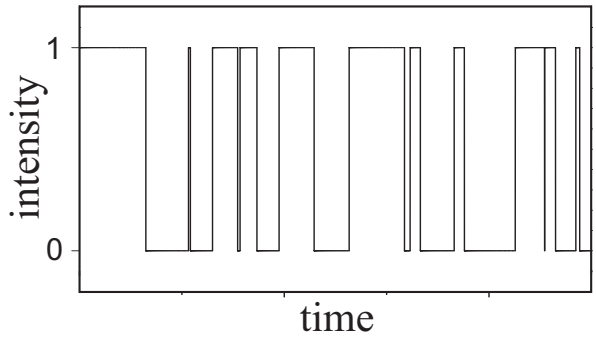

Figure 3.6: Schematic time variations of the signal of a random telegraph switching between on- and off-states.

Let us assume a fluctuating signal $S(t)$ randomly taking values 1 or 0 (Figure 3.6), and let us introduce the distributions $P_I(\tau)$ of the on-times and $P_O(\tau)$ of the off-times, which again are not necessarily single-exponential, and have Laplace transforms $p_I(s)$ and $p_O(s)$. Assuming them to exist, we define average durations of on- and off-times by

$$T_I = \int_0^\infty \tau P_I d\tau \qquad \text{and} \qquad T_O = \int_0^\infty \tau P_O d\tau \; .$$

If N_I and N_O are the average number of on- and off-periods during some long time interval, the average signal writes:

$$\langle S(t)\rangle = \frac{N_I T_I}{N_I T_I + N_O T_O} \, .$$

We define, as in Section 3.3, two probabilities: ϵ_I that an on-time is followed by an off-time, and ϵ_O that an off-time is followed by an on-time. We can then derive the average number of on- and off-times in a row, and therefore the average signal:

$$\langle S(t)\rangle = \frac{\epsilon_O T_I}{\epsilon_O T_I + \epsilon_I T_O} \, .$$

The probability density that any on-time starts at a given time is just given by the total number of on-times divided by the total duration:

$$D_I = \left(T_I + \frac{\epsilon_1}{\epsilon_O} T_O \right)^{-1} \, .$$

We still need two auxiliary probabilities, calculated as in Section 3.2: The probability that an on-time lasts longer than τ,

$$P_I^{'} = \int_0^\infty P_I(\tau + \alpha) d\alpha \, ,$$

and the probability *density* that an on-time which started earlier than time zero stops at time τ, which can be shown to be:

$$P_I^{''}(\tau) = P_I^{'}(\tau)/T_I \, .$$

We can now write the correlation function as a sum of probabilities for the signal of being "on" at time τ, knowing that it was "on" at time 0. The first term is the probability that it remained "on" all the time, the second one, that a first on-time finished between 0 and τ, and that a second on-time, immediately following the first one, lasted longer than τ, the third term that there is one off-time between these two on-times, etc. By working out and re-summing all the possible combinations, and replacing convolutions by products of Laplace transforms of the functions involved, we derive the following expression for the Laplace transform of the correlation function $G(\tau)$:

$$g(s) = \frac{1}{s} - \frac{\epsilon_I}{s^2 T_I} \times \frac{(1-p_I)(1-p_O)}{1-(1-\epsilon_I)p_I - (1-\epsilon_O)p_O + (1-\epsilon_I-\epsilon_O)p_I p_O} \, . \quad (3.7)$$

This expression may be rewritten for the special cases of Markovian random jumps between on- and off-times ($\epsilon_I + \epsilon_O = 1$), and for alternating on- and off-times ($\epsilon_I = \epsilon_O = 1$). Hereafter, we examine three important cases of alternating on- and off-times.

Single-exponential distributions of on- and off-times with rates (or inverse average times) a_I and a_O

The correlation function of the signal can be written

$$G(t) = \frac{a_O}{a_O + a_I}\left[1 + \frac{a_I}{a_O} exp[-(a_O + a_I)t]\right] ,$$

a well-known result for the correlation function of a single emitter coupled to a two-level system [72, 103].

Single-exponential distribution of on-times only, with rate a_I

This case may represent a single-exponential transfer to a distribution of traps, with complex non-exponential recovery kinetics arising from a distribution of recovery times represented by P_O. The Laplace transform of the correlation function simply writes:

$$g(s) = [s + a_I(1 - p_O)]^{-1} . \tag{3.8}$$

In the special case where the on-times are extremely short, this expression yields back Reynaud's formula [Equation 3.1], with the distribution $P_O(\tau)$ of waiting times, and with an initial delta-function contribution from the auto-correlation of the short on-times.

Power-law distributions

Here, we consider the case of broad, power-law distributions of off- and/or on-times. Such distributions have been found experimentally in the blinking of semiconductor nanocrystals [85, 86]. A power-law distribution could result from a waiting-time distribution to a population of traps at various distances from the nanocrystal. True power-law distributions of times are difficult to treat because of their infinite average value (first moment). The signal is non-stationary on all timescales [104,105], violating our second assumption (Section 3.1). Our treatment thus does not apply to true power laws. Jung et al. [106] handle the long time tails found in many systems within the formalism of Lévy walks. Here, to describe kinetics at times shorter than the experimental time,

we assume that the distribution follows a power law only within a certain range of times, and that it decreases much faster outside this range. We therefore introduce cutoffs for long and/or for short times, and we suppose that all experiments last much longer than the longest cutoff time, so that standard averages can again be defined. The assumption is then that experimental results on a long timescale are not too far from those of our analysis, if we take the experimental timescale as cutoff.

A power-law distribution $P(\tau)$ with exponent m requires cutoffs θ and Θ, $\theta \ll \Theta$: $P(\tau) = A\tau^{-m}$ for $\theta < \tau < \Theta$.

For $m > 1$, the usual case, the normalization factor writes:

$$A = (m-1)\theta^{m-1} .$$

The Laplace transform of this distribution is an incomplete gamma function:

$$p(s) = \int_{\theta}^{\Theta} A\tau^{-m} e^{-s\tau} d\tau ,$$

but we will simplify it by considering that the scale of times involved is very broad, and by replacing the exponential in the integral by 0 for $\tau > 1/s$ and by 1 for $\tau < 1/s$. We thus obtain

$$p(s) \approx 1 - (\theta s)^{m-1} .$$

In the case of short, single-exponentially distributed on-times, we obtain a normalized correlation function of the form:

$$\tilde{g}^{(2)}(s) = T_O(\theta s)^{1-m} .$$

By taking the inverse Laplace transform of the power law, we obtain a power-law correlation function with exponent $m-2$ (Γ is the usual gamma function):

$$g^{(2)}(\tau) = T_O \frac{\theta^{1-m}}{\Gamma(m-1)} \tau^{m-2} . \tag{3.9}$$

A physically meaningful correlation function should decrease with time, which occurs only for $m < 2$, in the range of exponents $1 < m < 2$ of experimental observations. Such power-law correlation functions have been observed experimentally for single uncapped nanocrystals [107]. Figure 3.7 shows the correlation function and the delay distribution in the special case of exponent

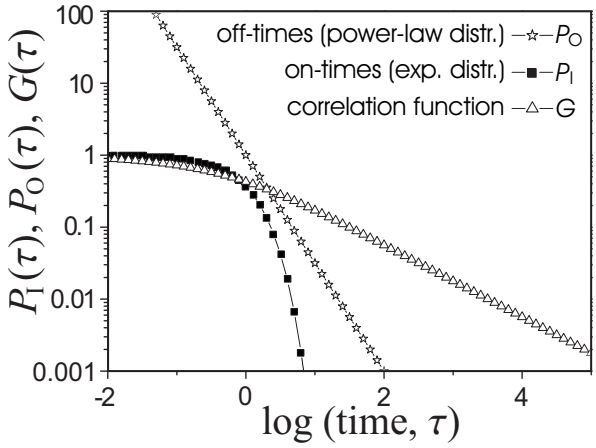

Figure 3.7: On-(squares) and off- (stars) times distributions and correlation function (triangles) of a random telegraph in the case of a single-exponential on-time distribution, and of a power-law off-time distribution with exponent $m = 1.5$. The correlation function is given by the inverse Laplace transform of Equation 3.8, which can be calculated analytically in the present case. It decreases like the inverse square-root of time (i.e. with power $m - 2$) for long times. The distribution of off-times has been shifted vertically for clarity.

$m = 1.5$, where the inverse Laplace transformation can be performed analytically[2]. The correlation function indeed decreases like the inverse square-root of time.

In the case where both the on- and the off-times distributions are power laws with exponents m_I and m_O, a similar analysis leads to the result:

$$g(s) = \frac{1}{s} - \frac{1}{s^2 T_I} \frac{1}{(\theta s)^{1-m_I} + (\theta s)^{1-m_O} - 1} \, .$$

The largest exponent gives the leading term in the denominator. Supposing m_I is larger, we can approximate the non-normalized correlation function by

$$G(\tau) \approx 1 - \frac{1}{T_I} \frac{\theta^{m_I - 1}}{\Gamma(3 - m_I)} \tau^{2 - m_I} \, ,$$

which is a sum of a constant and a power law with the opposite exponent of the previous case, and yields a much slower time dependence of the correlation

[2]For a single-exponential on-time distribution and a power-law distribution of off-times, Equation 3.8 gives for the Laplace transform of the correlation function $g(s) = (s + \lambda\sqrt{s})^{-1}$, which can be inverse Laplace-transformed analytically to give $G(t) = e^{\lambda^2 t}\mathrm{erfc}(\lambda\sqrt{t})$. This function decreases like $t^{1/2}$ for long times.

function than Equation 3.9. This is because there are long on-times, which lead to a nearly flat correlation for short times. Such flat correlation functions have been observed experimentally for capped quantum dots [99].

3.6 Conclusions

We have presented a general formalism relating the distribution of delays between consecutive photons to the second-order correlation function, including the case of non-exponential distributions. Our basic assumption is that each new photon is drawn in a Markovian process, with no memory of the preceding one. We have then extended our analysis to the case where the system can choose from two distributions of waiting times, with possible correlation between them (but not between photons within each distribution), and we have examined the influences of background and detection efficiency. We have considered in particular the case of power-law distributions, which have been observed in the blinking of nanocrystals, and found that correlation functions have simple expressions which can be related to published experimental data. We have shown that, although a long-term correlation of bright or dark intervals obviously fails to show up in the average distribution of delays, it does appear in the intensity correlation function at long times. The distribution of delays does not give access to these long times, not only because it decays exponentially for long times, but also for a more fundamental reason, namely because it is an average quantity. Other quantities than intensities, for example lifetimes, can be correlated in time [74, 91], and correlation functions of higher order than two can be measured and calculated [89, 90]. The rate coefficients can even fluctuate in arbitrary ways, and a general method to evaluate the effect of these fluctuations has been proposed recently [108]. It would be very desirable to encompass all those different approaches of the photon statistics in single-molecule fluorescence in a single compact formalism. This, however, exceeds the scope of the present work.

4 A model for nanocrystal blinking

abstract – We assign the blinking of semiconductor nanocrystals (NC's) to electron tunneling towards a uniform spatial distribution of traps. This model naturally explains the power-law distribution of off-times, and the power-law correlation function we measured on uncapped CdS NC's. This correlation function demonstrates that the power-law distributions are valid for times as short as microseconds. Capped NC's, on the other hand, present extended on-times leading to a radically different correlation function. This is readily described in our model by involving two different, dark and bright, charged states. Coulomb blockade prevents further ionization of the charged NC, thus giving rise to long, power-law distributed on- and off-times.

4.1 Introduction

Nanocrystals of II-VI semiconductors (e.g. CdS or CdSe), with a diameter of a few nanometers, present original optical properties due to quantum exciton confinement [48, 109]. In addition to their use as model systems for quantum optics and solid state physics [66, 98], single nanocrystals (NC's, often called quantum dots) are attracting much attention because of their potential use as luminescent probes in molecular biology [33, 36]. To improve their emission properties, one often protects them with 4 to 8 monolayers of a semiconductor with a higher band gap, for example ZnS [11,110] and an organic layer (capped NC's), or with an organic layer only (uncapped NC's). Under steady laser illumination, the photoluminescence of single NC's displays strong fluctuations [12], with long dark periods or off-times. This phenomenon called blinking is a hallmark of single fluorescent nano-objects [68]. It limits the brightness and visibility of NC's, and thus their potential applications. The mechanism of blinking is still an open problem, whose understanding may open new paths to improve luminescent nanoprobes.

We investigated the blinking of single uncapped CdS NC's and compared the results to data of capped NC's. We propose a model that describes all observations in a single framework. Numerical simulations are performed to make a good comparison between experiments and this model possible. An important feature of this model is the ability to explain the (counterintuitive) power-law distribution of on-times of capped NC's. It also gives an answer to the second main question: "How can a capping layer (shell) cause the statistical difference between capped and uncapped NC's?"

It is important to stress here the difference between blinking and bleaching. Blinking is a reversible process that does not limit the observational time, as the nano-object comes back to the fluorescing state. Bleaching on the other hand is an irreversible process, possibly due to a photochemical process, that determines the lifetime of the nano-object. One of the advantages of NC's as luminescent labels is their outstanding stability against photo degradation compared to conventional organic labels.

4.2 Acquisition and analysis

The most direct way to evaluate blinking is to record the luminescence intensity under continuous wave (cw) excitation as a function of time. By use of a pre-defined threshold, bright and dark periods can be determined. A period during which the luminescence is higher or lower than this threshold is called

an on- or off-time respectively. The next step is to make a histogram of the duration of either the on- or the off-times and measure this distribution. For a normal distribution the best fit to such a histogram is a single exponential function. If the data in such a histogram can be fit with a power law, it is called a power-law distribution for short. In this way, researchers have been able to obtain a wealth of experimental results on blinking of capped NC's [85, 86]. This method has several disadvantages though.

An alternative method to probe the dynamics of fluorescence intermittency is the auto-correlation function, defined for a time-dependent intensity $I(t)$ by

$$g^{(2)}(\tau) = \frac{\langle I(t)I(t+\tau)\rangle}{\langle I(t)\rangle^2} \,.$$

This function keeps track of all intensity fluctuations over a long acquisition time [93]. Whereas the on-time and off-time distributions are sensitive to detection yield and background, the normalized $g^{(2)}(\tau)$ is insensitive to detection yield, and only its overall contrast is reduced by background. (See Sections 3.2 and 3.2.) Furthermore, in contrast to measuring distributions of on- and off-times, measuring a correlation function does not require a threshold (an arbitrary, non-physical, parameter). In case of noise or if the intensity varies in a more complicated way than just alternating between strong and no luminescence, defining a threshold is hard and subjective. A fundamental advantage of a correlation function measurement over measurements of distributions is the higher time-resolution. The difference is typically a factor 1000, as in this example. If the luminescence intensity is in the order of 1000 counts per second, the time-resolution at which a trace can be recorded is at least a few milliseconds. The time-resolution of the correlation function is $\propto n\tau^2/T$. With the number of correlation events $n \sim 10^3$, the average delay time $\tau \sim 10^{-3}$ s and the acquisition time $T \sim 10^3$ s, the time-resolution is in the order of microseconds. Only in this way can one address the features in the important time regime of microseconds to milliseconds. Measured correlation functions are therefore reliable and particularly useful in comparing blinking data to theoretical models.

In order to compare the autocorrelation function with on- and off-time distributions, we derived a mathematical relation between the two. The present problem is an application of the work in Section 3.5. We consider a Markovian random telegraph whose on- and off-periods deterministically succeed one another, but without any memory of former on- and off-times. We have related $g^{(2)}(\tau)$ to the distributions $P_I(\tau)$ of on-times and $P_O(\tau)$ of off-times by expanding the probability of a photon pair as a series of probabilities of independent events occurring between $t = 0$ and $t = \tau$. The Laplace transform

$\tilde{g}^{(2)}(s)$ of $g^{(2)}(\tau)$ is related to those of the on- and off-time distributions, $p_I(s)$ and $p_O(s)$ respectively, by

$$\tilde{g}^{(2)}(s) = \left(1 + \frac{T_O}{T_I}\right) \frac{1}{s} \left(1 - \frac{(1-p_I)(1-p_O)}{sT_I(1-p_I p_O)}\right) , \tag{4.1}$$

where T_I (T_O) is the average on-time (off-time), supposed to be definable. This result is in fact the same as Equation 3.7 with $\epsilon_I = \epsilon_O = 1$ and normalized by the average intensity. For power-law distributions, this definition requires cutoffs at short or long timescales. [1] For the important special case of our uncapped NC's, when the on-times follow a single-exponential distribution $P_I(\tau) = a\mathrm{e}^{-a\tau}$ with an average on-time $T_I = a^{-1}$, Equation 4.1 becomes

$$\tilde{g}^{(2)}(s) = \frac{1 + aT_O}{s + a(1-p_O)} . \tag{4.2}$$

For off-times distributed according to a power law,

$$P_O(\tau) \propto \tau^{-m} , \tag{4.3}$$

the Laplace transform varies as $p_O(s) \approx 1-(\theta s)^{m-1}$, where θ is the shortest off-time (see Section 3.5). Equation 4.2 then shows that the correlation function is itself a power law at long times, varying as τ^{m-2} (see Equation 3.9):

$$g^{(2)}(\tau) \propto \tau^{m-2} . \tag{4.4}$$

4.3 Experiment and results

We investigated the blinking of single uncapped CdS nanocrystals. A solution of demineralized water with 0.5 % (w/w) polyvinylalcohol (MW 125,000) and 5×10^{-11}M CdS particles (5 nm in diameter, prepared in the group of Prof.dr. A. Meijerink at Utrecht University) was spin-cast onto a substrate of fused silica to obtain a film with an estimated thickness of less than 1 micron. The luminescence was measured with a home-built beam-scanning confocal microscope at 1.5 K, exciting with the 457.9 nm line of an argon-ion laser. The maximum count rate of a few thousands per second gave us a time-resolution of 10 ms for the luminescence intensity trace and about 2 μs for the correlation function.

As Figure 4.1(a) shows, the time traces of luminescence intensity display very strong blinking. Their appearance is self-similar on various timescales.

[1] There is some evidence that the power-law distributions have intrinsic lower and upper bounds [111].

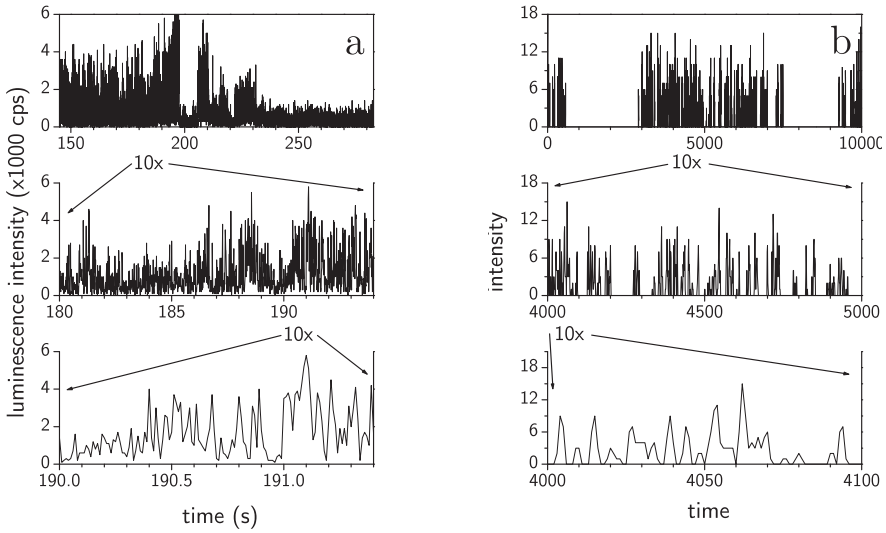

Figure 4.1: (a) Luminescence intensity trace of a single uncapped CdS nanocrystal, showing only short on-times at all timescales. (b) Simulated luminescence intensity trace of a single uncapped nanocrystal with parameter $m = 1.7$.

The corresponding distributions of the on- and off-times are shown in Figure 4.2(a). The distribution of off-times follows an inverse power law with exponent $m = 1.7 \pm 0.1$, whereas the distribution of on-times decays much faster and can be fitted with a single exponential function. The intensity correlation function of Figure 4.2(b) is a power law of time, with an exponent of about -0.3. According to Equation 4.4 this is in good agreement with the exponent of the off-time distribution: $m - 2 = 1.7 - 2 = -0.3$. This correlation function is the only measurement on NC blinking with a time-resolution of 2 μs. It demonstrates the the power-law distributions are still valid at these short times.

In a very similar way experiments are performed on capped NC's by Kuno *et al* [85] and Shimizu *et al* [86]. A striking observation in these studies is that both on-time and off-time distributions follow an inverse power law. Whereas power-law behavior of the off-times can easily be explained by a wide distribution of trapping potentials for a charge carrier that is ejected by an Auger process, the power-law behavior of the on-time distributions appears to be inconsistent with all proposed physical models. Models based on a single emitting state have the difficulty that a finite probability to leave this state naturally leads to a single exponential distribution of on-times. This problem

will be addressed in Section 4.5, where we explain the results of these studies with our model for capped NC's. But first we consider uncapped NC's only.

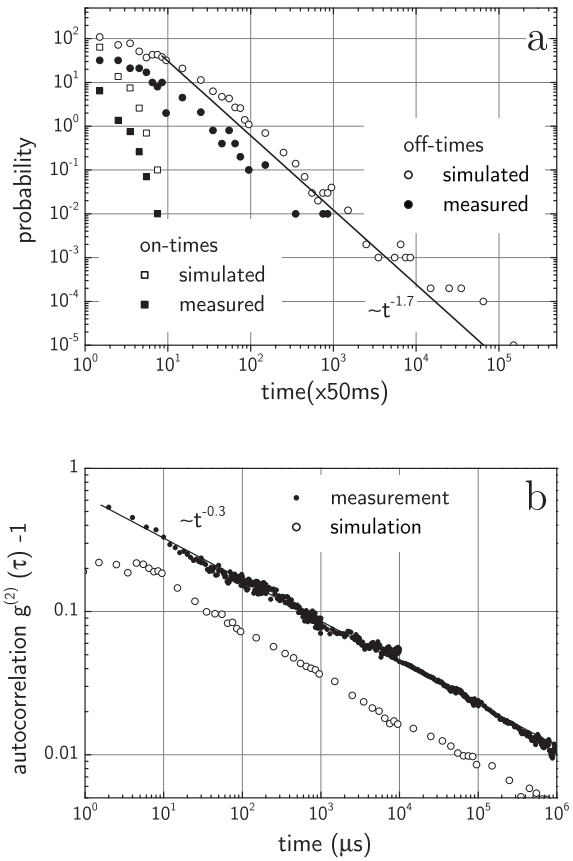

Figure 4.2: (a) Distributions of on- and off-times for a single CdS NC (filled symbols) and a simulated uncapped NC (open symbols). The off-time distributions (circles) follow a power law with exponent $m = 1.7$ and the on-times (squares; probabilities multiplied by 0.1 for clarity) have a single exponential distribution. (b) The corresponding correlation functions (filled symbols for experiment and open symbols for simulation) decay as a power law over 6 decades of time, with an exponent of about -0.3 (solid line).

4.4 Model for uncapped nanocrystals

In order to explain our observations on uncapped NC's, we propose a simple model, following the ideas of Efros and Rosen [112]. Upon excitation an exciton is created in the core of the NC, which normally recombines under emission of a photon. During this cycle the NC has no net charge and we call this the neutral state. There is a finite probability, however, that the electron tunnels from the excited NC to a trap in the surrounding matrix. (The effective mass of the electron is smaller than that of the hole and the electron is therefore more likely to tunnel: $m_e^* = 0.22$, $m_h^* = 0.70$ for the wurtzite structure and $m_e^* = 0.14$, $m_h^* = 0.51$ for the zincblende structure [113]. Experiments based on electrostatic force microscopy show indeed that ionized NC's are always positively charged [114, 115]. Although the effective mass approximation is commonly used in treatises on NC's, this might not always be justified. This will be discussed in Section 6.6.) The NC, now charged with the residual hole of the exciton, still absorbs, but is dark because of fast Auger recombination, i.e. charge-induced non-radiative relaxation of the exciton energy. The dark period ends, and the NC becomes bright again when the trapped electron hops back and recombines with the hole. To account for the broad distribution of off-times, we do not postulate a single trap, but a uniform distribution of traps in the matrix around the NC. Assuming spherical symmetry, the exciton wavefunction outside the dot decreases like $r^{-1}\mathrm{e}^{-\alpha r/2}$. Since the radial density of traps varies as r^2, the trapping probability decreases exponentially with distance r, just as in a one-dimensional model with a constant linear density of traps. The probability density to tunnel to a trap at distance r from the NC surface is therefore $p(r) = \alpha \mathrm{e}^{-\alpha r}$. The recovery rate, describing the back-tunneling rate of the trapped electron to the ionized NC also varies exponentially with distance r, like $\mathrm{e}^{-\beta r}$, but with a different decay length[2]. The distribution of off-times can be obtained by integrating over the distance r and taking into account that for every trap the distribution of times is an exponential function again. This calculation simplifies significantly by regarding a single rate for every trap-distance, leading to a simple relation between the average recovery time T and distance r: $T = T_0 \mathrm{e}^{\beta r}$. The probability density

[2] While we assumed the wavefunction of the electron in the trap to be hydrogen-like, we took that of the exciton in the core of the NC to be that of a neutral particle in a spherical box with a constant potential (muffin-tin potential). Upon trapping, the electron wavefunction also feels the Coulomb potential of the hole left on the NC. A different shape of the trapping dependence with distance would lead to slight deviations from power laws.

of T is now[3]:

$$\Pi(T) = \frac{\alpha}{\beta}\frac{1}{T}\left(\frac{T_0}{T}\right)^{\alpha/\beta} \propto T^{-m} \quad , \tag{4.5}$$

$$m = 1 + \frac{\alpha}{\beta} \, , \tag{4.6}$$

i.e. an inverse power law with exponent $m = 1 + \alpha/\beta$. Because this power-law distribution is much broader than the single-exponential Poisson distribution of off-times for a given average recovery time T for a distance r, we may approximate the overall distribution of off-times with the same power law.

Relating the decay coefficients α and β to the tunneling barriers, we obtain

$$\frac{\alpha}{\beta} = \sqrt{\frac{V_{\text{matrix}} - V_{\text{e}}}{V_{\text{matrix}} - V_{\text{trap}}}} \, , \tag{4.7}$$

where V_{matrix}, V_{e} and V_{trap} are the electron's potentials in the matrix, in the excited state of the NC, and in the traps, respectively (see Figure 4.3). The trap must be deeper than the excited state. Tunneling back to the NC is harder than tunneling to the trap, as the corresponding barrier is higher. In other words $\alpha < \beta$. Therefore, Equation 4.7 naturally explains why the exponent m lies between 1 and 2, just as we found for uncapped NC's and has been observed for capped NC's as well [85, 86, 116, 117]. Since the process is electron tunneling, m does not depend on temperature, as was observed in Reference [86]. Note that this model predicts a single-exponential distribution of on-times.

The results of simulations based on this model with $m = 1.7$ are shown in Figures 4.1(b) and 4.2. The luminescence trace in Figure 4.1(b) is self-similar on a wide range of timescales (as soon as these are much longer than the minimal hopping time to the closest trap) and resembles the trace of a single CdS NC in Figure 4.1(a). The distributions of on- and off-times are shown in Figure 4.2(a), together with the experimental findings. The agreement between experiment and simulation is good. The on-time distribution is not broader than a single exponential function, whereas the off-time distribution follows a power law with exponent $m = 1.7$. As can be seen in Figure 4.2(b), the correlation function, a power law with exponent -0.3, agrees very well with the experimental correlation function and confirms the relation between the exponents of Equations 4.3 and 4.4 again.

[3]The exact calculation leads to $\Pi(T) = \frac{\alpha}{\beta} T_0^{\alpha/\beta} T^{-m} \Gamma(m)$, were $\Gamma(m)$ is the Gamma function. For all relevant values of m ($1 < m < 2$), $\Gamma(m) \approx 1$.

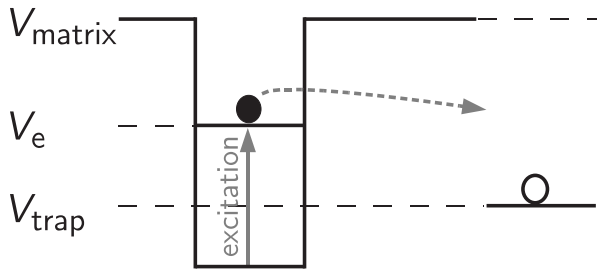

Figure 4.3: Relative potentials of the electron in the matrix, in the excited state, and in the trap. After excitation with a photon, the potential of the electron is higher than the potential of the electron in the trap. The electron can tunnel to the trap through the barrier $V_{matrix} - V_e$. The barrier for back-tunneling, $V_{matrix} - V_{trap}$, is higher. The ratio of these barrier heights is α/β.

The intensity traces were simulated in a personal computer by picking an exponentially distributed random time for each elementary process having a well-defined single rate (photon emission, electron trapping to a given distance, back-tunneling). We thus generated a series of detected counts similar to an experimental trace, which was further used as input for the correlation function and on/off-time counting. See Chapter 5 for more details on the simulations. The influence of, for example, the threshold and the total detection yield of the setup are discussed in this chapter, too. Also different values of the exponent m (which could correspond to various matrices or trap depths) are discussed.

4.5 Model for capped nanocrystals

We now consider the blinking of capped NC's, for which both the on- and off-time distributions have been found to obey power laws. See Refs. [85, 86] and Chapter 6. The difference in on-time statistics between uncapped and capped NC's appears in the intensity traces as much longer "average" on-times for capped NC's, as is clearly shown in Ref. [118]. This yields a completely different correlation function, too. The long on-times are heavily weighted in the average, giving rise to a nearly flat correlation. A steep decrease at times in the order of the integration time is caused by the limited integration time [99].

Quantitatively, power-law distributions of both on- and off-times, with n (defined as $P_I(\tau) \propto \tau^{-n}$) the larger exponent of the two[4], means that Equation

[4]If $n \approx m$, n in Equation 4.8 is replaced by a value close to the average value of n and m.

4.1 becomes:

$$g^{(2)}(\tau) = A(1 - B\tau^{2-n}) \,, \tag{4.8}$$

where A and B are two constants. (See also Section 3.5.) In accordance with experiments, this dependence indeed appears flat on a logarithmic timescale [99]. But in the present version of our model for uncapped NC's, the ionization rate of the NC (and therefore its probability to go to an off-state after each excitation) is always finite, leading to a single-exponential distribution of on-times. In the simulations even extreme values for background and quantum yield could not bias the on-time distribution towards a power law. The model must therefore be extended to describe the long on-times observed in the blinking of capped dots.

In order to allow for long on-times, a bright, long-living, charged state is introduced. As other blinking models postulate, a charged NC should not emit. This assumption, however, holds only as far as the residual hole is located in the core (charged-core state). If the hole is trapped further away, for example in the capping shell, or on the shell surface, the radiative recombination yield of a new exciton in the core of the NC may still be significant during this charged-shell state, because there is little overlap between the wavefunctions of the trapped hole and the exciton in the core. The exciton wavefunction decreases exponentially in the shell [110, 119, 120] and the wavefunction of the trapped hole is localized [46]. The idea that also charged NC's can emit is not completely new. NC's on a rough gold surface have two emitting states, of which the emission can spectrally be resolved. One of these bright states is probably a charged state [121]. The crystalline quality of the capping layer is believed to be so poor (Possibly because the lattice mismatch between CdSe and ZnS, the most common core and shell materials respectively, is as large as 12% [11] and the capping layer is normally only a few monolayers thick.) that even oxidation of the underlying core is possible [122]. This gives numerous opportunities to trap a hole. Moreover, the organic layer (e.g. trioctylphosphine oxide, TOPO) passivates the dangling bonds of Zn-atoms and therefore removes the surface electron traps, but it cannot remove the hole traps (which are dangling bonds of S-atoms) [46, 80].

The lifetime of this charged-shell state depends on the time that the electron stays in the far-away trap, just like the lifetime of the charged-core state. This naturally explains why the on- and off-time distributions are so similar. Long on-times are only possible if the charged-shell state is stable under repeated excitation. Second order NC ionization to far-away traps must be prevented. We propose Coulomb blockade as the ionization-stopping mechanism. Because

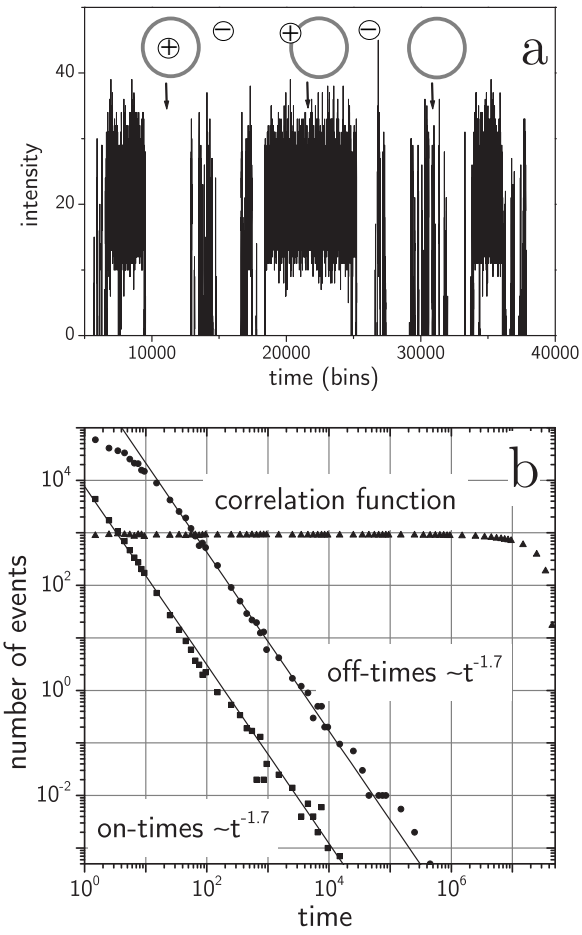

Figure 4.4: (a) Simulated luminescence intensity trace for a capped NC. Three different states can be distinguished in the trace: "off" (charged-core state), "on" (charged-shell state), and "blinking" (neutral state). (b) The on-time and off-time distributions are both inverse power laws of time with exponents 1.7. The distribution of off-times has been shifted upward by a factor of 50 for clarity's sake. Note that the correlation function is now much flatter than that of the uncapped NC (see Figure. 4.2(b) and compare with Ref. [99]).

the trapped hole's Coulomb potential varies slowly with distance, it still, even though it is not situated in the core, effectively prevents second order ionization. For a small enough NC, once one electron has been transferred to a far-away trap, another ionization would cost more electrostatic energy than the exciting photon can provide. Indeed, elegant experiments [114] have re-

cently shown that blinking is related to charge rearrangements via electron transfer, and that individual NC's accommodate at most one or two positive charges (or holes).

Depending on the distance of the trapped hole to the core, we may expect a broad range of luminescence levels. Neuhauser *et al* [123] presented a similar argument in their discussion of the correlation between spectral diffusion and blinking of NC's. In order to keep this model simple, we consider only two possibilities to trap the residual hole: either in the shell with probability ε, giving an extended on-time, or in the core with probability $(1 - \varepsilon)$, giving an extended off-time. These extended on- and off-times last until the far-away electron comes back.

Simulations of intensity traces based on this new model with $\varepsilon = 0.2$ are shown in Figure 4.4. The trace of Figure 4.4(a) consists of a random juxtaposition of three modes of luminescence pertaining to the three possible states of the NC: – with a charged core, corresponding to an off-time, – with a charged shell, leading to steady emission, i.e. an "extended" on-time, – and neutral, corresponding to "true" on-times, too short to be resolved on the long timescale of this figure. In practice, because of limited experimental time-resolution, the neutral state is likely to appear as a "gray", blinking trace, similar to those shown by the simulations of Figure 4.1. Some experimental evidence for three states can be seen in the trace published in Reference [99]. Simulated distributions of on-times and off-times, as well as the correlation function are shown in Figure 4.4(b). The simulations agree very well with the published power-law distributions of on- and off-times. Although Expression 4.8 for the correlation function does not rigorously apply here (because it pertains to a deterministic instead of random succession of on- and off-times), its form agrees qualitatively with experiments [99] and with the simulation of Figure 4.4(b).

4.6 Discussion

Hole surface traps

Our model for capped NC's requires for an extended on-time (charged-shell state) the hole to remain trapped in, or at the surface of, the shell as long as the electron stays in the matrix. In the mean time many cycles of creation and recombination of excitons take place in the core of the NC. On the other hand, we assume that in the neutral state the electron has a finite probability to tunnel to the environment. Recent improvements in the description of confinement effects in semiconductor NC's confirm that the wavefunction of

the electron may spread out beyond the surface of the NC [49]. But if the electron (in the neutral state) can explore the surrounding of the NC, the electron wavefunction of the second exciton in the charged-shell state, has to have a finite overlap with the wavefunction of the localized hole at the surface (which is even closer by than the traps in the matrix). The probability that this electron recombines with the hole in the shell can than not be ignored. This paradox cannot be explained satisfactory by kinetics only. This "recombination in the shell" has to be a forbidden process in order to have a smaller probability than the process of electron tunneling into the matrix. In other words, the hole prefers to be in the shell, rather than in the core. (Note that this type of recombination, which brings the NC from a charged-shell state to a charged-core state, is equivalent to moving the hole from the shell to the core.) Maybe the ideas of Bawendi *et al*, illustrated in Figure 4.5, are the answer to this problem [124]: The highest occupied molecular orbital (HOMO) in the interior of the NC lies just (0.1 eV for CdSe) below the top of the bulk valence band. The surface state, based of dangling bonds of S–atoms, lies in the band gap if surface reconstruction is ignored. For CdSe NC's this surface state is calculated to lie about 50 meV above the top of the valence band [125]. It might thus be energetically favorable for the hole to move from the interior (HOMO) to the surface (trap).

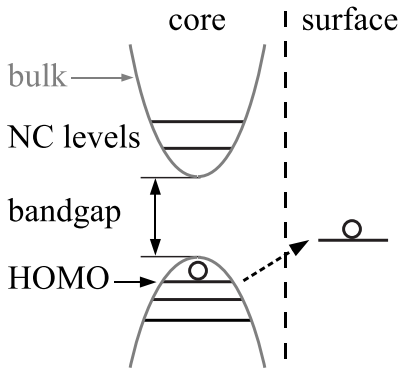

Figure 4.5: The highest occupied molecular orbital (HOMO) of CdSe NC's lies just below the top of the valence band of the bulk material. The energy levels of surface states fall in the band gap and are thus lower in energy than the HOMO. The hole could migrate to a surface state easily.

Experiments by Hohng and Ha [10] show how chemical modifications of the surface of CdSe/ZnS NC's can drastically change the blinking behavior. They showed that if small molecules (small enough to penetrate through the streptavidin coating) with thiol-groups reach the surface of the NC, the blinking

stops almost completely and the NC emits continuously. The slope of the off-time distribution didn't change, however. The change in blinking behavior was caused by a large increase of the on-times only. Our model could explain this unexpected observation as follows. If the thiol-group approaches the dangling bonds of surface S–atoms, an electron negative trap is created for the hole. This increases the chance of a charged-shell state and extended on-times dominate the luminescence time trace. Also Koberling *et al* demonstrated that the on-time statistics is much more sensitive to the atmosphere than the off-time statistics [118]. This agrees with our assumption that the wavefunction density of the relevant charge, i.e., the hole, is on average closer to the surface during an on-state (charged-shell state) than during an off-state (charged-core state).

It is interesting to note that for $ZnO/Zn(OH)_2$ nanocrystals the presence of hole traps in the capping layer has been demonstrated recently by electron paramagnetic resonance (EPR) measurements [126]. The presence of this acceptor was revealed by the observation of the EPR signal of a donor–acceptor pair when the donor is a shallow interstitial Li–atom. The acceptor has been identified as a Zn^{2+} vacancy at the interface between the ZnO core and the $Zn(OH)_2$ capping layer. It is suggested that one of its O^{2-} neighbors is replaced by an OH^- ligand of the $Zn(OH)_2$ capping layer, because of the observation of an ENDOR signal of ^1H in the EPR line of this acceptor. This substitution makes the Zn^{2+} vacancy a single acceptor and observable by EPR.

Power laws and (stretched) exponentials

One of the most appealing features of the model described above is its ability to explain in a natural way why some distributions follow an exponential function and others a power law function. The special relation between these two functions and their relevance for NC-blinking are discussed here.

i) We postulated a uniform distribution of traps in the surrounding matrix of the NC to account for the power-law distribution of off-times. In fact we used in this way a (large) sum of exponential functions (with different characteristic timescales) which is in good approximation a power law. In practice however, when the observable range is limited to only a few decades and in the presence of experimental noise, only a few exponential functions (with different weighting factors) are required to imitate a true power law. This is shown in Figure 4.6(a). Therefore, only a limited number of traps is required in this model. Variations in the depth of the traps in time, due to regular redistribution of charges in the surrounding of the NC [123], would

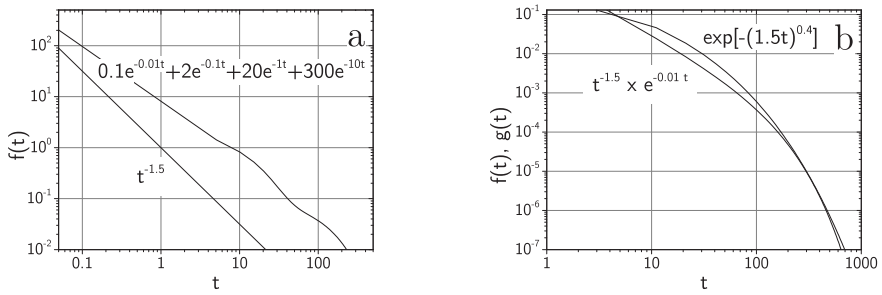

Figure 4.6: (a) A power law can be approximated by a sum of exponential functions if only a limited range is viewed. Here, only 4 exponential functions are required to resemble a power law over 3 decades. (b) Instead of a stretched exponential one could use a product of an exponential function and a power law. Plotted here: $f(t) = exp[(-1.5t)^{0.4}]$ and $g(t) = t^{-1.5} \times e^{-0.01t}$.

lead to an even better resemblance of a power-law distribution.

ii) Experimental data that resembles a power law at short times, but decays much faster, almost like an exponential function, at long times [86,116], is often fit with a Kohlrausch-Williams-Watts function, also known as the stretched exponential. But often there is no clear physical meaning for the "stretching factor", let alone an explanation for its value. A very similarly shaped function is obtained by the product of an exponential function and a power law. This is shown in Figure 4.6(b). One might consider to use this function instead of the stretched exponential in some cases. The next example shows how this product function suggests an alternative way to interpret some measured on-time distributions. Two independent physical processes, of which one causes a power law and the other one an exponential distribution, together give the correct overall shape of these on-time distributions in a natural way. All fitting parameters can be related to physical quantities. This product function, called "truncated power law" in economics [79], could also be relevant for other physical processes, as a good alternative for the stretched exponential.

The duration of long on-times in the charged-shell state is determined by the time that the electron remains trapped in the matrix. Due to a distribution of traps, the broad range of on-times is described by a power law. The recombination process described in Section 4.6 would be a completely independent process to terminate an on-time. This process of recombination in the shell has a finite probability to take place. Therefore, the distribution of on-times would follow an exponential function if this was the only way to end an on-time. If both processes would be relevant ways to terminate an on-time, would the histogram of on-times resemble the product of a power law and

an exponential function. This supposition is tested by simulations, of which the results are shown in Figure 4.7. Even a very small probability for this new recombination process to take place introduces a "truncation point" (the point where the function clearly starts to deviate from a power law) in the on-time distribution. Here, this probability ϕ is chosen to be three orders of magnitude smaller than the probability that an electron tunnels from a neutral dot to the surrounding, i.e. $\phi = 10^{-5}$. The shape of this distribution is in good agreement with the results of Shimizu *et al* [86]. Higher laser intensity or temperature leads to a shift of the truncation point to shorter times, because it causes more opportunities to recombine (more excitations are created per unit of time) or more randomness, respectively. This idea has recently been confirmed by successfully fitting experimentally obtained distributions of on-times with this product function. The average on-time, which is defined in case the power-law distributions have both upper and lower bounds, appeared as the parameter in the exponential function [111]. The distribution of off-times is not affected by this process.

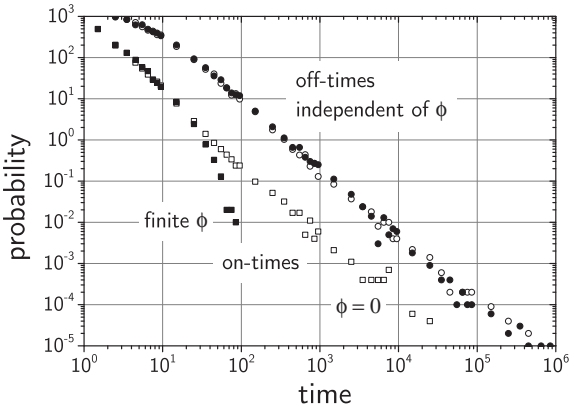

Figure 4.7: On- and off-time distributions in the case of a finite probability ϕ of recombination in the shell (closed symbols). The on-time distribution (squares) has an exponential tail or truncation point. The off-time distribution (circles) is independent of ϕ. The on- and off-time distributions for $\phi = 0$ are plotted for reference (open symbols).

Model predictions and possible tests

From this model a few predictions can be abstracted of which some can be tested experimentally.

Firstly, hole tunneling must be very unlikely or short-range, because the NC couldn't keep its positive charge very long under heavy laser illumination. It has been demonstrated by electrostatic force microscopy that very long living positively charged states exist [114]. Apparently, a position in the NC or on the surface is energetically favorable for the hole. The traps of Section 4.6 are a possible explanation. Moreover, the effective mass of the hole is much bigger than the effective mass of the electron [113] and increases even near the surface. The hole energy level spacing is about one order of magnitude smaller than that of the electron, resulting in a extremely fast relaxation to the top of the valence band [25, 127].

Further, Equation 4.7 indicates that blinking statistics and power-law exponents should depend on substrate material, and on doping with electron traps. Capping thickness and quality must be critical. The first proofs of the influence of surface chemistry are presented by Hohng [10]. Chapter 6 shows the first results of the experiments we performed to address this question.

Equation 4.7 also explains why all observed power laws have exponents valued between 1 and 2. Although this equation primarily deals with the distribution of off-times, it also holds for the on-time distribution of capped NC's. At long times (long compared to the "true" on-times of the neutral state), the on-time distribution (charged-shell state) is governed by the same distribution of traps that is responsible for the distribution of off-times (charged-core state).

Depending on the location of the hole, states with various luminescence yields could exist, i.e. with various luminescence intensities, lower than that of the "true" on-states of the neutral dot. Recent observations [128] of lifetime fluctuations correlated to changes in brightness in a single NC support this hypothesis.

Finally, our model suggests that the role of capping is not so much to prevent ionization, as was initially thought after the first experiments on uncapped NC's [12]. Ionization to far-away traps and very long off-times occur for both capped and uncapped NC's. We suggest that the main function of the capping layer is to keep the residual hole away from the emitting core by introducing possible trap sites, making long on-periods possible for capped dots.

4.7 Conclusions

Our model naturally accounts for most current observations of blinking in both uncapped ($\varepsilon = 0$) and capped nanocrystals ($\varepsilon \neq 0$), and provides a general frame for blinking kinetics. It deals with the most important questions

of semiconductor nanocrystal blinking; the power-law distribution of on-times for capped NC's, the role of the capping layer in the difference between capped and uncapped NC's, and the range of values of the power-law exponents. It is successfully tested against our experiments and those of several other investigators. Moreover, it shows how power-law distributions can arise from clear physical processes, down to the microsecond timescale. Even a "truncated" distribution could be described without introducing parameters that cannot directly be related to a physical process. Yet, the photophysics of real NC's, where charge rearrangements upon blinking cause spectral diffusion, is probably more complicated. We hope nevertheless that this model leads to a better understanding of blinking of NC's, and thereby to more efficient luminescent nanoprobes.

Acknowledgements

The author wants to thank Ageeth Bol and Prof.dr. Andries Meijerink from the Debye Institute (Utrecht University) for providing us with the CdS nanocrystals.

5 Simulations of the blinking behavior of individual nanocrystals

abstract – We simulated the streams of photons that are emitted by individual nanocrystals under continuous illumination, and compared the results to experimental data. These numerical simulations are based on the model described in Chapter 4, and demonstrate that this model could explain the experimental observations. For a reliable model it is important to consider luminescence time trace, distributions of on- and off-times, and the correlation function simultaneously. The influence of some experimental parameters (detection efficiency, threshold) is investigated explicitly.

5.1 Introduction

Simulations can be of great help to test a new model and to explain current experimental observations. A well-known method is to perform simulations based on the model and compare the results with experimental data. In doing so one can investigate the influence of individual parameters on the result to obtain a better understanding of the underlying physics and thus to improve the model.

This chapter describes simulations of the blinking behavior of single semiconductor nanocrystals. These simulations are based on the model described in Chapter 4. More specifically, we use the model for the capped nanocrystals (Section 4.5) and treat the uncapped nanocrystals as a special case in which the charged-shell state is not accessible ($\varepsilon = 0$). It will be shown that the luminescence time traces, distributions of on- and off-times, and correlation functions of both uncapped and capped NC's can be simulated satisfactorily. The influence of the major parameters is also demonstrated.

5.2 The model and its parameters

Based on the model described in Chapter 4, the stream of photons emitted by a nanocrystal under continuous illumination is simulated in a personal computer. Every state in the optical cycle has a fixed entering probability and the residence time is derived from appropriate distributions. The effect of the overall detection yield, threshold and bin time on the results are considered to allow a comparison with experimental data.

We consider first a system with only three electronic states: ground state G, excited state E and charged state C, see Figure 5.1. Relaxation from vibrational levels to the electronic states is much faster than the transitions discussed here and the vibronic levels are therefore ignored. Also stimulated emission is not taken into account because the NC is excited over the band gap. The laser is thus not in resonance with the G–E transition. The time that the NC spends in the ground state is randomly drawn from an exponential distribution (Poisson process). The inverse of the average value is the rate κ_{ge} of the transition to the excited state. The lifetime of the excited state is also randomly drawn from an exponential distribution. The inverse of the average lifetime equals the sum of the rate to the ground state, κ_{eg}, and the rate to the charged state, κ_{ec}. The transition rate from the charged state to the ground state, κ_{cg}, is defined in a similar way as κ_{ge}. This system can be described by

three rate equations:

$$\dot{p}_g = -\kappa_{ge}p_g + \kappa_{eg}p_e + \kappa_{cg}p_c$$
$$\dot{p}_e = -\kappa_{eg}p_e + \kappa_{ge}p_g - \kappa_{ec}p_e$$
$$\dot{p}_c = -\kappa_{cg}p_c + \kappa_{ec}p_e$$

with p_g, p_e and p_c the steady state populations of the ground, excited and charged states and κ_{ij} $(i, j = g,\ e \text{ or } c\ \&\ i \neq j)$ the rates of the transitions from state i to state j.

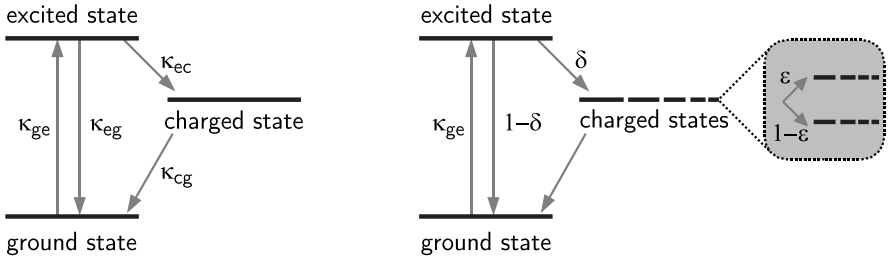

Figure 5.1: Energy-level diagrams of a simple three state system (left) and of a capped nanocrystal (right). The residence times of the simple system in one of its states are drawn from exponential distributions. Single transition rates can be defined. For a NC we use one rate, δ, to describe the probability to go to one of several charged states. The distribution of residence times of the electron in one of the traps outside the NC is described by a power law.

In the model for uncapped NC's the charged state is related to off-times. The NC becomes charged if the electron tunnels to a trap outside the NC, see Chapter 4. The time the electron resides in this trap determines the duration of the off-time. Finite probabilities to enter and leave a trap make up for an exponential distribution of residence times or off-times. Replacing the single trap of this simple three state model, including its single entrance rate κ_{ec} and its single exit rate κ_{cg}, by a distribution of traps, a power-law distribution of off-times is introduced. These N charged states, see Figure 5.1, have different entrance rates κ_{ec}^{j} and exit rates κ_{cg}^{j}, with $1 \leq j \leq \mathrm{N}$. The probability to tunnel to a trap decays exponentially with distance r; $p(r) = \alpha e^{-\alpha r}$. The probability to tunnel back to the NC depends on distance in a similar way; $p(r) = \beta e^{-\beta r}$. To simplify the calculations we replace the exponential distribution of residence times per trap by its average value. The residence time is then related to the distance of a trap to the NC by $T = T_0 e^{\beta r}$. The distribution of residence times is

$$\Pi(T) = \frac{\alpha}{\beta}\frac{1}{T}\left(\frac{T_0}{T}\right)^{\alpha/\beta} \propto T^{-1-\alpha/\beta}\,. \tag{5.1}$$

Because this power-law distribution is much broader than a single-exponential distribution of off-times per trap (or per distance r), we may approximate the overall distribution of residence times by the same power law. A single rate cannot be defined for the transition from the charged state(s) to the ground state, as the average value of this power-law distribution is not defined. Therefore the power-law distribution of residence times of Equation 5.1 is approximated by numerical simulations.

The residence time of an electron in a trap is calculated from the product of two factors. The first factor represents the exponential decay of the wave-function ($p(r) = \alpha e^{-\alpha r}$) and thus of the probability that the electron tunnels a distance r away. This is simulated by $-C \cdot log(x)$, with x randomly picked from the interval (0,1] and C a constant. The second factor represents the power-law distribution of trap times ($\Pi(T) \propto T^{-1-\alpha/\beta}$). It is simulated by $x^{-\alpha/\beta}$, with x again from the interval (0,1]. The constant C was used to scale the power law with respect to the average residence times in the ground and excited states. Although the average value of this power-law distribution is not defined, the constant C is a measure for the average value of the *observed* power-law distribution. The slope of the power-law distribution depends only on $\gamma \equiv \alpha/\beta$. The potential of the trap has to be lower than the potential of the excited state, thus $\alpha < \beta$ and $0 < \gamma < 1$.

As we consider the residence times of all traps as one distribution, we also have to consider only one entrance rate. The ratio of this transition rate from the excited state to the charged states, and the transition rate from the excited state to the ground state is $\delta = \sum_{j=1}^{N} \kappa_{ec}^{j} / \kappa_{eg}$. Information on the individual entrance rates κ_{cg}^{j} is obviously lost. The probability δ that the electron tunnels to a trap outside the NC is much lower than the probability $1 - \delta$ that it recombines with the hole, under emission of a photon. This means that $\delta \ll 1$, probably $\delta \approx 0.01$. This value is comparable to the intersystem crossing rate for some organic molecules. Although completely different physical processes are involved, similarities in the appearance of luminescence time traces suggest the same order of magnitude for the transition rates to the charged states and the triplet state. This value is also of the same order of magnitude as the ratio between ionization (tunneling) and recombination as estimated for the Auger excited state in silicon NC's [3].

The model can now easily be extended to describe capped NC's as well. In Chapter 4 we considered two different types of charged states. The first type is the charged-core state, from which no emission is possible, as the residual hole causes fast Auger recombination of the newly created exciton. The second type is the charged-shell state, in which the emission may proceed via a new

exciton. The cycle between ground and excited states is then restored, but with zero probability that the (second) electron tunnels out of the NC ($\delta = 0$), due to Coulomb blockade. We define a probability ε that a charged state is a charged-shell state, which is much smaller than the probability $1 - \varepsilon$ that a charged state is charged-core state. When a charged state ends (because the primary electron tunnels back) the NC relaxes to the ground state without emission of a photon. In order to simulate uncapped NC's the charged-shell state was excluded by setting $\varepsilon = 0$. Note that we did not redefine δ.

A few additional parameters are required from an experimental point of view. Every emitted photon is detected with probability η, the effective overall detection yield. For measurements at low temperatures, by use of a confocal microscope, the detection yield is typically 0.5%. We used this value throughout the simulations. The time-resolution T is introduced to obtain a luminescence time trace from this stream of photons. The number of detected photons per period of length T is calculated (the photons are binned with time T) for every multiple of $T/2$ and plotted as a function of bin-number. Distributions of on- and off-times are calculated from a luminescence time trace with the help of the parameter θ, representing the threshold. If the number of photons per bin is bigger (smaller) than θ the nanocrystal is "on"("off"). A sequence of one or more bins in the "on-state" ("off-state") is called on-time (off-time). The length of the on- and off-times is thus calculated in units of T. The auto-correlation function is directly calculated from the stream of photons. The time delay between any pair of photons in this series is calculated and plotted in a histogram. This "all pair distribution" of delays is equivalent (up to a normalization factor) to the correlation function, as was shown in Section 3.2. Note that, like in real experiments, no arbitrary parameters representing threshold or bin time are required in this case.

Under normal excitation intensities it takes about 100 ns before a nanocrystal absorbs a photon and leaves the ground state [85]. The fluorescence lifetime at room temperature is measured to be a few tens of nanoseconds [99]. Therefore, the rates κ_{ge} and κ_{eg} are initially expected to be of the same order of magnitude. The residence time of the electron in a trap is expected to be longer than the times related to the ground and excited states. The constant C is therefore probably about two orders of magnitude larger than κ_{ge}^{-1}. Measurements with a confocal microscope at low temperatures are often performed with 1 ms binning time, due to the limited collection efficiency. The time-resolution T should thus be about two orders of magnitude larger than C.

With this set of parameters our model is completely defined and supposedly

takes into account the most important features of the excitation-luminescence cycle of a nanocrystal under steady-state illumination. The number of independent parameters in the simulations is limited. The detection quantum yield and time-resolution are kept fixed at $\eta = 0.005$ and $T = 10^6$, respectively. We have no information on the time that the NC spends in the ground- or excited state. Only the total duration of the cycle between these two states appears in the simulations. We define the duration of this cycle as $\zeta = \kappa_{ge}^{-1} + \kappa_{eg}^{-1}$. Information on the tunneling barriers is limited to the ratio of α and β. The slope of the power law is determined by $\gamma = \alpha/\beta$. δ represents the ratio between the transition rates from the excited state to the charged states and from the excited state to the ground state. The probability ε to have a charged-shell state instead of a charged-core state equals zero for uncapped NC's and is finite for capped NC's.

5.3 Simulating blinking statistics

Comparison to experimental data

First, the data from our experiments on (uncapped) CdS NC's were simulated. The results in Figures 4.1 and 4.2 show the good agreement we obtained between simulations based on the model for uncapped NC's ($\varepsilon = 0$) and experimental data. This was possible with the following set of parameter values: $\gamma = 0.7, \quad \delta = 0.01 \quad \zeta = 2 \cdot 10^2$, and $C = 10^4$. Note that the agreement holds for all four aspects of the statistics; luminescence time trace, distribution of on-times, distribution of off-times and correlation function, and that these four aspects are all simulated with the same set of parameter values.

With minimum changes the results on capped NC's were also simulated. A finite value of the parameter ε opens the possibility for a charged-shell state. With $\varepsilon = 0.2$ the power-law distributions for on- and off-times are reproduced. For the optimum agreement with experiments the excitation-luminescence cycle has to be a bit faster than in the case of uncapped NC's; now $\zeta = 1.1 \times 10^2$. The results are shown in Figure 4.4(a) and (b). The luminescence time traces and distributions of on- and off-times resemble those of References [85] and [86], and the correlation function is similar to the one in Reference [99].

The tunneling barriers

For a better understanding of the model the influence of individual parameters was investigated. The parameters that are not mentioned explicitly are kept

at the values as mentioned above.

Obviously, the parameter γ is very important. It represents a measure for the depths of the electron traps. Figure 5.2(a-c) and (e-g) show how drastically the appearance of luminescence time traces changes upon small variations of γ, for uncapped and capped NC's respectively. The traces change from almost empty at $\gamma = 0.6$ to dense at $\gamma = 0.8$.

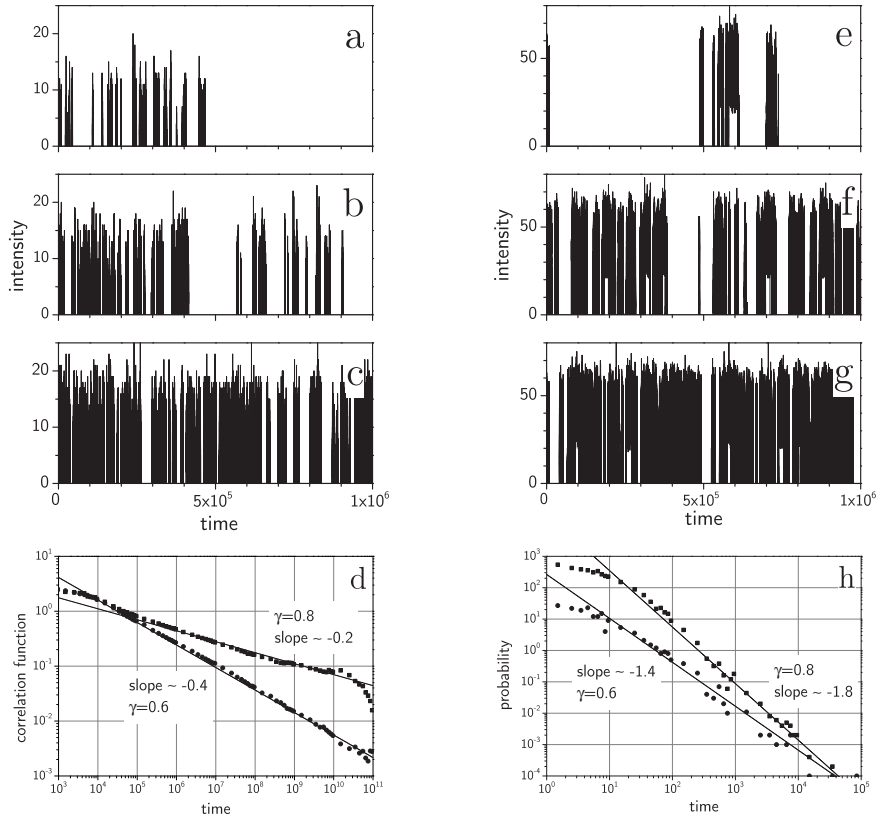

Figure 5.2: Influence of γ on the blinking statistics of uncapped (left) and capped (right) NC's. (a-c) The trace of uncapped NC's becomes denser for bigger values of γ, as long off-times become less dominating. (d) As a result, the correlation function becomes flatter. (e-g) For capped NC's, short on- and off-times become more important in the trace for bigger values of γ. Long off-times, already dominating over the long on-times, occur less often. (h) Therefore, the distribution of off-times gets steeper.

The distributions and correlation functions change accordingly. For uncapped NC's this is best illustrated by the correlation function, as is shown in

Figure 5.2(d). Its slope changes from -0.4 for $\gamma = 0.6$ to -0.2 for $\gamma = 0.8$. Figure 5.2(h) shows the effect of a small variation in γ on the off-time distributions of capped NC's.

The slope of the distributions of on- and off-times cannot be efficiently changed by varying the values of ζ, C or δ, without changing the shape of the distribution or the appearance of the trace. The only parameter that directly controls the slope of the distributions is γ. All experimental data (the appearance of traces, the slopes of on- and off-time distributions, and the correlation function of uncapped NC's), indicate that the value for γ is about 0.7.

A bigger value of γ represents a faster decay of the wavefunction of the exciton outside the nanocrystal, leading to a much smaller probability for the electron to tunnel to a more remote trap. Therefore long off-times (and for capped NC's also long on-times) become less likely and the traces show faster blinking. A good estimation of γ is important for understanding the tunneling probabilities. Fortunately the system is very sensitive to γ. From Equation 4.7 and detailed knowledge about the materials involved it may be possible to determine the energy levels involved. This is further discussed in Chapter 6.

The detection efficiency

We have seen in Section 3.2 that the total detection efficiency of the setup is an important parameter in photon statistics. The statistics of the detected photons may differ significantly from that of the emitted photons. This is clear from Equation 3.3 and worked out in detail in Table 3.1 for two special distributions. Figure 5.3 demonstrates that the detection yield is also important in case of power-law statistics. For different values of η, the distribution remains a power law. But the slope of the measured distribution of on-times ($\eta = 0.005$) differs significantly from the true distribution of on-times, which would be measured if every photon was detected ($\eta = 1$).

The correlation function, however, is independent of detection yield. This was already demonstrated in Section 3.2. If the correlation function is not normalized, only its shape is independent of η.

The threshold

The threshold parameter θ is used to determine the on- and off-times from a stream of photons. Although important for the evaluation of the data, there is no clear physical argument for setting its value. Therefore it is important to know what the influence is of small changes in the threshold value, on the

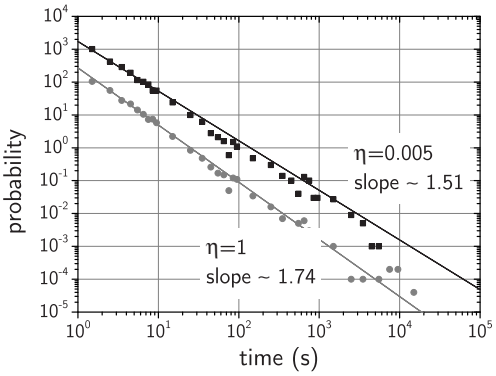

Figure 5.3: Distributions of on-times depend on the detection yield. The slope of the power-law distribution, as measured on a capped NC with $\eta = 0.005$, differs form the slope of the power law of the true distribution, as would be measured if $\eta = 1$.

distributions of on- and off-times. Figure 5.4(a) shows a simulated luminescence time trace for a capped NC. The three horizontal lines indicate values of the threshold that could be used to determine the on- and off-time distributions. The distributions of off-times are very similar for all three values of θ. However, the distribution of on-times changes significantly. This is shown in Figure 5.4(b). A relatively small value for the threshold ($\theta = 8$) leads to a power-law distribution of on-times with a slope of -1.9. A moderate value of the threshold, $\theta = 23$, gives the correct distribution with a slope of -1.65. For too high values of the threshold ($\theta = 38$) the distribution does not follow a power law anymore. Whether the signal drops below the threshold is now determined by shot noise, rather than by blinking. One has to consider the combined action of threshold, detection yield and bin time to describe the statistics of detected photons in detail [129]. A measurement with an unfortunate choice of bin time or threshold, together with a strong background signal or poor statistics, might even lead to power-law exponents smaller than -2. However, the assumption that the (true) exponents lie between -1 and -2 (and $0 < \gamma < 1$) does not have to be violated (see Equation 4.7). If the dynamics exceeds bin time and resolution by a few orders of magnitude, the data at long times resemble the correct power law. The influence of the detection yield remains, and measured distributions ($\eta \ll 1$) are never identical to the true distributions of on and off-times ($\eta = 1$).

This example demonstrates that the exponents of the on- and off-time distributions n and m, respectively, depend on the choice of the threshold value.

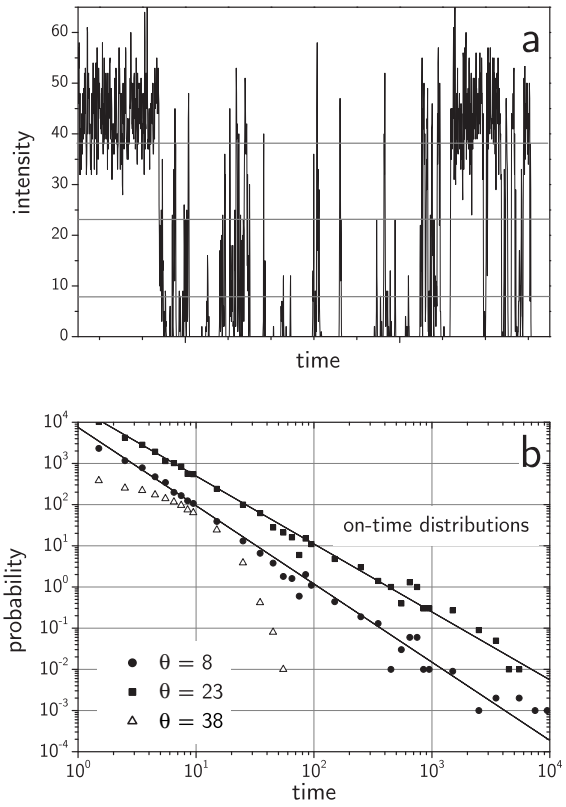

Figure 5.4: On- and off-time distributions depend on the threshold that is used to obtain them from a luminescence time trace. (a) Simulated luminescence time trace for a capped NC. The horizontal gray lines represent the threshold values that were used to calculate the on-time distributions in figure (b). A threshold of $\theta = 38$ is obviously too high. The on-time distribution does not follow a power law anymore. The distributions obtained by $\theta = 23$ and $\theta = 38$ are multiplied by, respectively, 10 and 0.1 for clarity.

Determining the correct value of θ, in a reproducible way, is even harder for a real trace, which includes noise and possibly more than just two luminescence intensity levels. Measuring the correlation function (which doesn't require a threshold) and knowing the relation between distributions of on- and off-times and the correlation function (Chapter 3), is therefore indispensable for a reliable interpretation of the data.

Lifetimes

The simulations also give information about the (relative) average residence time in the ground-, excited-, and charged states. The residence time of the ground- and excited states are supposed to be four orders of magnitude shorter than the bin time (100 ns versus 1 ms). For larger values of ζ, the cycle time between ground state and excited state, the count rate is so low that long on-times are not possible anymore. Even during the charged-shell state the luminescence intensity can drop below the threshold value, aborting the on-time. Larger values of C, δ, and ε cannot compensate this effect. For much lower values of ζ the count rate becomes very high. The noise is then much lower during on-times than what is observed experimentally.

The parameter C, a measure for the duration of the charged states, is studied together with the probability δ to enter the charged states. For a smaller product of C and δ, too few long off-times appear in the simulated traces of uncapped NC's. Correlation at relatively long times is lost and the correlation function resembles an exponential function. For bigger values of $C \cdot \delta$, the correlation function breaks up into two regimes. The blinking due to the cycle between the ground state and excited states on the one hand, and the long off-times due to the charged (core) state on the other hand, take now place on completely different timescales. The optimum values are $10^3 < C < 10^5$ and $0.005 < \delta < 0.05$.

Narrowed on-time distribution

Finally, we have tried to simulate the on-time distributions as shown in Ref. [86]. Here, the distribution of on-times follows a power law up to a certain duration. For longer times the histogram decays much faster. This behavior could not be simulated without introducing a new process.

As discussed in Section 4.6, experimentally obtained distributions, which decay faster than a power law at long times, are often fitted with a "stretched exponential". We had no physical arguments to use this function, however, and found an alternative process that may cause this on-time distribution. A charged-shell state (long on-time) is terminated when the electron tunnels back from a trap outside the NC. We now introduce the possibility that an on-time can also be terminated by a process that effectively moves the hole from the shell to the core. See Section 4.6 for further details. This second way to end an extended on-time (by transformation into an off-time for the rest of the duration of the charged state) has a finite probability, causing an exponential tail to the distribution. With probability $\phi = 10^{-5}$ (1000 times

smaller than the probability δ that the primary electron tunnels to a trap in the surrounding matrix) for this process, the histogram of on-times of Ref [86] is well reproduced. Although there is no evidence for this transformation to take place, this simulation might indicate a possible way to improve our model.

5.4 Conclusions

The simulations described in this chapter are based on the model as described in Chapter 4. They illustrate how this model accounts for the power-law distributions of on- and off-times. With only a few parameters, several aspects of the statistics are reproduced at the same time; luminescence time trace, distribution of on-times, distribution of off-times, and the correlation function. Moreover, the simulations show how a single model accounts for both uncapped and capped nanocrystals.

All parameters that were used in these simulations are related to physical processes or quantities. Even quantitatively we found some agreement between the parameters and the physics they represent. Investigations of the influence of individual parameters on the blinking statistics again demonstrate the relations between physical processes and mathematical distributions. The influence of the detection yield and the threshold value are also shown, demonstrating the importance of the correlation function.

6 Influence of the environment on nanocrystal blinking

abstract – Decreasing fluorescence signals from ensembles are compared with blinking statistics of individual nanocrystals in various environments. For most substrates, the ensemble decay follows a power law of time, the exponent being the difference between the power-law exponents of the on- and off-time distributions of individual NC's. We derive an analytical relation between these three exponents. The decay exponent is also found to depend on substrate. We discuss possible mechanisms for this dependence in conjunction with previously published models. Other experiments presented here concern the dependence of the blinking behavior on atmosphere, distance to the substrate interface, and excitation intensity.

6.1 Introduction

Due to quantum confinement effects, semiconductor nanocrystals (NC's) have interesting physical and optical properties that are relevant for many applications, from multidimensional data storage to labeling in molecular biology. In all these applications the environment of the NC's is different. Due to the large surface–to–volume ratio and the assumed tunneling of charges from the NC to the surrounding matrix and back, the photophysics and photochemistry of NC's may depend strongly on the environment matrix. For a full use of their potential, it is crucial to first understand how the NC's respond to different environments, down to the single-NC level.

One approach to study NC's is to investigate the luminescence intermittency (blinking). This property is very important in single-molecule microscopy, where it is often used as evidence for single quantum systems [12] and led to determination of, e.g., triplet lifetimes. For NC's however, the mechanism that causes blinking is still under debate. It is well known that the distributions of bright and dark periods of ZnS-capped CdSe NC's follow power laws with exponents between -1 and -2 [85, 86, 116, 117]. Such distributions give rise to unusual properties governed by Lévy statistics, and to statistical aging [104, 105]. Although this type of statistics complicates the interpretation of blinking data, it gives valuable information about the physical processes taking place in the NC. The ensemble decay, on the other hand, is also predicted to follow a power law, its exponent being intimately related to those of the on- and off-time distributions. However, no rigorous experiments to test this prediction have been published, yet. This is the prime focus of the current chapter. We also present a mathematical derivation of the relation between the power-law luminescence decay for ensembles and the blinking statistics for individual NC's, in the framework set in Chapter 3.

The second topic we address here is the influence of the environment on the blinking behavior of individual NC's. The model described in Chapter 4 predicts that blinking statistics depends on the direct environment of the NC. In Section 6.3 we briefly discuss some experiments that demonstrate the influence of the atmosphere. The influence of the surrounding matrix is demonstrated by the experiments of Section 6.4. Here, we compare luminescence decays of NC-ensembles with the blinking statistics of individual NC's in various matrices. Section 6.5 deals with the influence of the excitation intensity on the blinking statistics. Again, both ensembles and individual NC's are studied. Section 6.6 discusses possible ionization processes for NC's under illumination.

6.2 Experiments

We used 3.4 nm core diameter CdSe NC's capped with 2 monolayers of ZnS, passivated with a mixture of trioctylphosphine oxide (TOPO), trioctylphosphine (TOP), and hexadecylamine (HDA). A solution of chloroform containing 3×10^{-10} M nanocrystals was spin-cast on substrates of fused silica (FS), indium tin oxide (ITO), glass, or lithium fluoride (LiF). For samples in poly(methyl methacrylate) (PMMA), the same solution of chloroform was mixed with a 6 mg/ml solution of PMMA in toluene and spin-cast on a substrate of FS. On average, the concentration of NC's on the surface of a substrate was $0.1/\mu m^2$ for all types of samples, ensuring that the measurements were not performed on aggregated samples. Good reproducibility of the sample preparation made it possible to measure a number of NC's on several samples, for each system. Measurements were performed with a home-built beam-scanning confocal microscope, using the 514 nm line of an argon-ion laser for excitation (continuous wave). During experiments the sample chamber was either flushed with dry nitrogen or filled with ambient air, at room temperature. For measurements on individual NC's, the excitation intensity was about 100 kW/cm^2 and the luminescence was recorded with an avalanche photodiode (APD; EG&G) with 10–100 ms resolution. For measurements on ensembles, we used epi-fluorescence detection with a CCD camera, 5 s integration time, at an intensity of 1 kW/cm^2. On average, there were about 100 NC's present in the detection volume. The samples that were used for the measurements described in Section 6.3 were very different from the other samples. Not only was the concentration of NC's in the stock solution 1000 times higher, also the preparation method was different. Instead of spin-casting the solution on a substrate, a droplet was put on it. The solvent evaporated and the NC's stayed behind on the substrate. Not only does the average distance between the NC's decrease with increasing concentration, the NC's may also aggregate at high concentrations. This aggregation effect is enhanced by the preparation method.

6.3 Blinking of nanocrystals in different atmospheres

Luminescence of highly concentrated samples of capped nanocrystals was recorded as a function of time. These samples were created from a droplet of chloroform with 10^{-7} M NC's on a substrate. The solvent evaporated and a high concentration of NC's was left behind, without any polymer matrix.

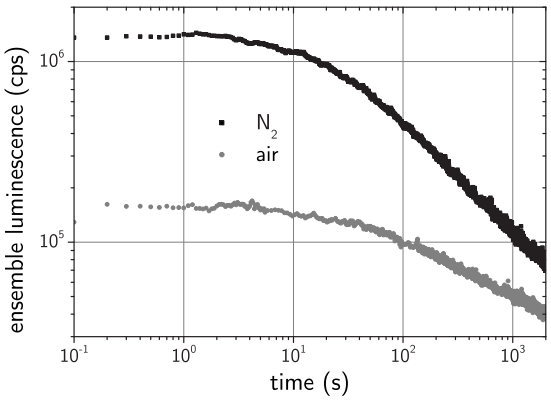

Figure 6.1: Ensemble luminescence of a highly concentrated sample of capped NC's on ITO, in two different atmospheres. For long times, the luminescence decay follows a power law, the exponent (slope) depending on the atmosphere.

Four different types of substrates were used: glass, fused silica (FS), indium tin oxide (ITO), and lithium fluoride (LiF). All four types of samples were studied in ambient air and nitrogen (N_2). The luminescence was recorded for 2000–6000 seconds with 100 ms resolution.

Figure 6.1 shows that the ensemble luminescence decays in time. The decay follows a power law (a straight line in a double logarithmic plot) at long times. To determine whether this decay is caused by reversible or irreversible processes, the laser was sometimes blocked for several minutes, after which excitation was resumed. The luminescence level was recovered to at least 90% of its initial value, and higher that the luminescence intensity shortly before the break, directly after the interruption. A longer break would lead to a more complete recovery. Obviously, the ensemble luminescence decay was not caused by irreversible processes (bleaching).

substrate	N_2	air
glass	0.1 ± 0.05	0.2 ± 0.02
fused silica	0.3 ± 0.05	0.5 ± 0.05
ITO	0.2 ± 0.1	0.5 ± 0.1
LiF	0.24 ± 0.02	-

Table 6.1: The ensemble luminescence decays in time as a power law. The exponent of the power law depends on substrate as well as on atmosphere. For all four substrates (glass, fused silica, indium tin oxide (ITO), and lithium fluoride (LiF)) the exponent is bigger in air atmosphere.

Variations in time of ensemble properties, that are caused by reversible processes only, can be explained by statistical aging. The ensemble luminescence is the sum of the luminescence intensities of all NC's in the ensemble. As NC's blink under (cw) illumination this sum is generally lower than the theoretical maximum (all NC's in the emitting state). In fact, it depends on the fraction of NC's in the on-state. On average, this fraction equals the ratio of the average on-time and the average off-time. But as stated before, the average values of the on- and off-times are not defined for NC's, because the distributions follow power laws with exponents between -1 and -2. As the experiment continues, longer on- and off-times can occur, even as long as the duration of the experiment itself. However, the distribution of off-times is broader (has a less negative exponent) than the distribution of on-times. The average value of all off-times that are observed for a single NC (which is not the average value of the distribution of off-times) grows faster than the "average" of all on-times. With time, the probability to be "off" (vs "on") increases slowly for every NC. This means for the ensemble that the fraction of NC's in the "off-state" increases in time and that the total luminescence decreases correspondingly. The relation between the blinking behavior of single NC's and the ensemble luminescence is described in more detail in the next section. It will be demonstrated that power-law distributions of on- and off-times cause a power-law decay of the ensemble luminescence. Note that statistical aging can only be observed if the system is physically stable for a long time (aging is often a slow process) and if it is not overruled by irreversible processes.

The decay at short times is slow and not well understood. On these short timescales the blinking behavior might be dominated by fast charge hopping between aggregated NC's, resulting in different distributions of on- and off-times. The ensemble decay is also measured on samples with a lower concentration (and no aggregation). In that case it follows a power law over the whole range of times, as is shown in Figure 6.5. The ensemble luminescence decay is measured on four different substrates and in two different atmospheres. The values of the power-law exponents are summarized in Table 6.1. Two conclusions can be drawn from this overview. In the first place, there is a clear influence of the atmosphere. For all substrates, the values are bigger in air than in nitrogen. Secondly, the exponents depend on substrate material.

If the ensemble decay depends on atmosphere, and is only caused by the blinking statistics of individual NC's, individual NC's are apparently affected by the atmosphere. This is confirmed by the luminescence time traces (luminescence intensity as a function of time) of individual NC's in Figure 6.2. A low concentration (10^{-10}M) of NC's was spin-cast on FS substrates to make

this experiment possible. The luminescence of these NC's was recorded while the atmosphere was changed. The nitrogen atmosphere was replaced by air, about halfway the upper trace. The second NC was situated in air, but from the start a constant flow of nitrogen slowly replaced the air. In nitrogen atmosphere the density of intense bursts of luminescence is higher and also the average intensity goes up, in agreement with Ref. [118]. Surprisingly, Müller *et al.* showed that the fluorescence bursts are enhanced upon sudden exposure to air, compared to vacuum [130]. The influence of the atmosphere on the ensemble decay is now demonstrated by the influence of the atmosphere on the blinking behavior of individual NC's.

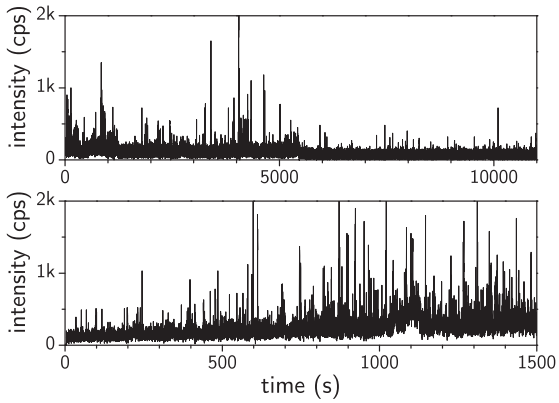

Figure 6.2: Luminescence time traces of two individual capped NC's on FS substrates. In the upper case the nitrogen atmosphere was replaced by air, at about 5500 s. During the lower trace a constant flow of nitrogen slowly replaced the air.

In summary, the influence of the atmosphere on the blinking behavior of individual NC's has been demonstrated in two ways. In the first place, the slope of the power-law ensemble decay depends on the atmosphere. On the other hand, the influence of the atmosphere on individual NC blinking is clear from the luminescence time traces shown in Figure 6.2. The latter effect is hard to quantify, however. It is difficult to understand the relevant processes that take place in these highly concentrated samples. Sometimes the decay was even faster than a power law. This may indicate that aggregation alters the luminescence decay. We expect this to happen via charge hopping between aggregated NC's and induced electric fields [8]. Comparison of different rows of Table 6.1 shows that the value of the power-law decay exponent also depends on the material of the substrate. This will be investigated in more detail in the next section.

6.4 Blinking of nanocrystals in different matrices

Changing the local environment

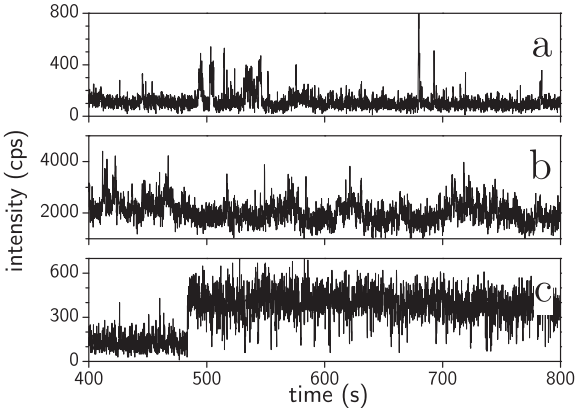

Figure 6.3: The appearance of a luminescence time trace of a single CdSe/ZnS nanocrystal depends on the environment: (a) A NC on fused silica shows short bursts of luminescence. (b) The luminescence intensity of a NC on indium tin oxide fluctuates. It is hard to discriminate on- and off-times. (c) On- and off-times are easier to recognize for a NC in a PMMA matrix.

The influence of the surrounding matrix on the blinking behavior of semiconductor nanocrystals is investigated by studying both individual nanocrystals and ensembles. Nanocrystals from the same batch were deposited on fused silica, on ITO or in a PMMA film. All experiments were performed in nitrogen atmosphere, at room temperature and with constant excitation intensity. Figure 6.3 shows typical luminescence time traces of single NC's on the three different substrates. The three systems differ qualitatively. NC's on FS (Figure 6.3a) show many short bursts of luminescence and a constant off-level, while on ITO (Figure 6.3b) the luminescence is strongly fluctuating, which makes discrimination between the on- and off-states difficult. NC's in a PMMA matrix (Figure 6.3c) show more telegraph-like on- and off-states, with relatively long on-times.

A more quantitative picture of the differences in blinking between NC's under these three conditions is obtained by considering distributions of on- and off-times. A threshold intensity defined as twice the background level determined the state of the NC. The NC is in the "on-state" if the luminescence intensity is higher than the threshold, or in the "off-state" if it's lower. The durations of the on- and off-times are collected and a probability density is

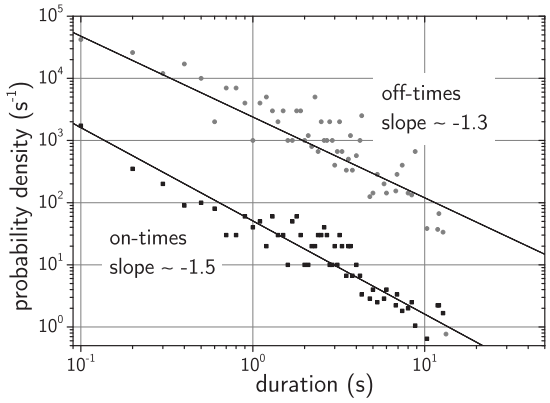

Figure 6.4: Probability-density distributions generated from a histogram of on- and off-times for a single nanocrystal in PMMA. The procedure to calculate these distributions is explained in the text. Both on- and off-times follow a power law, with the biggest exponent (in absolute value) for the on-times. (The off-time probability density is multiplied by 100 for clarity.)

plotted. In this chapter the distributions of on- and off-times are not depicted in histograms (number of occurrences per time bin), but plotted in probability density graphs. Although the same information is displayed in both cases, the latter has the advantage that the function is smoother, whereas a histogram can be very noisy. Especially at long durations, where the statistics is poor because very little events of long duration are observed during the finite experimental observation time, a probability density function is easier to analyze (fit) than a histogram. It is obtained from a histogram by weighing every element in the histogram by the inverse of the average distance to its two nearest neighbors (one to shorter and one to longer times). This has clearly no effect on data at short durations, where every bin has multiple entries, but it makes the plot smoother at long durations.

Figure 6.4 shows probability densities of the on- and off-times for a NC in PMMA. The straight lines in a double-logarithmic plot indicate power-law distributions. The exponents n and m of the power laws for on- and off-times, respectively, are summarized for different environments in Table 6.2. The exponent of on-times is found to be larger than that of the off-times, in agreement with earlier observations [85]. Note that several NC's measured in each environment showed the same difference between the exponents, $n - m$, within experimental error. In the case of an ITO substrate it was difficult to set a threshold, and the values of the exponents are therefore rough and tentative.

	FS				PMMA		ITO
NC	1	2	3	4	1	2	-
n	2.2	1.9	2.3	1.9	2.1	1.5	-
m	1.5	1.3	1.7	1.4	1.8	1.3	-
$n-m$	0.7	0.6	0.6	0.5	0.3	0.2	-
r	0.5 ± 0.1				0.23 ± 0.07		0.3 ± 0.1

Table 6.2: The relation between the exponents of the power-law distributions of on-times (n, first row) and off-times (m, second row), and the exponent for the ensemble luminescence power-law decay (r, last row) is tested for several NC's. The results are shown for 4 NC's on fused silica and 2 in PMMA. Distribution of on- and off-times could not be measured for single NC's on ITO.

Figure 6.5 shows the decay of the luminescence of an ensemble of NC's with time. These experiments are done on the same samples as the single-NC experiments. The concentration is thus about 1000 times lower than in the samples that were used for the experiments described in Section 6.3. The NC's did not aggregate in these samples. The decay clearly follows a power law. Its exponent equals the difference between those of the on- and off-time distributions [104], i.e., $r \approx n - m$ (compare the last 2 rows in Table 6.2). In the next section, the relation between n, m, and r is derived mathematically.

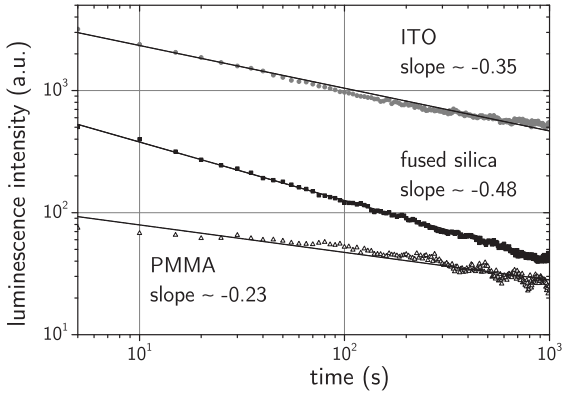

Figure 6.5: The total luminescence of an ensemble of nanocrystals decays with a power law. The exponents, shown in the figure, depend on the environment: indium tin oxide (ITO), fused silica (FS), or organic polymer (PMMA).

The relation between ensemble decay and single NC's

A returning question in single-molecule spectroscopy is whether the sum of spectra of single molecules resembles the spectrum of an ensemble of molecules. A similar question is possible in the time domain. Does the "sum" of single-NC photon statistics resemble the ensemble statistics? To understand the relation between the on- and off-time distributions $P_I(t)$ respectively $P_O(t)$ of a single NC, and the ensemble-averaged fluorescence $\langle I(t)\rangle$, we derive an expression related to the correlation function of a random telegraph, in analogy to Section 3.5.

We assume all time traces to start with an on-time when the laser is switched on. The average intensity can be written as a series of probabilities to have a single (long) on-time, or one with one, two... interruptions (See Section 3.5). With $\otimes$ for convolution products:

$$\langle I(t)\rangle = Y(t) + P_I(\alpha) \otimes P_O(\beta) \otimes Y(t-\alpha-\beta) + \ldots \quad , \tag{6.1}$$

where $Y(\alpha) = \int_\alpha^\infty P_I(\beta)d\beta$ is the probability that an on-time lasts longer than time α. If the Laplace transforms of $P_I(t)$, $P_O(t)$, and $Y(\tau)$ are expressed as $p_I(s)$, $p_O(s)$, and $y(s) = (1/s)(1 - p_I(s))$, respectively, then the Laplace transform of $I(t)$ is expressed as

$$i(s) = y(s) + p_I(s)p_O(s)y(s) + \ldots = \frac{1}{s}\,\frac{1-p_I}{1-p_Ip_O} \quad . \tag{6.2}$$

For capped NC's, the on- and off-time distributions follow power laws, $P_I(t) \propto t^{-n}$ and $P_O(t) \propto t^{-m}$, respectively. The corresponding Laplace transforms $p_I(s) \approx 1 - (\theta s)^{n-1}$ and $p_O(s) \approx 1 - (\theta s)^{m-1}$ were already derived in Section 3.5. (θ is a cutoff for short times.) Knowing that $n > m$ (see Table 6.2 and Ref. [85]), Equation 6.2 gives for long times $i(s) = (\theta s)^{n-m-1}$. The inverse Laplace transform gives the relation between the average intensity and the exponents n and m:

$$\langle I(t)\rangle \propto t^{-(n-m)} \equiv t^{-r} \quad , \tag{6.3}$$

which is a power law again[1]. Within experimental error, the relation holds for our measurements both on FS (e.g. $n = 1.9$, $m = 1.3$, $r = 0.5$) and in PMMA (e.g. $n = 1.5$, $m = 1.3$, $r = 0.23$). This is in agreement with the results of Brokmann *et al.* As explained by these authors, the decay arises from non-stationary NC blinking, i.e., whenever n is bigger than m, the total

[1] For a distribution of r-values the ensemble averaged function $\langle I(T)\rangle$ is not a pure power law. The deviation is very small, however, especially compared to experimental errors.

time spent in the off-state grows faster than that in the on-state for every NC [104]. This means that information on the blinking behavior of single NC's can also be obtained from less difficult ensemble measurements. This was recently confirmed by Pelton *et al.*, who used an equivalent method based on noise power spectra [131].

Changing the distance to the substrate

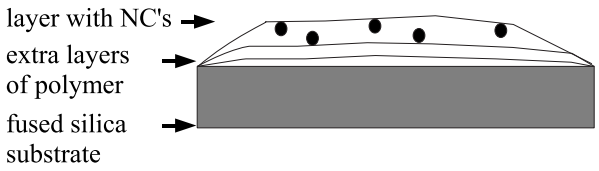

Figure 6.6: Schematic picture of a multilayered sample. Several layers of polymer are spin-cast on a substrate of fused silica. Only the top layer contains nanocrystals.

If blinking is governed by electron tunneling to traps outside the NC's, it is interesting to investigate where those traps are located. For samples where the NC's are embedded in a polymer layer on top of a substrate, the traps are located either in the polymer or in the substrate (or on its surface). By varying the average distance from the NC's to the substrate it should be possible to find out whether the traps are mainly located in the polymer (the blinking behavior is independent of the NC–substrate distance) or mainly in (or at the surface of) the substrate (the blinking statistics depends on the NC–substrate distance). The experiments described in this section are a first attempt to investigate whether the blinking behavior depends on the distance between the NC and the substrate. The results shown are preliminary.

Several layers of polymer are spin-cast on a FS substrate from a polymer/chloroform solution. On top of this polymer matrix a new layer is spin-cast from a polymer/chloroform solution containing NC's. The NC's are thus only present in the top layer of this multilayered structure, see Figure 6.6. By varying the number of polymer layers that are spin-cast on the substrate before the layer containing the NC's is added, the average distance between the NC's and the substrate is changed. For this experiment we used the polymer Zeonex and capped nanocrystals from Evident Technologies (3.95 nm diameter "Fort Orange" Evidots). The number of layers between the substrate and the final layer was varied from 0 to 8.

Figure 6.7 shows luminescence time traces of individual NC's in multilayered samples of different thickness. For thick samples, where the NC's are far from

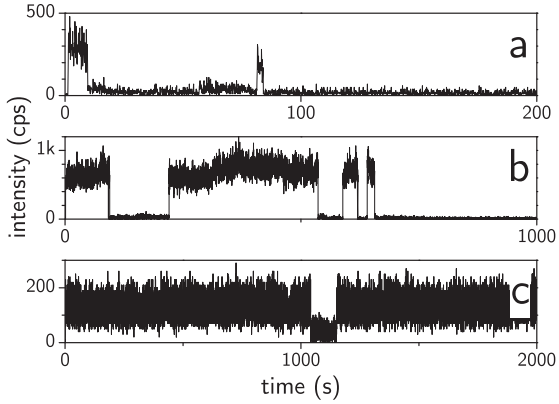

Figure 6.7: Luminescence time traces of nanocrystals in a polymer matrix on fused silica. From top to bottom the nanocrystals are further away from the substrate, due to (respectively 3, 5, and 8) extra polymer layers between the substrate and the layer containing the NC's.

the substrate, the on-times are much longer than for thinner samples. As stated before, the average values are not defined for the power-law distributions of on- and off-times. The statistics of these preliminary results is too poor, however, to calculate the exponents of the power laws. For this reason we define the "average" on-time of a NC as the average of all on-times that are measured for this NC. This "average" (we use quotes to indicate that this is not a true average) is used here as a measure for the on-times of a NC, although it is not equal to the average of the on-time distribution and even depends on the observation time. For samples with only three extra layers, the on-times are typically in the order of seconds (Figure 6.7a). The thickest samples show on-times in the order of 1000 seconds (Figure 6.7c). For samples where the layer containing the NC's was directly deposited on the substrate, no single-NC traces could be recorded. The results are summarized in Table 6.3, where every entry is the average value of about 10 NC's. Some on-times lasted longer than the experiment and are therefore cut off. The "average" on-time can therefore be calculated in two ways. Either by simply averaging over all on-times of all NC's in one type of sample, or by taking the average value of the "average" on-time per NC. Both values are shown in the table, and both numbers indicate that on-times last longer in thicker samples. Aging of the samples also influences the typical duration of on-times. As is shown in Table 6.3, the on-times are significantly longer in "old" samples (7–10 days old) than in "fresh" samples (samples that were prepared and investigated on

the same day). This aging effect may be related to drying of the samples. In time, water or solvents from the original polymer/chloroform solution diffuses out of the sample. This effect was not studied in more detail.

# of extra layers	⟨on-time⟩ (s)		⟨⟨on-time⟩ per NC⟩ (s)	
	fresh	old	fresh	old
2	-	15	-	28
3	42	187	65	312
5	57	384	93	452
7	109	-	138	-
8	1021	-	1031	-

Table 6.3: The "average" on-time depends on the distance between the NC's and the fused silica substrate. This distance depends on the thickness of the polymer matrix underneath the layer containing the NC's. The two types of averaging are explained in the text. The "average" on-time increases also if the sample ages. (Compare "fresh" columns with "old" columns.) Every entry in this table is the average of several NC's.

The "average" on-time lasts longer if the distance between the NC and the substrate is larger. To obtain more information about these distances, the thickness of some samples was measured by atomic force microscopy (AFM). A sample of one polymer layer was about 18 nm thick, a sample constructed by spin-casting the polymer/chloroform solution 6 times was about 26 nm thick, see Figure 6.8. Apparently, adding a layer increases the total sample thickness by about 1.5 nm. A possible explanation is that the underlying polymer is (re-)dissolved during the process of spin-coating, except the lowest 1.5 nm of the polymer matrix[2]. When the final layer is added, the NC's are distributed over the whole (re-)dissolved part of the matrix. Diffusion is so fast compared to the spin-coating process that the NC's are distributed over this whole layer. If this is true, 2 to 8 extra layers create a NC-free polymer barrier layer of 3 to 12 nm. The outer diameter of a NC including its capping and passivating layers is much bigger than the core diameter of 4 nm, maybe up to 13 nm. The organic layers are very flexible, however, making it hard to estimate the "effective diameter". But high-resolution AFM images show that the nanocrystals do not stick out of the sample, but are completely embedded in the polymer, see Figure 6.8. This confirms our idea that the top layer containing the NC's is not very thin[3].

These preliminary data show that the blinking behavior of capped NC's depends on the distance between the NC and the fused silica substrate. This

[2] Another possibility is that the whole matrix redissolves during spin-coating and the sample becomes thicker because the polymer concentration (and thus the viscosity of the

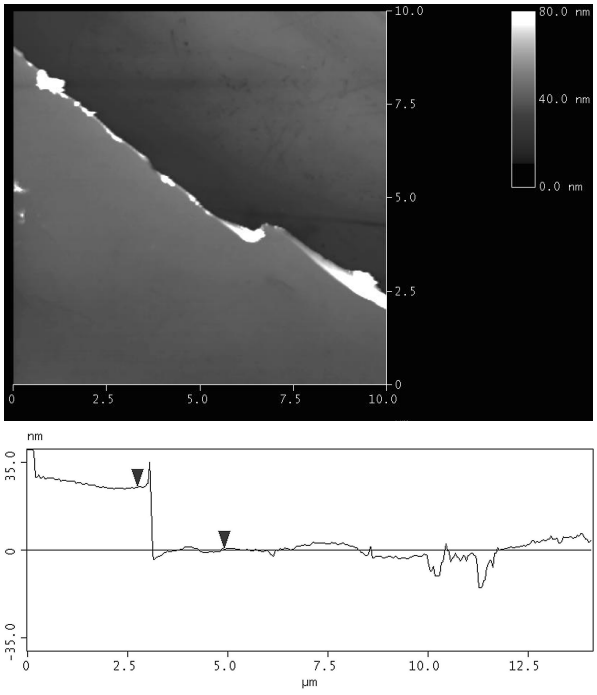

Figure 6.8: (top) Topographical image of a sample consisting of a thick PMMA matrix on top of a fused silica substrate, obtained by atomic force microscopy (AFM). The polymer matrix was partly removed with a razor blade (top right part of the image) to measure its thickness. The surface of the matrix is smooth; no NC's stick out of the surface. (bottom) Cross-section (from bottom left to top right) of the sample shown in the top figure. The matrix is about 26 nm thick, as indicated by the black triangles. The dips between 10 and 12 μm from the left indicate where the razor blade cut into the substrate.

indicates that the traps are mainly located at the polymer–substrate interface or in the silica substrate. It would be desirable, however, to fabricate samples with better control over the distances between the NC's and the substrate. This should be done by adding the NC's to the sample without affecting the underlying polymer matrix. Also improved statistics is desirable, which makes it possible to calculate the exponents of the on- and off-time distributions.

solution) increases every time a new layer is added.

[3] If the first layer would be 18 nm thick and every additional layer would add only 1.5 nm to the total sample thickness, the NC's would stick out of the 1.5 nm thin top layer.

6.5 Blinking of nanocrystals at different excitation intensities

In this section we shortly discuss the influence of the excitation intensity on the blinking behavior. To determine which of the several possible processes, which are discussed in the next section, are responsible for the ionization and neutralization of NC's under (cw) excitation, it is important to know whether the luminescence intensity shows a linear or a quadratic dependence with the excitation intensity. We also want to know if the assumption is correct, that the duration of the off-times does not depend on excitation intensity.

The samples we used for this experiment are very similar to the samples of the former section. 5 layers of polymer were spin-cast on a fused silica substrate. Only the sixth Zeonex layer contained CdSe/ZnS NC's (3.95 nm diameter "Fort Orange" Evidots from Evident Technologies). The results presented here are the average behavior of six NC's, monitored over several hundreds to 2400 seconds. From every recorded luminescence time trace, we calculated the exponents of the on- and off-time distributions, respectively n and m. Like in the former section, we also use the "average" on-time (off-time), defined as the average of all on-times (off-times) measured for a single NC, as a measure for the on- and off-time distributions.

The intensity of the luminescence was measured as a function of excitation intensity. This dependence was linear in the range from 1.9 kW/cm^2 to 9.6 MW/cm^2. By increasing the excitation intensity from 1.9 to 200 kW/cm^2, n increased from about 1.6 to 2.0. This increase of n was confirmed by a decrease of the "average" on-time from about 1 to 0.5 seconds, in agreement with Refs. [12, 86]. The exponent of the off-times, m, was in the order of 1.5 and decreased only very little upon the increase of excitation intensity. The "average" off-time, in the order of 2 seconds, showed a correspondingly small increase.

The decrease of the "average" on-time for higher excitation intensities is caused by the higher rate of exciton creation. At higher intensity, a neutral NC is in the excited state for a larger fraction of time. The probability per unit of time that the NC ionizes due to electron tunneling increases correspondingly. If the NC is in the charged-shell state, the probability that the extended on-time will be terminated is higher at high excitation intensity because the probability of recombination in the shell is larger. On-times are thus shorter at higher excitation intensity. It is not obvious why the value of n increases for increasing intensities. The duration of off-times is independent of the excitation intensity, in agreement with Refs. [12, 86]. The process of electron

tunneling from a trap to the NC is not photo-assisted. The small changes in m (and of the "average" off-time) could be an artefact. The duration of this experiment is limited and the next off-time to be measured can be of the same order of magnitude as the total time spent in the off-state up to that time (see Section 2.5). At high excitation intensities the "average" on-time is shorter, and more (on- and) off-times are measured during the experiment. This increases the probability to measure a very long off-time which enlarges the "average". This increase of the "average" has a statistical rather than a physical reason and is only a small effect. It happens to the on-times as well, but is then dominated by a decrease of the "average" for physical reasons.

6.6 Discussion

The experiments described in this chapter demonstrate the sensitivity of NC blinking to changes in the environment. The atmosphere, material of the substrate, distance to the polymer–substrate interface, excitation intensity and even the concentration have all an effect on the statistics of on- and off-times. This agrees well with the assumption that traps outside the NC, and tunneling barriers for electrons leaving and returning to the NC, play an important role in blinking, according to the model described in Chapter 4. Other arguments for the assumption that traps are situated outside the NC are direct [114,115] and indirect [123] observations of charged NC's, the values of the tunneling rates and residence times in the traps [132], and the required number of traps [3]. However, details about the processes of ionization and neutralization, probably through tunneling, are not known, yet. Consistent observations of the dependence of m, n, and r on the material of the substrate give some quantitative information and may help to interpret the relevant barrier heights and energy level schemes.

Both Kuno *et al* [132] and ourselves (Chapter 4) have proposed a simple charge tunneling model where the off-times exponent m is related to the tunneling barrier heights $V_m - V_e$ and $V_m - V_t$ for tunneling out and into the NC as:

$$m = 1 + \sqrt{\frac{V_m - V_e}{V_m - V_t}} \quad , \tag{6.4}$$

with V_m, V_e, and V_t the electron's potentials in the matrix, in the excited state of the nanocrystal and in the traps, respectively (See Section 4.5.). A first idea would be to extract these values from the band structures of bulk materials [132], as depicted in Figure 6.9 for a 5 nm (capped) CdSe nanocrystal

on a FS substrate, with band gaps of $E_g \approx 1.8$ eV [5] and 10.4 eV respectively [133]. Changes in the band structure, due to Coulomb interactions, upon rearrangements of charges are only a small correction. Due to the high values of the relative dielectric constants in semiconductors, these interactions can be ignored at the relatively large distances that are relevant to the movements of the charges (in the order of nanometers). Upon excitation over the band gap (the energy of a photon at 514 nm is 2.4 eV) an electron is promoted to the conduction band and a hole is created in the valence band, see Figure 6.9(b). The electron relaxes to the bottom of the conduction band within picoseconds. From there, the barrier for ionization, $V_m - V_e$, is about 3.6 eV. The trap has to be deeper than the excited state of the NC and is situated somewhere in the band gap of the NC. The barrier for back tunneling is thus higher, about 4.5 eV. This gives for the exponent $m \approx 1 + \sqrt{3.6/4.5} \approx 1.9$, which is higher than the values measured here and published earlier [85, 86, 116, 117], about 1.5. In order to obtain $m \approx 1.5$ we require V_e to be only ~ 1.2 eV below V_m, which is an unlikely scenario for the given FS bulk energy level structure.

Kuno *et al* give a qualitative possible explanation for this discrepancy in barrier heights. If the V_e level is assumed to be high above the band edge of the NC, the $V_m - V_e$ barrier is effectively lowered and a smaller exponent is expected. We consider three possible processes to achieve this. In the process called two-photon excitation, schematically depicted in Figure 6.9(b), two photons are absorbed simultaneously. The excited state of the NC, V_e, lies 2 times 2.4 eV above the top of the valence band. The barrier for ionization is now only about 0.6 eV. The resulting exponent is $m \approx 1 + \sqrt{0.6/4.5} \approx 1.4$, which is close to the measured value of m. For excitation intensities below the saturation intensity, ionization via a two-photon absorption process should lead to a quadratic dependence of the ionization rate with excitation intensity. However, measurements of the ionization rate [114] showed a linear dependence in the range of 0.1–2 W/cm^2. Moreover, pulsed excitation, with the same average intensity as cw excitation but a probability of generating two electron-hole pairs which is over two orders of magnitude higher, showed the same excitation rate leading to an off-state [12].

The process of Auger-assisted tunneling [134] is pictured in Figure 6.9(c). If the excitation intensities is not too low, two electron-hole pairs can be present in a NC at the same time. The electrons are supposed to quickly relax to the bottom of the valence band. If one of the electron-hole pairs recombines, the energy can be transferred to the other exciton, of which the electron is now promoted to a level 1.8 eV above the band edge. This leads to an exponent of $m \approx 1 + \sqrt{(3.6 - 1.8)/4.5} \approx 1.6$, again close to the observed value. While it

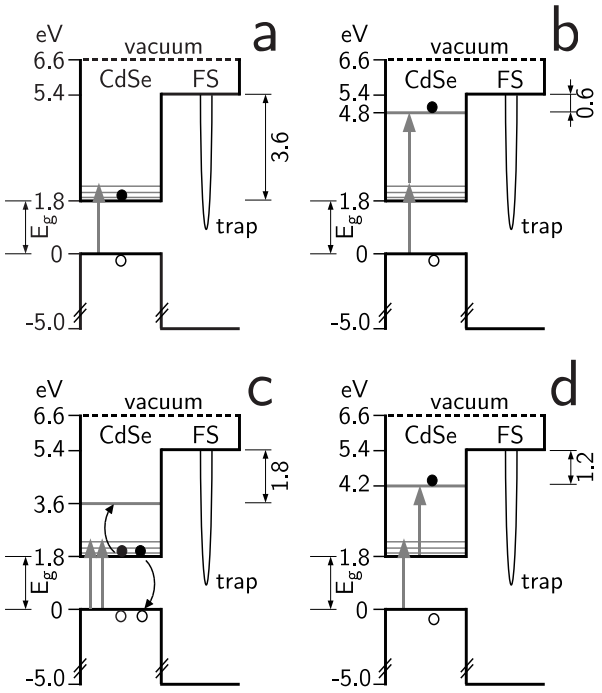

Figure 6.9: Band-energy diagram of a NC on fused silica and four possible processes of ionization. The energy scale on the left is set to 0 eV at the top of the valence band of CdSe. After excitation, tunneling to a deep trap is possible. The height of the barrier (indicated on the right and relative to the bottom of the conduction band of FS) depends on the position of the excited state, which depends on the excitation process. (a) One-photon absorption followed by intra-band relaxation brings the electron to the bottom of the conduction band. (b) Two-photon excitation results in a much smaller barrier. (c) Auger-assisted tunneling is possible if two excitons are created in a NC. The recombination energy of one exciton is transferred to the second one, of which the electron is promoted to a higher level. (d) Absorption of one photon is followed by intra-band relaxation and absorption of a second photon. The processes in (b) and (d) give also access to traps that are higher in energy than the band gap of CdSe.

accurately predicts for the observed variation in m values, whether the Auger-assisted tunneling process can compete with the fast relaxation down to the band-edge level remains to be clarified [3, 65]. The same objection holds for two-photon excitation.

Figure 6.9(d) represents another possible process for ionization. It requires an intermediate state and absorption of two photons. The NC is first excited to the intermediate state by absorption of a single photon. From here, a second

photon is absorbed to reach V_e. Note that this process is different from two-photon excitation, where two photons have to be absorbed *simultaneously*. This process does not require the high excitation intensities needed for two-photon excitation. Moreover, if one of the two transitions is saturated, the probability of this process depends linearly on excitation intensity[4] (versus the quadratic dependence of two-photon absorption). In the band structure of the NC, the only level in which a significant population can be built up is at the bottom of the valence band. We think that the electron, after excitation by of the first photon, relaxes to the band edge before the second photon is absorbed. The lifetime of this state is about 17 ns [99]. The excitation rate at a typical intensity of 1 kW/cm^2 and with an absorption cross section of $\sim 10^{-14}$ cm^2 [36,38] is in the order of once per 10 ns. A significant population can thus be build up in this intermediate state. An alternative level that could serve as an intermediate state, is a shallow surface trap at the fused silica surface (~ 2 eV below the conduction band [136]) and close to the NC. The surface of fused silica is expected to possess many defect sites. The two processes in which the absorption of two photons is involved, illustrated in Figures 6.9(b) and 6.9(d), may seem much less likely to happen than the other processes. But the lower probability to reach the levels at 4.2 eV or higher, and the shorter lifetimes of these levels, could be compensated by the higher probability of tunneling from these levels. Not only is the tunneling barrier much lower, tunneling is now also possible to traps that lie above the band gap of the NC and were inaccessible from the excited states that are involved in the other processes. At this stage, it is not clear which of these processes is more likely to be the main process of ionization.

The positions of the energy levels discussed above are not accurately known. But it is doubtful whether more precise values are relevant for this approach. The use of energy levels of bulk FS to describe the energy scheme close to the surface might not be justified at all. The vast majority of defect states that a surface of FS is expected to possess does not simplify this situation. Especially the relative positions of the band structures of the NC and the substrate are uncertain. Furthermore, electrons and holes can be trapped at the surfaces of the substrate and the NC, respectively, and induce electric fields that deform the band structure.

For the same reason, the band structure of the capping layer could be deformed when a hole is trapped in the shell (charged-shell state). As a result,

[4]For intensities below the saturation intensities of both transitions, this dependence is quadratic. This has not been demonstrated, yet, maybe due to difficulties in measurements in this intensity regime [135].

the energy-level scheme could be somewhat different during the charged-shell state and during the charged-core state. The probabilities of back-tunneling during an (extended) on-state and the off-state could differ correspondingly. As a result, the exponents n and m of the on- and off-time distributions, respectively, are slightly different, although the mechanisms for (extended) on- and off-times are very similar.

The experiments in which we varied the distance between the NC's and the substrate (Section 6.4), seem to support the hypothesis that the substrate surface is the main source of (electron) traps, in agreement with [115]. These samples differ only in the distance between the NC's and the substrate, while the on-times change dramatically. The substrate surface can only be reached through the dielectric polymer matrix, suggesting again that tunneling is the active mechanism (see Chapter 4). The number of traps at the substrate–polymer interface is at least 10^{17} m^{-2}. This is the number of charges or traps at the interfaces of a polymer light-emitting diode, where this number is kept minimum [137]. This corresponds to about 100 traps on 10 nm^2, that are relatively close to the NC.

In Chapter 4 the question was already raised, whether it is correct to use the effective mass approximation in descriptions of NC's, as is often done. It has recently been demonstrated that this approximation is no longer valid for ZnO/Zn(OH)$_2$ NC's that are of the same size, or even smaller, than the Bohr radius [138]. By means of electron paramagnetic resonance (EPR) experiments on ZnO/Zn(OH)$_2$ NC's, the electronic wavefunction of a shallow donor electron was monitored. The density of the wavefunction increased both in the core and at the surface for decreasing radius R of the NC, like R^{-3}. This dependence on volume is well described by the effective mass approximation for NC's that are larger than the Bohr radius (1.5 nm in ZnO). This theory turned out to break down at NC dimensions very close to the Bohr radius. It could no longer be used for NC's with $R = 1.5$ nm or smaller. For models that are based on optical experiments of NC's, is it important to know whether these convincing results can be translated to other materials directly. NC's used in optical studies are often made of CdS or CdSe and about 5 nm in diameter. The exciton Bohr radius in CdS is 2.8 nm [5], i.e., comparable to the radius of the particle. Whether the effective mass approximation can be used for these NC's is questionable. The Bohr radius in CdSe is even larger; 4.9 nm [5]. An appropriate description of the wavefunction can probably be obtained by molecular-cluster-type calculations as carried out recently for Si nanoparticles [139]. On the other hand, it is desirable to investigate whether this type of EPR-experiments can be performed on CdS or CdSe NC's. The

results could be compared to the calculations already performed on this type of NC's [119,120]. There are more indications that the effective mass approximation is not valid for NC's. Calculations on confinement effects indicate that the dielectric constant depends on the size of the (nano)crystal [49]. Application of the effective mass approximation is thus not straightforward. Moreover, the Bohr radius indicates only the decay length of the wavefunction of a donor electron. The wavefunction extends to much larger distances [140]. This makes an accurate calculation of the effective mass of an electron in a NC (with a radius similar to the electron Bohr radius) impossible.

6.7 Conclusions

We have investigated the luminescence-intensity decay of ensembles of NC's in various environments, and found power-law decays with the exponents dependent on the surrounding materials. For FS and PMMA, we have demonstrated that the power-law exponents are closely related to the exponents of the on- and off-time distributions of single NC's. This relation is also derived mathematically. The influence of the environment on the blinking behavior confirms that our assumption is correct, that charge rearrangements outside the NC are relevant for the blinking statistics.

Nanocrystals placed on a substrate without a covering polymer matrix are sensitive to the atmosphere. The blinking behavior is different for air and nitrogen atmospheres, which affects also the ensemble decay, and depends on aggregation as well. For nanocrystals in a polymer matrix, the distance to the substrate has a strong influence on the blinking statistics. This indicates that the traps, which play a role in the blinking dynamics, are located outside the NC's and probably at the interface of the substrate. The duration of on-times depends on excitation intensity, the duration of off-times does not. For the whole range of promising applications for nanocrystals, attention should be paid to the exact conditions in which the dots will be used. On the one hand, the sensitivity of nanocrystals to their local environment complicates their use in many different matrices. On the other hand, it makes them very sensitive nanoprobes and careful tuning of the environment makes the nanocrystals even more suited for numerous applications or as model systems for fundamental research.

Acknowledgements

The author wants to thank Celso de Mello Donega and Prof.dr. Andries Meijerink from the Debye Institute (Utrecht University) for providing us with the CdSe/ZnS nanocrystals, and James W.M. Chon for his contributions to the work described in this chapter.

Bibliography

[1] F. Cichos, J. Martin, and C. von Borczyskowski, "Characterizing the non-stationary blinking of silicon nanocrystals", *J. Lumines.* **107** (2004) 160–165.

[2] J. Martin, F. Cichos, and C. von Borczyskowski, "Spectroscopy of single silicon nanoparticles", *J. Lumines.* **108** (2004) 347–350.

[3] F. Cichos, J. Martin, and C. von Borczyskowski, "Emission intermittency in silicon nanocrystals", *Phys. Rev. B* **70** (2004) 115314.

[4] A. P. Alivisatos, "Perspectives on the physical chemistry of semiconductor nanocrystals", *J. Phys. Chem.* **100** (1996) 13226–13239.

[5] S. Gaponenko, *Optical properties of semiconductor nanocrystals*, Cambridge University Press (1998).

[6] T. Vossmeyer, L. Katsikas, M. Giersig, I. G. Popovic, K. Diesner, A. Chemseddine, A. Eychmuller, and H. Weller, "CdS nanoclusters - synthesis, characterization, size-dependent oscillator strength, temperature shift of the excitonic-transition energy, and reversible absorbency shift", *J. Phys. Chem.* **98** (1994) 7665–7673.

[7] M. A. Kastner, "The single-electron transistor", *Rev. Mod. Phys.* **64** (1992) 849–858.

[8] B. C. Hess, I. G. Okhrimenko, R. C. Davis, B. C. Stevens, Q. A. Schulzke, K. C. Wright, C. D. Bass, C. D. Evans, and S. L. Summers, "Surface transformation and photoinduced recovery in CdSe nanocrystals", *Phys. Rev. Lett.* **86** (2001) 3132–3135.

[9] E. Rabani, "Structure and electrostatic properties of passivated CdSe nanocrystals", *J. Chem. Phys.* **115** (2001) 1493–1497.

[10] S. Hohng and T. Ha, "Near-complete suppression of quantum dot blinking in ambient conditions", *J. Am. Chem. Soc.* **126** (2004) 1324–1325.

[11] M. A. Hines and P. Guyot-Sionnest, "Synthesis and characterization of strongly luminescing ZnS-Capped CdSe nanocrystals", *J. Phys. Chem.* **100** (1996) 468–471.

[12] M. Nirmal, B. O. Dabbousi, M. G. Bawendi, J. J. Macklin, J. K. Trautman, T. D. Harris, and L. E. Brus, "Fluorescence intermittency in single cadmium selenide nanocrystals", *Nature* **383** (1996) 802–804.

[13] C. Brunel, B. Lounis, P. Tamarat, and M. Orrit, "Triggered source of single photons based on controlled single molecule fluorescence", *Phys. Rev. Lett.* **83** (1999) 2722–2725.

[14] B. Lounis and W. E. Moerner, "Single photons on demand from a single molecule at room temperature", *Nature* **407** (2000) 491–493.

[15] F. Treussart, R. Alleaume, V. L. Floc'h, L. T. Xiao, J. M. Courty, and J. F. Roch, "Direct measurement of the photon statistics of a triggered single photon source", *Phys. Rev. Lett.* **89** (2002) 093601.

[16] Y. Ebenstein, T. Mokari, and U. Banin, "Fluorescence quantum yield of CdSe/ZnS nanocrystals investigated by correlated atomic-force and single-particle fluorescence microscopy", *Appl. Phys. Lett.* **80** (2002) 4033–4035.

[17] X. Brokmann, E. Giacobino, M. Dahan, and J. P. Hermier, "Highly efficient triggered emission of single photons by colloidal CdSe/ZnS nanocrystals", *Appl. Phys. Lett.* **85** (2004) 712–714.

[18] P. Lodahl, A. F. van Driel, I. S. Nikolaev, A. Irman, K. Overgaag, D. L. Vanmaekelbergh, and W. L. Vos, "Controlling the dynamics of spontaneous emission from quantum dots by photonic crystals", *Nature* **430** (2004) 654–657.

[19] X. Brokmann, L. Coolen, M. Dahan, and J. P. Hermier, "Measurement of the radiative and nonradiative decay rates of single CdSe nanocrystals through a controlled modification of their spontaneous emission", *Phys. Rev. Lett.* **93** (2004) 107403.

[20] F. Koberling, U. Kolb, G. Philipp, I. Potapova, T. Basche, and A. Mews, "Fluorescence anisotropy and crystal structure of individual semiconductor nanocrystals", *J. Phys. Chem. B* **107** (2003) 7463–7471.

[21] H. J. Eisler, V. C. Sundar, M. G. Bawendi, M. Walsh, H. I. Smith, and V. Klimov, "Color-selective semiconductor nanocrystal laser", *Appl. Phys. Lett.* **80** (2002) 4614–4616.

[22] Y. Chan, J. M. Caruge, P. T. Snee, and M. G. Bawendi, "Multiexcitonic two-state lasing in a CdSe nanocrystal laser", *Appl. Phys. Lett.* **85** (2004) 2460–2462.

[23] S. A. Ivanov, J. Nanda, A. Piryatinski, M. Achermann, L. P. Balet, I. V. Bezel, P. O. Anikeeva, S. Tretiak, and V. I. Klimov, "Light amplification using inverted core/shell nanocrystals: Towards lasing in the single-exciton regime", *J. Phys. Chem. B* **108** (2004) 10625–10630.

[24] S. A. Empedocles, R. Neuhauser, K. Shimizu, and M. G. Bawendi, "Photoluminescence from single semiconductor nanostructures", *Adv. Mater.* **11** (1999) 1243–1256.

[25] A. L. Efros, V. A. Kharchenko, and M. Rosen, "Breaking the phonon bottleneck in nanometer quantum dots - role of Auger-like processes", *Solid State Commun.* **93** (1995) 281–284.

[26] H. Htoon, J. A. Hollingsworth, R. Dickerson, and V. I. Klimov, "Effect of zero- to one-dimensional transformation on multiparticle Auger recombination in semiconductor quantum rods", *Phys. Rev. Lett.* **91** (2003) 227401.

[27] V. I. Klimov, D. W. McBranch, C. A. Leatherdale, and M. G. Bawendi, "Electron and hole relaxation pathways in semiconductor quantum dots", *Phys. Rev. B* **60** (1999) 13740–13749.

[28] R. D. Schaller and V. I. Klimov, "High efficiency carrier multiplication in PbSe nanocrystals: Implications for solar energy conversion", *Phys. Rev. Lett.* **92** (2004) 186601.

[29] D. J. Binks, D. P. West, S. Norager, and P. O'Brien, "Field-independent grating formation rate in a photorefractive polymer composite sensitized by CdSe quantum dots", *J. Chem. Phys.* **117** (2002) 7335–7341.

[30] J. W. M. Chon, P. Zijlstra, and M. Gu, "Two-photon-induced photoenhancement of densely packed CdSe/ZnSe/ZnS nanocrystal solids and its application to multilayer optical data storage", *Appl. Phys. Lett.* (2004).

[31] M. Achermann, M. A. Petruska, S. Kos, D. L. Smith, D. D. Koleske, and V. I. Klimov, "Energy-transfer pumping of semiconductor nanocrystals using an epitaxial quantum well", *Nature* **429** (2004) 642–646.

[32] G. W. Walker, V. C. Sundar, C. M. Rudzinski, A. W. Wun, M. G. Bawendi, and D. G. Nocera, "Quantum-dot optical temperature probes", *Appl. Phys. Lett.* **83** (2003) 3555–3557.

[33] M. Dahan, S. Levi, C. Luccardini, P. Rostaing, B. Riveau, and A. Triller, "Diffusion dynamics of glycine receptors revealed by single- quantum dot tracking", *Science* **302** (2003) 442–445.

[34] X. Michalet, F. Pinaud, T. D. Lacoste, M. Dahan, M. P. Bruchez, A. P. Alivisatos, and S. Weiss, "Properties of fluorescent semiconductor nanocrystals and their application to biological labeling", *Single Mol.* **2** (2001) 261–276.

[35] R. E. Bailey, A. M. Smith, and S. M. Nie, "Quantum dots in biology and medicine", *Physica E* **25** (2004) 1–12.

[36] M. Bruchez, M. Moronne, P. Gin, S. Weiss, and A. P. Alivisatos, "Semiconductor nanocrystals as fluorescent biological labels", *Science* **281** (1998) 2013–2016.

[37] W. C. W. Chan, D. J. Maxwell, X. H. Gao, R. E. Bailey, M. Y. Han, and S. M. Nie, "Luminescent quantum dots for multiplexed biological detection and imaging", *Curr. Opin. Biotechnol.* **13** (2002) 40–46.

[38] C. A. Leatherdale, W. K. Woo, F. V. Mikulec, and M. G. Bawendi, "On the absorption cross section of CdSe nanocrystal quantum dots", *J. Phys. Chem. B* **106** (2002) 7619–7622.

[39] R. Zondervan, F. Kulzer, S. B. Orlinskii, and M. Orrit, "Photoblinking of rhodamine 6G in poly(vinyl alcohol): Radical dark state formed through the triplet", *J. Phys. Chem. A* **107** (2003) 6770–6776.

[40] J. W. M. Chon, M. Gu, C. Bullen, and P. Mulvaney, "Three-photon excited band edge and trap emission of CdS semiconductor nanocrystals", *Appl. Phys. Lett.* **84** (2004) 4472–4474.

[41] W. C. W. Chan and S. M. Nie, "Quantum dot bioconjugates for ultrasensitive nonisotopic detection", *Science* **281** (1998) 2016–2018.

[42] S. Pathak, S. K. Choi, N. Arnheim, and M. E. Thompson, "Hydroxylated quantum dots as luminescent probes for in situ hybridization", *J. Am. Chem. Soc.* **123** (2001) 4103–4104.

[43] S. Weiss, "Fluorescence spectroscopy of single biomolecules", *Science* **283** (1999) 1676–1683.

[44] C. R. Kagan, C. B. Murray, M. Nirmal, and M. G. Bawendi, "Electronic energy transfer in CdSe quantum dot solids", *Phys. Rev. Lett.* **76** (1996) 1517–1520.

[45] S. A. Empedocles and M. G. Bawendi, "Quantum-confined stark effect in single CdSe nanocrystallite quantum dots", *Science* **278** (1997) 2114–2117.

[46] P. Guyot-Sionnest, M. Shim, C. Matranga, and M. Hines, "Intraband relaxation in CdSe quantum dots", *Phys. Rev. B* **60** (1999) R2181–R2184.

[47] M. Shim, C. J. Wang, and P. Guyot-Sionnest, "Charge-tunable optical properties in colloidal semiconductor nanocrystals", *J. Phys. Chem. B* **105** (2001) 2369–2373.

[48] L. Brus, "Quantum crystallites and nonlinear optics", *Appl. Phys. A-Mater. Sci. Process.* **53** (1991) 465–474.

[49] B. Pejova and I. Grozdanov, "Three-dimensional confinement effects in semiconductor zinc selenide quantum dots deposited in thin-film form", *Mater. Chem. Phys.* **90** (2005) 35–46.

[50] E. Barkai, Y. J. Jung, and R. Silbey, "Theory of single-molecule spectroscopy: Beyond the ensemble average", *Annu. Rev. Phys. Chem.* **55** (2004) 457–507.

[51] G. Binnig and H. Rohrer, "Scanning tunneling microsopy - from birth to adolescence", *Rev. Mod. Phys.* **59** (1987) 615–622.

[52] G. Binnig, C. F. Quate, and C. Gerber, "Atomic force microscope", *Phys. Rev. Lett.* **56** (1986) 930–933.

[53] W. E. Moerner and L. Kador, "Optical detection and spectroscopy of single molecules in a solid", *Phys. Rev. Lett.* **62** (1989) 2535–2538.

[54] M. Orrit and J. Bernard, "Single pentacene molecules detected by fluorescence excitation in a p-terphenyl crystal", *Phys. Rev. Lett.* **65** (1990) 2716–2719.

[55] R. M. Dickson, A. B. Cubitt, R. Y. Tsien, and W. E. Moerner, "On/off blinking and switching behaviour of single molecules of green fluorescent protein", *Nature* **388** (1997) 355–358.

[56] G. Jung, J. Wiehler, W. Göhde, J. Tittel, T. Basché, B. Steipe, and C. Bräuchle, "Confocal microscopy of single molecules of the green fluorescent protein", *Bioimaging* **6** (1998) 54–61.

[57] A. M. van Oijen, M. Ketelaars, J. Kohler, T. J. Aartsma, and J. Schmidt, "Unraveling the electronic structure of individual photosynthetic pigment-protein complexes", *Science* **285** (1999) 400–402.

[58] D. A. Vanden Bout, W. T. Yip, D. H. Hu, D. K. Fu, T. M. Swager, and P. F. Barbara, "Discrete intensity jumps and intramolecular electronic energy transfer in the spectroscopy of single conjugated polymer molecules", *Science* **277** (1997) 1074–1077.

[59] A. Hartschuh, H. N. Pedrosa, L. Novotny, and T. D. Krauss, "Simultaneous fluorescence and Raman scattering from single carbon nanotubes", *Science* **301** (2003) 1354–1356.

[60] W. E. Moerner, T. Plakhotnik, T. Irngartinger, M. Croci, V. Palm, and U. P. Wild, "Optical probing of single molecules of terrylene in a Shpol'skii matrix: A two-state single-molecule optical switch", *J. Phys. Chem.* **98** (1994) 7382–7389.

[61] A. Bloess, Y. Durand, M. Matsushita, R. Verberk, E. J. J. Groenen, and J. Schmidt, "Microscopic structure in a Shpol'skii system: A single-molecule study of dibenzanthanthrene in n-tetradecane", *J. Phys. Chem. A* **105** (2001) 3016–3021.

[62] F. Kulzer and M. Orrit, "Single-molcule optics", *Annu. Rev. Phys. Chem.* **54** (2004) 585–611.

[63] J. B. Pawley (editor), *Handbok of biological confocal microscopy*, Plenum Press, New York (1995).

[64] M. Dahan, T. Laurence, F. Pinaud, D. S. Chemla, A. P. Alivisatos, M. Sauer, and S. Weiss, "Time-gated biological imaging by use of colloidal quantum dots", *Opt. Lett.* **26** (2001) 825–827.

[65] S. A. Blanton, M. A. Hines, and P. GuyotSionnest, "Photoluminescence wandering in single CdSe nanocrystals", *Appl. Phys. Lett.* **69** (1996) 3905–3907.

[66] S. A. Empedocles, D. J. Norris, and M. G. Bawendi, "Photoluminescence spectroscopy of single CdSe nanocrystallite quantum dots", *Phys. Rev. Lett.* **77** (1996) 3873–3876.

[67] M. E. Schmidt, S. A. Blanton, M. A. Hines, and P. GuyotSionnest, "Size-dependent two-photon excitation spectroscopy of CdSe nanocrystals", *Phys. Rev. B* **53** (1996) 12629–12632.

[68] W. E. Moerner, "Polymer luminescence - those blinking single molecules", *Science* **277** (1997) 1059–1060.

[69] J. Bernard, L. Fleury, H. Talon, and M. Orrit, "Photon bunching in the fluorescence from single molecules: a probe for intersystem crossing", *J. Chem. Phys.* **98** (1993) 850–859.

[70] H. P. Lu and X. S. Xie, "Single-molecule kinetics of interfacial electron transfer", *J. Phys. Chem. B* **101** (1997) 2753–2757.

[71] T. Christ, F. Kulzer, P. Bordat, and T. Basché, "Watching the photo-oxidation of a single aromatic hydrocarbon molecule", *Angew. Chem.-Int. Edit.* **40** (2001) 4192–4195.

[72] L. Fleury, A. Zumbusch, M. Orrit, R. Brown, and J. Bernard, "Spectral diffusion and individual two-level systems probed by fluorescence of single terrylene molecules in a polyethylene matrix", *J. Lumin.* **56** (1993) 15–28.

[73] L. A. Deschenes and D. A. Vanden Bout, "Single-molecule studies of heterogeneous dynamics in polymer melts near the class transition", *Science* **292** (2001) 255–258.

[74] X. S. Xie, "Single-molecule approach to dispersed kinetics and dynamic disorder: Probing conformational fluctuation and enzymatic dynamics", *J. Chem. Phys.* **117** (2002) 11024–11032.

[75] J. A. Astrom, R. P. Linna, J. Timonen, P. F. Moller, and L. Oddershede, "Exponential and power-law mass distributions in brittle fragmentation", *Phys. Rev. E* **70** (2004) 026104.

[76] R. Albert and A. L. Barabasi, "Statistical mechanics of complex networks", *Rev. Mod. Phys.* **74** (2002) 47–97.

[77] S. Eubank, H. Guclu, V. S. A. Kumar, M. V. Marathe, A. Srinivasan, Z. Toroczkai, and N. Wang, "Modelling disease outbreaks in realistic urban social networks", *Nature* **429** (2004) 180–184.

[78] W. Cook and P. Ormerod, "Power law distribution of the frequency of demises of US firms", *Physica A* **324** (2003) 207–212.

[79] J. P. Bouchaud, "An introduction to statistical finance", *Physica A* **313** (2002) 238–251.

[80] M. G. Bawendi, "Synthesis and spectroscopy of II-VI quantum dots: An overview", in E. Burnstein and C. Weisbuch (editors), "Confined Electrons and Photons", Plenum Press (1995), 339–356.

[81] C. D. Donega, S. G. Hickey, S. F. Wuister, D. Vanmaekelbergh, and A. Meijerink, "Single-step synthesis to control the photoluminescence quantum yield and size dispersion of CdSe nanocrystals", *J. Phys. Chem. B* **107** (2003) 489–496.

[82] W. E. Moerner and M. Orrit, "Illuminating single molecules in condensed matter", *Science* **283** (1999) 1670–1676.

[83] H. P. Lu and X. S. Xie, "Single-molecule spectral fluctuations at room temperature", *Nature* **385** (1997) 143–146.

[84] S. Kummer, T. Basché, and C. Bräuchle, "Terrylene in p-terphenyl: a novel single crystalline system for single molecule spectroscopy at low temperatures", *Chem. Phys. Lett.* **229** (1994) 309–316, 1995. *ibid.* 232:414.

[85] M. Kuno, D. P. Fromm, H. F. Hamann, A. Gallagher, and D. J. Nesbitt, ""on"/"off" fluorescence intermittency of single semiconductor quantum dots", *J. Chem. Phys.* **115** (2001) 1028–1040.

[86] K. T. Shimizu, R. G. Neuhauser, C. A. Leatherdale, S. A. Empedocles, W. K. Woo, and M. G. Bawendi, "Blinking statistics in single semiconductor nanocrystal quantum dots", *Phys. Rev. B* **63** (2001) 205316.

[87] A. Molski, J. Hofkens, T. Gensch, N. Boens, and F. De Schryver, "Theory of time-resolved single-molecule fluorescence spectroscopy", *Chem. Phys. Lett.* **318** (2000) 325–332.

[88] A. Molski, "Photon-counting distribution of fluorescence from a blinking molecule", *Chem. Phys. Lett.* **324** (2000) 301–306.

[89] V. Barsegov, V. Chernyak, and S. Mukamel, "Multitime correlation functions for single molecule kinetics with fluctuating bottlenecks", *J. Chem. Phys.* **116** (2002) 4240–4251.

[90] V. Barsegov and S. Mukamel, "Multidimensional spectroscopic probes of single molecule fluctuations", *J. Chem. Phys.* **117** (2002) 9465–9477.

[91] H. Yang and X. S. Xie, "Probing single-molecule dynamics photon by photon", *J. Chem. Phys.* **117** (2002) 10965–10979.

[92] V. Barsegov and S. Mukamel, "Probing single molecule kinetics by photon arrival trajectories", *J. Chem. Phys.* **116** (2002) 9802–9810.

[93] R. Loudon, *The quantum theory of light*, Oxford University Press, Oxford, 3rd edition (1983).

[94] T. Basché, W. E. Moerner, M. Orrit, and H. Talon, "Photon antibunching in the fluorescence of a single dye molecule trapped in a solid", *Phys. Rev. Lett.* **69** (1992) 1516–1519.

[95] S. Reynaud, "Resonance fluorescence - the dressed atom approach", *Ann. Phys.-Paris* **8** (1983) 315–370.

[96] L. Fleury, J. M. Segura, G. Zumofen, B. Hecht, and U. P. Wild, "Nonclassical photon statistics in single-molecule fluorescence at room temperature", *Phys. Rev. Lett.* **84** (2000) 1148–1151.

[97] P. Michler, A. Imamoğlu, M. D. Mason, P. J. Carson, G. F. Strouse, and S. K. Buratto, "Quantum correlation among photons from a single quantum dot at room temperature", *Nature* **406** (2000) 968–970.

[98] B. Lounis, H. A. Bechtel, D. Gerion, P. Alivisatos, and W. E. Moerner, "Photon antibunching in single CdSe/ZnS quantum dot fluorescence", *Chem. Phys. Lett.* **329** (2000) 399–404.

[99] G. Messin, J. P. Hermier, E. Giacobino, P. Desbiolles, and M. Dahan, "Bunching and antibunching in the fluorescence of semiconductor nanocrystals", *Opt. Lett.* **26** (2001) 1891–1893.

[100] R. Short and L. Mandel, "Observation of sub-poissonian photon statistics", *Phys. Rev. Lett.* **51** (1983) 384–387.

[101] Y. R. Shen, *The principles of nonlinear optics*, Wiley, New York (1984).

[102] R. Verberk and M. Orrit, "Photon statistics in the fluorescence of single molecules and nanocrystals: Correlation functions versus distributions of on- and off-times", *J. Chem. Phys.* **119** (2003) 2214–2222.

[103] M. Boguna, A. M. Berezhkovskii, and G. H. Weiss, "Residence time densities for non-Markovian systems. (I). The two-state system", *Physica A* **282** (2000) 475–485.

[104] X. Brokmann, J. P. Hermier, G. Messin, P. Desbiolles, J. P. Bouchaud, and M. Dahan, "Statistical aging and nonergodicity in the fluorescence of single nanocrystals", *Phys. Rev. Lett.* **90** (2003) 120601.

[105] G. Margolin and E. Barkai, "Aging correlation functions for blinking nanocrystals, and other on-off stochastic processes", *J. Chem. Phys.* **121** (2004) 1566–1577.

[106] Y. Jung, E. Barkai, and R. J. Silbey, "Lineshape theory and photon counting statistics for blinking quantum dots: a Lévy walk process", *Chem. Phys.* **284** (2002) 181–194.

[107] R. Verberk, A. M. van Oijen, and M. Orrit, "Simple model for the power-law blinking of single semiconductor nanocrystals", *Phys. Rev. B* **66** (2002) 233202.

[108] M. O. Vlad, F. Moran, and J. Ross, "Lifetimes and on-off distributions for single-molecule kinetics. Stochastic approach and extraction of information from experimental data", *Chem. Phys.* **287** (2003) 83–90.

[109] A. P. Alivisatos, "Semiconductor clusters, nanocrystals, and quantum dots", *Science* **271** (1996) 933–937.

[110] B. O. Dabbousi, J. RodriguezViejo, F. V. Mikulec, J. R. Heine, H. Mattoussi, R. Ober, K. F. Jensen, and M. G. Bawendi, "(CdSe)ZnS core-shell quantum dots: Synthesis and characterization of a size series of highly luminescent nanocrystallites", *J. Phys. Chem. B* **101** (1997) 9463–9475.

[111] I. H. Chung and M. G. Bawendi, "Relationship between single quantum-dot intermittency and fluorescence intensity decays from collections of dots", *Phys. Rev. B* **70** (2004) 165304.

[112] A. L. Efros and M. Rosen, "Random telegraph signal in the photoluminescence intensity of a single quantum dot", *Phys. Rev. Lett.* **78** (1997) 1110–1113.

[113] O. Madelung (editor), *Numerical data and functional relationships in science and technology*, volume III-17: semiconductors, Springer Verlag, Berlin (1988).

[114] T. D. Krauss, S. O'Brien, and L. E. Brus, "Charge and photoionization properties of single semiconductor nanocrystals", *J. Phys. Chem. B* **105** (2001) 1725–1733.

[115] O. Cherniavskaya, L. W. Chen, and L. Brus, "Imaging the photoionization of individual CdSe/CdS core-shell nanocrystals on n- and p-type silicon substrates with thin oxides", *J. Phys. Chem. B* **108** (2004) 4946–4961.

[116] A. Y. Kobitski, C. D. Heyes, and G. U. Nienhaus, "Total internal reflection fluorescence microscopy - a powerful tool to study single quantum dots", *Appl. Surf. Sci.* **234** (2004) 86–92.

[117] W. G. J. H. M. V. Sark, P. L. T. M. Frederix, D. V. D. Heuvel, M. A. H. Asselbergs, I. Senf, and H. C. Gerritsen, "Fast imaging of single molecules and nanoparticles by wide-field microscopy and spectrally resolved confocal microscopy", *Single Mol.* **1** (2000) 291–298.

[118] F. Koberling, A. Mews, and T. Basche, "Oxygen-induced blinking of single CdSe nanocrystals", *Adv. Mater.* **13** (2001) 672–676.

[119] J. B. Li and L. W. Wang, "First principle study of core/shell structure quantum dots", *Appl. Phys. Lett.* **84** (2004) 3648–3650.

[120] D. Schooss, A. Mews, A. Eychmuller, and H. Weller, "Quantum-dot quantum-well CdS/HgS/CdS - theory and experiment", *Phys. Rev. B* **49** (1994) 17072–17078.

[121] K. T. Shimizu, W. K. Woo, B. R. Fisher, H. J. Eisler, and M. G. Bawendi, "Surface-enhanced emission from single semiconductor nanocrystals", *Phys. Rev. Lett.* **89** (2002) 117401.

[122] W. G. J. H. M. van Sark, P. L. T. M. Frederix, A. A. Bol, H. C. Gerritsen, and A. Meijerink, "Blueing, bleaching, and blinking of single CdSe/ZnS quantum dots", *ChemPhysChem* **3** (2002) 871–879.

[123] R. G. Neuhauser, K. T. Shimizu, W. K. Woo, S. A. Empedocles, and M. G. Bawendi, "Correlation between fluorescence intermittency and spectral diffusion in single semiconductor quantum dots", *Phys. Rev. Lett.* **85** (2000) 3301–3304.

[124] M. G. Bawendi, P. J. Carroll, W. L. Wilson, and L. E. Brus, "Luminescence properties of CdSe quantum crystallites - resonance between interior and surface localized states", *J. Chem. Phys.* **96** (1992) 946–954.

[125] A. Franceschetti and A. Zunger, "Optical transitions in charged CdSe quantum dots", *Phys. Rev. B* **62** (2000) R16287–R16290.

[126] S. B. Orlinskii and J. Schmidt, private communications.

[127] H. Htoon, P. J. Cox, and V. I. Klimov, "Structure of excited-state transitions of individual semiconductor nanocrystals probed by photoluminescence excitation spectroscopy", *Phys. Rev. Lett.* **93** (2004) 187402.

[128] G. Schlegel, J. Bohnenberger, I. Potapova, and A. Mews, "Fluorescence decay time of single semiconductor nanocrystals", *Phys. Rev. Lett.* **88** (2002) 137401.

[129] M. Lippitz, F. Kulzer, and M. Orrit, "Statistical evaluation of single nano-object fluorescence", *submitted to Chem. Phys. Chem.* (2005).

[130] J. Muller, J. M. Lupton, A. L. Rogach, J. Feldmann, D. V. Talapin, and H. Weller, "Air-induced fluorescence bursts from single semiconductor nanocrystals", *Appl. Phys. Lett.* **85** (2004) 381–383.

[131] M. Pelton, D. G. Grier, and P. Guyot-Sionnest, "Characterizing quantum-dot blinking using noise power spectra", *Appl. Phys. Lett.* **85** (2004) 819–821.

[132] M. Kuno, D. P. Fromm, S. T. Johnson, A. Gallagher, and D. J. Nesbitt, "Modeling distributed kinetics in isolated semiconductor quantum dots", *Phys. Rev. B* **67** (2003) 125304.

[133] C. G. V. de Walle and J. Neugebauer, "Universal alignment of hydrogen levels in semiconductors, insulators and solutions", *Nature* **423** (2003) 626–628.

[134] D. I. Chepic, A. L. Efros, A. I. Ekimov, M. G. Vanov, V. A. Kharchenko, I. A. Kudriavtsev, and T. V. Yazeva, "Auger ionization of semiconductor quantum drops in a glass matrix", *J. Lumines.* **47** (1990) 113–127.

[135] U. Banin, M. Bruchez, A. P. Alivisatos, T. Ha, S. Weiss, and D. S. Chemla, "Evidence for a thermal contribution to emission intermittency in single CdSe/CdS core/shell nanocrystals", *J. Chem. Phys.* **110** (1999) 1195–1201.

[136] R. Williams, "Photoemission of electrons from silicon into silicon dioxide", *Phys. Rev.* **140** (1965) A569.

[137] T. van Woudenbergh, J. Wildeman, P. W. M. Blom, J. J. A. M. Bastiaansen, and B. M. W. Langeveld-Voss, "Electron-enhanced hole injection in blue polyfluorene-based polymer light-emitting diodes", *Adv. Funct. Mater.* **14** (2004) 677–683.

[138] S. B. Orlinskii, J. Schmidt, E. J. J. Groenen, P. G. Baranov, C. de Mello Donega, and A. Meijerink, "Shallow donors in semiconductor nanoparticles and the limit of the effective mass approximation", *accepted for publication in Phys. Rev. Lett* (2005).

[139] D. V. Melnikov and J. R. Chelikowsky, "Quantum confinement in phosphorus-doped silicon nanocrystals", *Phys. Rev. Lett.* **92** (2004) 046802.

[140] R. T. Cox and J. J. Davies, "Electron-hole exchange interaction for donor-acceptor pairs in CdS determined as a function of separation distance by optically detected magnetic-resonance", *Phys. Rev. B* **34** (1986) 8591–8610.

Statistiek van fotonen en het blinken van individuele halfgeleider nanokristallen

Dit is een vereenvoudigde samenvatting van het onderzoek dat in dit proefschrift is beschreven. De twee vraagstukken die hierin worden behandeld zijn gerelateerd. Het eerste draait om het ritme waarmee lichtdeeltjes (fotonen) door een enkel molecuul of nanokristal worden uitgezonden onder continue belichting. Na het oplossen van enige wiskundige problemen ontstond een veelzijdig en praktisch raamwerk dat helpt om experimentele data te interpreteren en om de resultaten van verschillende experimenten te vergelijken. Het tweede vraagstuk draait om de emissie van halfgeleider nanokristallen. We hebben niet alleen metingen gedaan aan deze deeltjes, maar ook een model ontwikkeld om de waarnemingen te verklaren. Om deze samenvatting voor een breed publiek toegankelijk te maken, begin ik met een korte uitleg van de noodzakelijke begrippen.

Moleculen

"Een molecuul is het kleinste deeltje van een stof, dat nog alle eigenschappen van die stof heeft." Deze regel leren we op de middelbare school en is misschien wel de meest beroemde regel van alle scheikundelessen. Eigenlijk zijn de eigenschappen waarover hier wordt gesproken niet meer terug te vinden bij individuele moleculen en zou deze regel beter kunnen luiden: "Een molecuul is het kleinste bouwsteentje van een stof waarin deze stof kan worden opgedeeld, zodanig dat het samenvoegen van de bouwsteentjes weer de oorspronkelijke stof oplevert." Het bekendste voorbeeld is het watermolecuul, dat wordt aangeduid met H_2O. Wie verder graaft, ontdekt dat een molecuul weer is opgebouwd uit nog kleinere bouwsteentjes: de atomen. In het voorbeeld van water is een molecuul opgebouwd uit een zuurstofatoom (aangeduid met "O") en twee waterstofatomen (aangeduid met "H"). Nu is ook duidelijk waar de afkorting H_2O vandaan komt: twee atomen waterstof plus een atoom zuurstof[5]. Het aantal soorten atomen is beperkt, en deze soorten worden ook de

[5]Deze aanduiding wordt daarom ook wel eens als naam gebruikt voor water als materiaal.

elementen genoemd (omdat lange tijd werd gedacht dat atomen niet zijn op te splitsen, en dus elementaire deeltjes zijn). De ruim 100 bekende elementen staan netjes gerangschikt in het bekende "Periodiek systeem der elementen". Met deze bescheiden verzameling elementen zijn echter heel veel verschillende moleculen (en dus materialen) te maken. Een van de grootste verzamelingen is bijvoorbeeld die der organische materialen. Ondanks dat deze materialen bestaan uit moleculen die zijn opgebouwd uit slechts een paar elementen, is de verzameling zeer groot en divers: eiwitten, hout, aardolie/benzine, azijnzuur, polymeren, suiker en alcohol. Hierin komt met name het element koolstof (C) voor en verder vooral zuurstof (O), waterstof (H) en stikstof (N). De verzameling van anorganische materialen, zoals metalen en halfgeleiders, wordt niet gedomineerd door koolstof. Een nog belangrijker verschil is dat deze materialen niet zijn opgebouwd uit moleculen! Om dit te kunnen begrijpen, moeten we eerst iets meer weten over de opbouw van atomen.

Een atoom is opgebouwd uit positief elektrisch geladen deeltjes, neutrale deeltjes en elektrisch negatief geladen deeltjes. Ze heten respectievelijk protonen, neutronen en elektronen. De protonen en neutronen vormen een klontje in het centrum van het atoom. Dit heet de atoomkern. De elektronen, wel 1800 keer lichter dan de protonen en neutronen, cirkelen daar op relatief grote afstand omheen. Stel het eenvoudigweg voor zoals de planeten (o.a. de aarde) om de veel zwaardere zon draaien. Het aantal elektronen is altijd gelijk aan het aantal protonen, zodat een atoom elektrisch neutraal is. De hoeveelheid protonen (of elektronen) bepaalt welk element het is. Waterstof heeft bijvoorbeeld slechts één proton en elektron (en geen neutron) en lood (Pb) heeft 82 protonen en elektronen (en 126 neutronen). De eigenschappen van de elementen worden voor een groot deel bepaald door de paar buitenste, relatief vrij bewegende, elektronen. Dit zijn de valentie-elektronen. De atoomkern met alle sterker gebonden (dieper liggende) elektronen kunnen vereenvoudigd worden voorgesteld als een positief geladen bol. Dit heet een ion. Als atomen een binding aangaan, bijvoorbeeld om een molecuul te vormen, naderen de ionen tot de gewenste onderlinge afstand. De valentie-elektronen van beide atomen vormen een soort plaksel tussen de ionen. Ze zorgen voor precies voldoende aantrekkende en afstotende krachten om de onderlinge afstand tussen de ionen ongeveer constant te houden. Voordat de anorganische materialen (inclusief de halfgeleiders waar dit proefschrift eigenlijk om gaat) aan bod komen, wil ik aan de hand van moleculen een en ander uitleggen over de gebruikte techniek.

Spectroscopie aan individuele moleculen

Door de aantrekkende en afstotende krachten tussen de elektronen en ionen komt een molecuul nooit tot rust. De onderlinge afstanden van de deeltjes variëren continu. Deze trillingen zorgen ervoor dat een molecuul niet makkelijk uit elkaar valt. Hoe hard de deeltjes trillen, bepaalt hoeveel energie er in het molecuul zit opgesloten. Hoeveel energie een molecuul bevat, wordt beschreven door de quantummechanica, de meest revolutionaire natuurkundige theorie van de 20^e eeuw. Op de schaal van moleculen (en kleinere deeltjes) blijkt onze wereld er opeens heel anders uit te zien dan de mens gewend is. Energie blijkt bijvoorbeeld te zijn opgesplitst in kleine, ondeelbare porties, genaamd "quanta". (Vergelijk dit met de definitie van een molecuul: Een watermolecuul is de kleinst mogelijke portie, een quantum, water.) Normaal gesproken merken wij hier niets van omdat zelfs een pluisje al zo groot is en zoveel energie bevat, dat toevoeging van één quantum energie nauwelijks uitmaakt. Maar voor een molecuul is dit wel een aanzienlijke hoeveelheid energie. De toestand waarin een molecuul zo weinig mogelijk energie bevat, en alle trillingen zo klein mogelijk zijn, heet de grondtoestand. Opname van één of meerdere energiequanta brengt het molecuul in een aangeslagen toestand. Dit betekent ook dat het molecuul slechts een paar toestanden kan aannemen, dit zijn de (toegestane) energieniveaus.

Overgangen tussen deze energieniveaus zijn alleen mogelijk als we het molecuul precies de juiste hoeveelheid energie aanbieden (of afpakken). Dit kan eenvoudig worden gedaan met behulp van licht, dat, evenals energie, is gequantiseerd. De deeltjes waaruit licht is opgebouwd heten fotonen. De hoeveelheid energie die in een foton ligt opgeslagen hangt af van de kleur. Een blauw foton bevat bijvoorbeeld meer energie dan een rood foton. De quantummechanica vertelt ons ook dat elk deeltje een golflengte heeft. De golflengte is een nauwkeurige maat voor de kleur van een foton, waarbij een kortere golflengte staat voor meer energie. Een blauw foton met een golflengte van 400 nm bevat bijvoorbeeld twee keer zoveel energie als een rood foton met een golflengte van 800 nm. Omdat de verschillen tussen de toegestane energieniveaus van een molecuul toevallig vergelijkbaar zijn met de energieën die fotonen bevatten, kunnen de energieverschillen met licht worden gemeten. Deze techniek heet spectroscopie. Als de energie van een foton precies gelijk is aan het verschil tussen het energieniveau van een molecuul op dit moment en een ander (hoger) toegestaan energieniveau van het molecuul, kan het foton worden geabsorbeerd. Het foton verdwijnt dan en het molecuul neemt zijn energie over. Het omgekeerde proces is ook mogelijk. Een molecuul kan "terugvallen" naar een lager energieniveau door het energieverschil mee te geven aan een foton.

Dit heet het uitzenden van een foton, luminescentie of emissie. (De bekendste vormen hiervan zijn fluorescentie en fosforescentie.) Om een molecuul een foton te kunnen laten uitzenden, moet het natuurlijk wel eerst naar een hoger energieniveau gebracht worden. Dit heet het aanslaan van een molecuul. Dit kan bijvoorbeeld door er met licht op te schijnen totdat een foton is geabsorbeerd. Er zijn dus twee methoden om met behulp van licht de energieniveaus, of eigenlijk de verschillen tussen de energieniveaus, van een molecuul te onderzoeken. Enerzijds kunnen we met steeds verschillende kleuren licht op een molecuul schijnen en onderzoeken welke kleuren het absorbeert. Anderzijds kunnen we heel nauwkeurig kijken welke kleuren licht een molecuul uitzendt.

Spectroscopie wordt al jaren gebruikt om informatie te verkrijgen over de energieniveaus van moleculen. Maar omdat moleculen maar één foton tegelijkertijd absorberen of uitzenden, zijn steeds vele miljarden moleculen tegelijk nodig om deze absorptie of emissie duidelijk waar te kunnen nemen. Het nadeel hiervan is dat alleen gemiddelde waarden gemeten konden worden. We kunnen bijvoorbeeld uitrekenen hoeveel fotonen worden gedetecteerd en hoeveel moleculen aan dit signaal hebben bijgedragen. Hieruit is het gemiddelde aantal fotonen per molecuul te berekenen. Maar als we naar individuele moleculen zouden kijken, zouden we veel meer informatie kunnen verkrijgen. Dragen bijvoorbeeld alle moleculen evenveel bij aan het totale signaal, of zenden sommige moleculen veel fotonen uit en andere helemaal geen? En verandert dit in de loop van de tijd? Uiteraard zijn alle moleculen van het materiaal dat we onderzoeken identiek. Dat ze zich toch verschillend kunnen gedragen komt doordat ze elk in een andere omgeving zitten. Ik loop bijvoorbeeld in de bergen van Costa Rica een stuk langzamer dan tijdens een wandeling in een Nederlandse polder. Toch ben ik nog steeds dezelfde persoon. In dit voorbeeld is de gemiddelde snelheid van deze twee wandelingen weinig interessant. Maar de individuele metingen kunnen wel iets vertellen over hoe warm het is of hoe steil de bergen zijn. Met andere woorden, door metingen te doen aan individuele moleculen is ook iets te leren over de omgevingen waarin zij zich bevinden. Pas sinds ongeveer 15 jaar is het mogelijk om spectroscopie te doen aan individuele moleculen! Hiervoor waren tenminste drie ontwikkelingen noodzakelijk. Ten eerste zijn heel gevoelige detectoren nodig om het zwakke signaal van een enkele molecuul waar te kunnen nemen. Ten tweede moeten we over een microscoop beschikken die goed genoeg is om een stukje van een preparaat te bekijken dat zo klein is, dat zich daarin slechts één molecuul bevindt van onze interesse. Ten derde was de uitvinding van de laser belangrijk. Hierdoor is het mogelijk om de golflengte van het licht nauwkeurig te variëren en om het licht in een microscoop optimaal te kunnen focusseren.

Halfgeleiders

Anorganische materialen zijn niet opgebouwd uit moleculen, maar uit atomen. Zoals knikkers in een grote bak na enig schudden netjes geordend liggen, liggen de atomen in deze materialen gerangschikt met steeds dezelfde afstand (vaak in alle drie de dimensies (lengte × breedte × hoogte)) tussen twee buren. Als we nauwkeuriger kijken, zijn het eigenlijk de ionen die op deze manier gerangschikt liggen en zwemmen de valentie-elektronen daar tussendoor om overal de gewenste afstanden tussen de ionen te bewaken. De materialen bestaan vaak uit slechts één element, zoals een stuk ijzer bijvoorbeeld alleen uit ijzeratomen (Fe) bestaat[6], of uit slechts enkele elementen, waarbij de atomen van de verschillende elementen elkaar zeer regelmatig afwisselen. Er zijn diverse manieren om de atomen te rangschikken, maar altijd is het patroon regelmatig. Materialen met een dergelijke regelmatige structuur heten kristallijn, of een kristal.

De anorganische materialen zijn onderverdeeld in drie groepen; metalen (of geleiders), halfgeleiders en isolatoren (niet-geleiders). De groep van de metalen is het bekendst: ijzer (Fe), koper (Cu), lood (Pb), goud (Au), enz. Metalen geleiden stroom heel goed. Met name koper wordt daarom gebruikt in elektriciteitssnoeren. De reden dat metalen goed geleiden is te vinden bij de valentie-elektronen. Deze elektronen voelen overal in het materiaal dezelfde ionen. Midden tussen twee ionen zou het elektrische veld precies nul kunnen zijn en is het elektron vrij om te gaan waar het wil. Omdat de elektronen niet meer tot een bepaald ion behoren, hebben ze slechts een klein zetje nodig om zich vrij door het metaal te kunnen bewegen. De elektronen zijn daarom in metalen veel beweeglijker dan in andere materialen. Zo'n zetje kan gegeven worden door een trilling in het metaal (veroorzaakt door warmte), de elektrische spanning die over het stuk metaal wordt gezet ("onder stroom zetten"), of door de energie die een foton kan leveren. Heel anders is het bij de isolatoren, zoals keukenzout[7] (NaCl), zand (SiO_2), diamant (C) en ijzeroxide (roest, Fe_2O_3). Bij de elementen die hierin voorkomen zijn de elektronen veel sterker gebonden aan "hun" atoom. Alleen een flinke zet kan ze vrijmaken, maar ook dat is dan slechts van korte duur. De elektronen kunnen dus niet vrij bewegen, waardoor het materiaal stroom niet goed geleid. De halfgeleiders zitten, zoals de naam al doet vermoeden, tussen deze twee groepen in. Een voorbeeld is silicium (Si) in computers. In principe geleiden deze materialen niet, maar het

[6] Als een materiaal is opgebouwd uit slechts één element, is de naam vaak identiek aan de naam van het element, zoals bij metalen.

[7] Ik beschouw hier alleen de materialen in vaste toestand. De eigenschappen van een materiaal veranderen sterk als het smelt of wordt opgelost.

zetje dat elektronen nodig hebben om zich vrij te kunnen gaan bewegen is veel kleiner dan bij de isolatoren. De benodigde hoeveelheid energie kan nog juist worden geleverd door een foton. Maar ook het verhogen van de temperatuur of het aanbrengen van een spanning is voldoende om de elektronen vrij te maken. Op deze manieren kunnen vrij veel elektronen worden vrijgemaakt en kan de geleiding van een halfgeleider opeens heel goed zijn. (Overigens geleiden halfgeleiders pas echt goed als ze met opzet worden verontreinigd met andere elementen.)

Halfgeleider nanokristallen

De halfgeleiders die in dit proefschrift worden gebruikt zijn Cadmiumselenide (CdSe), cadmiumsulfide (CdS) en zinksulfide (ZnS). Toch komen de eigenschappen van deze materialen nauwelijks aan bod! Dit komt omdat de stukjes halfgeleider die we bestudeerd hebben zo klein zijn, dat de eigenschappen heel anders zijn dan de eigenschappen van een groot stuk. De deeltjes zijn slechts een paar nanometer groot (1 meter = 1000 millimeter = 1.000.000.000 nanometer), maar de atomen zijn nog netjes gerangschikt zoals bij kristallen. Ze worden daarom nanokristallen genoemd. Bij deze afmetingen zijn de energieniveaus weer bepaald door de quantummechanica, net als bij moleculen. De nanokristallen kunnen slechts een paar verschillende energieniveaus aannemen. De verschillen hiertussen kunnen worden onderzocht met behulp van spectroscopie. Door de belangrijke rol van de quantisatie, worden nanokristallen ook quantum dots genoemd. De emissie van nanokristallen is sterk genoeg om ze individueel waar te kunnen nemen.

De energie van een geabsorbeerd foton wordt overgedragen op een van de elektronen in het nanokristal. Dit elektron kan zich nu vrij(er) bewegen door het materiaal en zal in het algemeen zijn oorspronkelijke positie verlaten. Op de plaats waar het elektron vandaan komt, ontstaat lokaal een positieve lading, omdat daar het evenwicht tussen positieve en negatieve ladingen is verstoord. Het is gebruikelijk om de afwezigheid van een elektron aan te duiden met de aanwezigheid van een gat. Na enige tijd zullen het elektron en het gat elkaar weer vinden (geholpen door de aantrekkende kracht tussen negatieve en positieve ladingen). In een proces genaamd recombinatie verdwijnen het elektron en het gat en wordt de energie die hierbij vrijkomt uitgezonden als een foton. Op deze manier kan een nanokristal licht uitzenden, luminesceren. Het onderzoek in dit proefschrift richt zich op deze vorm van luminescentie van halfgeleider nanokristallen.

We onderscheiden hierbij twee typen nanokristallen: met en zonder be-

schermlaag ("capping layer"). Nanokristallen zonder beschermlaag, ("uncapped nanocrystals", afgekort: uncapped NC's) bestaan uit een klein, puur bolletje CdS of CdSe. De nanokristallen met beschermlaag ("capped nanocrystals", afgekort: capped NC's) bestaan meestal uit CdSe met daaromheen een dunne schil van ZnS van slechts enkele atomen dik. Overigens zijn beide soorten omgeven door een laagje organische moleculen om ze te beschermen en op te kunnen lossen.

Blinken

Onderzoek aan individuele nanokristallen heeft aangetoond dat de intensiteit van hun luminescentie fluctueert in de loop van de tijd! Ook als ze continu met een stabiele laser worden aangeslagen. De intensiteit blijkt te fluctueren tussen slechts twee intensiteitsniveaus: De luminescentie is sterk (vergeleken met individuele moleculen) of (bijna) nul. Zie voor een voorbeeld Figuur 1.1 op pagina 2. Dit lijkt op het knipperen van de richtingaanwijzer van een auto. Het verschil is echter dat de duur van de perioden met sterke of zwakke luminescentie ook varieert. De duur van een periode van sterke luminescentie (dit noemen we een aan-tijd) kan variëren van een microseconde (1 miljoenste deel van een seconde) tot enkele minuten. Periodes zonder emissie (dit noemen we uit-tijden) variëren op dezelfde wijze. Het fluctueren van de intensiteit van de luminescentie heet blinken. Het blinken van individuele moleculen is in veel gevallen al verklaard (en een van de bekendste voorbeelden van verschijnselen die pas werden ontdekt na de introductie van spectroscopie aan individuele moleculen), maar wij willen graag begrijpen waarom ook nanokristallen dit gedrag vertonen.

In verband hiermee moeten we ook leren begrijpen waarom de verdelingen van de aan- en uit-tijden van nanokristallen zo bijzonder zijn. Een verdeling is een soort samenvatting van een meting. Bijvoorbeeld een verdeling van aan-tijden vertelt hoe lang alle aan-tijden duurden. Voor een richtingaanwijzer is dit heel eenvoudig: alle aan-tijden duren 0.1 seconde. Voor een nanokristal is dit heel anders: aan-tijden duren vaak maar heel kort (bijvoorbeeld 0.01 seconde), soms wat langer (1 seconde) en heel soms heel lang (2 minuten). De verdelingen van aan- en uit-tijden die voor nanokristallen zijn waargenomen, zijn wezenlijk anders dan de verdelingen die voor moleculen zijn waargenomen, en wijzen op een bijzondere vorm van statistiek. Het begrijpen van het blinken van nanokristallen en deze bijzondere vorm van statistiek zijn hiermee verwante problemen geworden. In de volgende twee paragrafen laat ik zien hoe wij deze vraagstukken hebben aangepakt.

Statistiek van fotonen

Het ritme waarmee fotonen door een molecuul of nanokristal worden uitgezonden, kan op verschillende manieren worden onderzocht. De eerste methode is gebaseerd op het meten van de duur van de aan- en uit-tijden, zoals hierboven besproken. De tweede methode is gebaseerd op het meten van de tijd die verstrijkt tussen de detectie van elke twee fotonen. Dus de tijd die verstreek tussen de detectie van foton 1 en foton 2, tussen 1 en 3, 1 en 4, maar ook tussen 2 en 3, 2 en 4, enz. Deze miljoenen tijden samen zijn evenredig aan de zogenaamde correlatie functie. Het is echter niet direct eenvoudig in te zien of deze twee methoden dezelfde informatie opleveren, en of de verdelingen vertaald kunnen worden naar een correlatie functie of andersom. In hoofdstuk 3 geven we een wiskundige afleiding van de formules waarmee deze vertalingen uitgevoerd kunnen worden. Naast de algemene afleiding geven we specifieke voorbeelden van mogelijke experimentele situaties. Hiermee kunnen experimenten die volgens de twee verschillende methoden zijn uitgevoerd goed met elkaar vergeleken worden. We bespreken ook de voor- en nadelen van de twee methoden. De correlatie functie is bijvoorbeeld meer geschikt om veranderingen op zeer korte tijdschalen te onderzoeken. Bovendien kan de correlatie functie juist informatie geven over trends op zeer lange tijdschalen, die in de verdelingen verloren gaat. Daarnaast laten we zien wat de invloeden zijn van experimentele omstandigheden op de uitkomst van de metingen. Zo blijkt bijvoorbeeld dat het meten van de correlatie functie veel minder wordt gehinderd door de aanwezigheid van een achtergrondsignaal (ruis) of door een lage efficiëntie van detectie, dan het meten van verdelingen van aan- en uit-tijden.

Een belangrijke eigenschap van onze afleiding is dat hij ook geldig is voor Lévy statistiek. Deze statistiek wijkt fundamenteel af van Poisson statistiek, welke bekend is van normale processen, zoals het gooien met een dobbelsteen of het grabbelen uit een pot met knikkers van verschillende kleuren. De opvallendste eigenschap van Lévy statistiek, welke o.a. het ritme beschrijft waarmee nanokristallen fotonen uitzenden, is dat gemiddelde waarden niet zijn gedefinieerd. Met andere woorden, er is geen karakteristieke tijd waarover het *gemeten* gemiddelde overeenkomt met het echte gemiddelde. Dit komt omdat er altijd een (heel kleine) kans bestaat dat de eerstvolgende meting zo'n vreselijk grote waarde zal geven, dat het gemiddelde significant zou veranderen. Ik zal dit verduidelijken met een voorbeeld.

De uit-tijden van een molecuul duren vaak ongeveer 1 ms (milliseconde), soms 5 ms en heel zelden 20 ms. Om het gemiddelde te bepalen tellen we de duur van 100 uit-tijden bij elkaar op en delen deze totale duur door 100. Hetzelfde gemiddelde zouden we berekenen na 101 of 1000 uit-tijden. Dit is een

voorbeeld van normale, of Poisson, statistiek met een exponentiële verdeling van de uit-tijden. De uit-tijden van een nanokristal hebben een veel bredere verdeling. Veel uit-tijden duren korter dan 1 ms, soms 5 ms of 20 ms, maar er is ook een kans dat een uit-tijd 1000 ms of langer duurt. Als we het gemiddelde berekenen over 100 uit-tijden, kan de uitkomst bijvoorbeeld 10 ms zijn. De som van deze 100 uit-tijden is dan 1000 ms. Er is echter een kans dat de 101-ste uit-tijd net zo lang duurt als de som van de eerste 100 uit-tijden (1000 ms)! Het gemiddelde zou dus opeens bijna twee keer zo groot zijn: 2×1000 ms$/101 \simeq 20$ ms. Zelfs het gemiddelde dat over 1000 of 10000 uit-tijden wordt berekend, kan nog flink veranderen als de 1001-ste of 10001-ste uit-tijd ook meegenomen zou worden. De vraag is dus over hoeveel uit-tijden we moeten middelen. Met andere woorden, hoe lang moet ons experiment duren om een betrouwbare meting te doen. Het antwoord hierop is onbekend. De verdeling van uit-tijden is zo breed, dat hij beschreven kan worden met een machtswet (power law). Er kan geen karakteristieke tijdsduur bepaald worden die het experiment minimaal moet duren voor een correcte meting. Dit is kenmerkend voor Lévy statistiek. Het verschil tussen exponentiële verdelingen en verdelingen volgens een machtswet, is te zien in Figuur 4.2(a). De vierkantjes geven de aan-tijden weer, welke hier een exponentiële verdeling volgen. De rondjes representeren de uit-tijden, welke een brede, machtswet verdeling volgen (let op: beide assen van deze grafiek zijn logaritmisch!).

Model voor het blinken van halfgeleider nanokristallen

Hoofdstukken 4 tot en met 6 concentreren zich op de halfgeleider nanokristallen. Uit eerdere metingen was al gebleken dat de verdelingen van aan- en uit-tijden van capped NC's een machtswet volgen. Maar onze metingen laten zien dat voor uncapped NC's alleen de uit-tijden een machtswet volgen. De aan-tijden volgen een normale, exponentiële verdeling. We hebben een model ontwikkeld om al deze waarnemingen in één keer te beschrijven. Belangrijke eisen hierbij waren dat het model kan verklaren i) hoe een dunne schil zo'n groot verschil in de statistiek van aan-tijden (tussen uncapped NC's en capped NC's) kan veroorzaken en ii) hoe een machtsverdeling van aan-tijden (voor capped NC's) mogelijk is (in het algemeen leiden natuurlijke processen tot exponentiële verdelingen).

Het elektron-gat paar dat wordt gecreëerd door de absorptie van een foton, recombineert meestal onder uitzending van een foton. Dit verklaart de luminescentie van nanokristallen. Er kan echter iets met het nanokristal gebeuren

waardoor het niet langer in staat is om licht uit te zenden. Het kan bijvoorbeeld zijn dat het elektron weglekt naar de omgeving. Het evenwicht tussen positieve en negatieve ladingen is nu verstoord, er is immers sprake van een gat in het centrum van het nanokristal, waardoor luminescentie niet langer mogelijk is. Omdat het elektron op ieder willekeurig moment kan weglekken, is de duur van de aan-tijden exponentieel verdeeld. (Een willekeurig ("random") process leidt in het algemeen tot Poisson statistiek.) Het elektron kan ook weer terugkeren naar het nanokristal en recombineren met het gat. Hiermee is het evenwicht tussen positieve en negatieve lading hersteld, komt een einde aan de uit-tijd en is luminescentie weer mogelijk. Als we veronderstellen dat het elektron verschillende logeeradressen in de omgeving heeft, waar het soms kort verblijft en soms heel lang, is het mogelijk te verklaren waarom de uit-tijden zo'n brede (machtswet)verdeling hebben. Het blinken van uncapped NC's lijkt hiermee te kunnen worden verklaard.

Tot zover komt ons model overeen met bestaande vermoedens dat een neutraal (evenveel positieve als negatieve lading bevattend) nanokristal wel kan luminesceren, maar een geladen (meer of minder positieve dan negatieve ladingen bevattend) nanokristal niet. Maar wij vermoeden dat de situatie iets ingewikkelder is door de aanwezigheid van de beschermlaag. Naast de twee bovenstaande toestanden, introduceren wij daarom een derde, nieuwe, mogelijke toestand voor capped NC's. Wanneer het elektron naar de omgeving lekt, kan het gat ook in de beschermlaag verblijven. (Ook een gat kan zich door het kristal bewegen, op een manier die doet denken aan schuifpuzzels.) Hoewel het nanokristal nu geladen is, kan het toch luminesceren omdat het centrum neutraal is. De duur van deze nieuwe aan-tijd is vergelijkbaar met de uit-tijden omdat ze wordt bepaald door de verblijfsduur van het elektron buiten het nanokristal. Dit leidt tot een brede (machtswet)verdeling van aan-tijden en verklaart het verschil in blinken tussen capped en uncapped NC's.

Dit is het eerste gedetailleerde model voor het blinken van (twee typen) nanokristallen dat alle waarnemingen kan verklaren. In hoofdstuk 4 wordt het model uitgebreid beschreven en vergeleken met experimentele data. Hoofdstuk 5 gaat over de simulaties die ik heb uitgevoerd om de voorspellingen van het model inzichtelijk te maken. Vermoedelijk is de situatie in werkelijkheid nog wel iets gecompliceerder dan dit model aangeeft, maar het is een goede stap op weg naar een beter begrip van de processen die zich in nanokristallen afspelen.

De invloed van de omgeving op het blinken van nanokristallen

Nanokristallen worden niet alleen bestudeerd vanwege hun interessante eigenschappen of omdat ze kunnen worden gezien als een modelsysteem om iets te leren over de overgang tussen de gewone wereld en de wereld van de quantummechanica. Er zijn ook diverse gebieden waarin nanokristallen een toepassing vinden. Nanokristallen worden bijvoorbeeld toegevoegd aan biologische systemen, welke vervolgens met behulp van microscopie en spectroscopie worden onderzocht. Als bekend is op welke posities de nanokristallen zich hechten, kan met behulp van de luminescentie van de nanokristallen informatie worden verworven over de veranderingen in dit systeem. Deze toepassingen vereisen dat nanokristallen in verschillende omgevingen gebruikt kunnen worden. Maar ons model en andere metingen geven aan dat de omgeving waarschijnlijk een belangrijke invloed heeft op het blinken van de nanokristallen. In hoofdstuk 6 worden daarom enkele metingen beschreven die tot doel hebben de gevoeligheid van nanokristallen voor veranderingen in de omgeving te onderzoeken. We hebben onder andere gekeken naar de invloed van de intensiteit van het laserlicht, de atmosfeer en het materiaal van de omgeving. De informatie die hierbij is verkregen is ook gebruikt om ons model te toetsen. Met name voor het proces dat de bewegingen van het elektron (naar de omgeving en terug naar het nanokristal) bepaald, is deze informatie van belang.

Het tweede aandachtspunt in hoofdstuk 6 is de relatie tussen metingen die worden verricht aan grote groepen (ensembles) en aan individuele nanokristallen. Door de zeer lange tijd waarover nanokristallen onderzocht kunnen worden (tientallen minuten, vergeleken met seconden voor veel moleculen) en de bijzondere statistiek is het mogelijk met ensemblemetingen nauwkeurige informatie te verkrijgen over het blinken van nanokristallen. Ik heb eerder gezegd dat informatie over individuele nanokristallen normaal gesproken verloren gaat in een ensemble. Maar de soort statistiek die alle nanokristallen volgen, kan in dit geval al worden bepaald aan de hand van ensemblemetingen. Het verband tussen de ensemblemetingen enerzijds en de verdelingen van aan- en uit-tijden van individuele nanokristallen anderzijds, hebben wij zowel wiskundig als experimenteel aangetoond.

List of Publications

- R. Verberk, J. W. M. Chon, M. Gu, and M. Orrit, "Environment-dependent blinking of single semiconductor nanocrystals and statistical aging of ensembles", Physica E **26** (2005) 19–23.
- R. Verberk and M. Orrit, "Photon statistics in the fluorescence of single molecules and nanocrystals: Correlation functions versus distributions of on- and off-times", J. Chem. Phys **119** (2003) 2214–2222.
- R. Verberk, A. M. van Oijen, and M. Orrit, "Simple model for the power-law blinking of single semiconductor nanocrystals", Phys. Rev. B **66** (2002) 233202.
- A. M. van Oijen, R. Verberk, Y. Durand, J. Schmidt, J. N. J. van Lingen, A. A. Bol, and A. Meijerink, "Continuous-wave two-photon excitation of individual CdS nanocrystallites", Appl. Phys. Lett. **79** (2001) 830–832.
- A. Bloess, Y. Durand, M. Matsushita, R. Verberk, E. J. J. Groenen, and J. Schmidt, "Microscopic structure in a Shpol'skii system: A single-molecule study of dibenzanthanthrene in n-tetradecane", J. Phys. Chem. A **105** (2001) 3016–3021.
- A. van Duijn-Arnold, J. Mol, R. Verberk, J. Schmidt, E. N. Mokhov, and P. G. Baranov, "The spatial distribution of the electronic wave function of the shallow boron acceptor in 4H- and 6H-SiC", Materials Science Forum **338-3** (2000) 799-803.
- A. van Duijn-Arnold, J. Mol, R. Verberk, J. Schmidt, E. N. Mokhov, and P. G. Baranov, "Spatial distribution of the electronic wave function of the shallow boron acceptor in 4H- and 6H-SiC", Phys. Rev. B **60** (1999) 15829–15847.

Curriculum Vitae

van Rogier Verberk, geboren op 19 oktober 1976 te Papendrecht.

In 1995 behaalde ik mijn VWO-diploma aan het Willem de Zwijger College te Papendrecht en begon ik aan de studie natuurkunde aan de Universiteit Leiden. Mijn afstudeerstage verrichtte ik in de werkgroep onder leiding van prof.dr. J. Schmidt. Tijdens deze stage heb ik met behulp van microscopie en spectroscopie bij lage temperaturen onderzoek gedaan aan het Shpol'skii-effect, waarbij individuele moleculen fungeerden als nanoprobes. In april 2000 heb ik het doctoraal examen afgelegd.

In mei 2000 trad ik als onderzoeker in opleiding in dienst bij de Stichting voor Fundamenteel Onderzoek der Materie (FOM). Mijn werkzaamheden verrichtte ik in de werkgroep MoNOS (Molecular NanoOptics and Spins), onder leiding van prof.dr. J. Schmidt en later prof.dr. M. Orrit. Centraal in mijn onderzoek stonden anorganische materialen, die ik heb onderzocht met technieken die bekend zijn uit de spectroscopie en microscopie aan individuele moleculen. Dit resulteerde in een model voor het blinken ("intermittency") van halfgeleider nanokristallen, ondersteund door simulaties en experimentele data. Daarnaast heb ik een wiskundig raamwerk opgesteld waarin de statistiek wordt beschreven die relevant is voor fotonen die door een individueel molecuul of nanokristal worden uitgezonden. Mijn bijdrage aan het onderwijs bestond uit het begeleiden van studenten bij de practica "Digitale signaalverwerking en programmeren in LabVIEW" en "Optisch pompen in rubidium".

Nawoord

Met het voltooien van dit proefschrift sluit ik een decennium af dat voor mij in het teken stond van de natuurkunde en de stad Leiden. De relatie tussen deze stad en wetenschap komt voor mij het best tot uiting in de werkgroep MoNOS. Hoewel er veel is veranderd in de jaren dat ik deel uit mocht maken van deze groep, zijn een aantal pijlers gelukkig niet veranderd. Ik heb genoten en geleerd van de interessante wetenschap, de gezellige atmosfeer en de aanwezigheid van Edgar Groenen.

Met veel genoegen heb ik ook specialisten aan het werk gezien, zoals ze steeds zeldzamer worden. Ik ben zeer dankbaar voor de hulp van Arno, Bert, Harmen en Jos, zonder wie ik nauwelijks aan onderzoek zou zijn toegekomen. Hun kennis lijkt onuitputtelijk op het gebied van computers, respectivelijk elektronica, fijnmechanische metaalbewerking en wetenschappelijke instrumentatie in zeer ruime zin.

De beginselen van de spectroscopie heb ik geleerd van de vorige lichting onderzoekers. Ik dank daarvoor met name Antoine, Albert-Jan (ook als LabVIEW-expert!), Andreas, Yannig en Michio. Het werk dat in dit proefschrift staat beschreven, heb ik vooral uitgevoerd in aanwezigheid van een nieuwe lichting jonge wetenschappers. Ik bedank Rob, Alexander, Markus en de andere leden van MoNOS voor de discussies en onderlinge steun die voor jonge onderzoekers onontbeerlijk is. Daarnaast ben ik vooral dank verschuldigd aan Florian, waarmee ik veel lol heb gehad, ondanks dat we jarenlang een veel te klein kantoortje moesten delen. Ik heb dankbaar gebruik gemaakt van zijn Duitse Gründlichkeit en kennis van IT en optica. Gelukkig kon ik hem ook nog een en ander leren, hoewel ik hem vaak teleur moest stellen als het ging om het taalgebruik van de Nederlanders. I thank James Chon for his visit to Leiden and his contributions to the work of chapter 6.

Ik dank ook mijn ouders voor de mogelijkheden die ze voor mij hebben gecreëerd en hun steun. Tot slot dank ik Janet voor haar onvoorwaardelijke steun en geduld.